SPATIAL VARIABILITY IN RECRUITMENT OF CHILIPEPPER ROCKFISH (*Sebastes goodei*) IN THE CALIFORNIA CURRENT SYSTEM

By

Laura Katelyn Solinger

A Thesis Presented to

The Faculty of Humboldt State University

In Partial Fulfillment of the Requirements for the Degree

Master of Science in Natural Resources: Fisheries

Committee Membership

Dr. Eric Bjorkstedt, Committee Chair

Dr. Andre Buchheister, Committee Member

Dr. Mark Henderson, Committee Member

Dr. Andrew Stubblefield, Graduate Coordinator

May 2019

ABSTRACT

SPATIAL VARIABILITY IN RECRUITMENT OF CHILIPEPPER ROCKFISH (*Sebastes goodei*) IN THE CALIFORNIA CURRENT SYSTEM

Laura Katelyn Solinger

Properly describing variability in population dynamics (e.g., growth, fecundity, recruitment) is expected to improve management of important fisheries stocks (Maunder & Piner, 2014). As recruitment to most fish stocks is determined during early life history stages (Houde, 1997; Iles & Beverton, 2000), and early life history stages are influenced by oceanographic conditions (Bjorkstedt et al. 2002; Laidig, 2010), understanding how environmental stochasticity influences recruitment deviations has potential to improve estimates of stock productivity and how productivity might change over time to support more effective management. Chilipepper Rockfish (*Sebastes goodei*) are an important commercial species that is managed as a single population throughout the continental US (Field et al. 2015), yet spatiotemporal heterogeneity of oceanographic conditions is likely to cause variability in recruitment deviations throughout this range. Field and Ralston (2005) used region-based catch-at-age data from 1967-1997 to determine that 72% of recruitment deviations were shared throughout their range, though a substantial amount of the variability was coherent over smaller scales. I extended and enhanced the analysis presented in Field and Ralston (2005) to encompass data from the last two decades, a period in which there was considerable rebuilding of stocks, generally favorable

oceanographic conditions, and a rise in the understanding of spatial oceanography in the California Current System (CCS). In doing so, we confirmed results from Field and Ralston (2005), demonstrating that 70% of the variability in Chilipepper Rockfish recruitment deviations were shared coastwide between 1973 and 2015, though north-south and core (approximate center of biomass) -boundary spatial patterns did emerge. Generalized additive models were then used to examine oceanographic conditions as predictors of both coastwide coherence and spatial heterogeneity in recruitment deviations. Spatial patterns in recruitment emerged as a product of oceanographic conditions in the winter, at least in part due to high- and low-frequency transport dynamics, captured by sea level anomalies and the North Pacific Gyre Oscillation, respectively. Magnitude of recruitment success, which was generally shared coastwide, was best captured by upwelling anomalies during spring. This work demonstrates a method to empirically estimate spatial variability in recruitment deviations, which may facilitate current efforts to develop spatially-explicit stock assessment models, which are currently forced to make the assumption that recruitment is equally distributed across space (Thorson and Wetzel, 2013). Furthermore, understanding how oceanographic conditions may predict temporal shifts in that recruitment distribution may enhance the effectiveness of these stock assessment models.

ACKNOWLEDGEMENTS

Firstly, I would like to thank the many funding resources that supported me throughout this project including the Southwest Fisheries Science Center, James Joseph/ Inter-American Tropical Tuna Commission scholarship, and Ernest P. Fusi scholarship.

I would also like to thank my wonderful advisor, Dr. Eric Bjorkstedt, for accepting me to this position despite my ghastly first attempts at proposal-writing. Eric took a leap of faith in me, and with this thesis he is either very proud, or has learned a very big lesson. There is not a better-spirited, more quantitatively-savvy committee to be had than these fellows, Dr. Andre Buchheister and Dr. Mark Henderson. They mentored me like a student, but questioned me like a colleague. I am grateful to be in the down-line of their prestige.

I would also like to thank my cohort, and a few members in particular. Hannah Coe, in addition to many lessors, you showed me why I don't like field work, and for that, I thank you. Emily Chen, thank you for always inspiring the competitive spirit in me, even if you always won. I'm infinitely happy to call you two my friends.

Finally, words cannot describe the appreciation I have for my family. My mother was consistently the matriarch I needed, and my sisters, Amy Wise and Sarah Solinger, have always been driving forces and inspirations for the work I do, if nothing but to have more to brag about at Christmas. Y'all are truly fabulous, and I'm lucky to call you my family.

TABLE OF CONTENTS

LIST OF TABLES

LIST OF FIGURES

LIST OF APPENDICES

INTRODUCTION

Incorporating spatial structure in assessments for managed stocks is a critical goal for fisheries management (Berkeley et al. 2004; Forgarty & Botsford, 2007; Goethel et al. 2011), and in particular for management of stocks that occupy extensive, spatially heterogeneous ranges along the U.S. West Coast (Berkeley et al. 2004). Management of U.S. West Coast fisheries is largely guided by estimates of stock size and productivity generated through stock assessments, though most of these assessments assume that biological characteristics of a stock are homogenous throughout its range. This issue was addressed in the 2015 Canary Rockfish stock assessment, which incorporated stock structure in the assessment model, though doing so required an *a priori* designation of spatial pattern in recruitment (for our purposes, defined as the point at which individuals recruit to the fishery) (Thorson & Wetzel, 2015). Spatially-discrete stock assessment models (models built to span only a portion of the stock range) can empirically estimate recruitment and improve *a priori* designation (Field and Ralston, 2005). Even so, interannual variability in how recruitment is proportioned across space can contribute to uncertainty in stock assessment outputs important to fisheries management. These impacts can be reduced by understanding the degree of variability in recruitment dynamics and the factors that drive this variability (Charles, 1998; Uusitalo et al. 2015).

Of particular interest is how oceanographic conditions influence recruitment dynamics (Secor, 2007; Galindo-Cortes et al. 2010; Peterson et al. 2014). Oceanographic conditions in the California Current System (CCS) exhibit substantial temporal and

alongshore variability that affects productivity and transport dynamics likely to influence recruitment in coastal species. Many studies across a wide range of taxa have established the effect of oceanographic variability on recruitment (Allain et al. 2001; Wilderbuer et al. 2002; Schirripa & Colbert, 2006; Galindo-Cortes et al. 2010; Kilduff et al. 2014), and rockfish are no exception (Sakuma et al. 2006; Laidig et al. 2007; Laidig, 2010; Ralston et al. 2013). Several of these studies link recruitment dynamics of rockfishes to oceanographic variability in specific regions (e.g., central California [Ralston et al. 2013], southern California [Caselle et al. 2010]), but relatively less attention has been given to understanding how oceanographic variability affects recruitment in broadly distributed stocks at coastwide scales (but see Laidig, 2010, though they examined characteristics of recruits rather than recruitment success), perhaps due to the considerable data-needs associated with developing spatially-explicit recruitment indices.

Limitations in understanding the impact of environmental covariates on recruitment and how that varies with the spatial distribution of species inhibit the use of recent advancements to incorporate environment in stock assessment models. Environmental drivers are incorporated into recruitment estimates of stock assessment models in two main ways: 1) including environmental drivers as covariates in the stock-recruit function (Maunder & Watters, 2003) or 2) using environmental time series functions as an age-0 index of recruitment variability (Schirripa et al. 2009). Utilization of these methods requires understanding of what environmental drivers influence recruitment success and the functional form of this response, and how this influence varies over space.

Hesitation to include environmental indices into stock assessments is warranted, in part because Myers (1998) established that few recruitment-environment relationships have proven to be sufficiently enduring through time. Through time, these relationships often break down because another factor arises that limits recruitment success, the functional form of the modeled relationship changes, or large-scale controls (e.g., basin-scale climate variability) shift regional ecosystems to a new state that exhibits different dynamics (Lindegren & Checkley, 2012). Despite this variability, incorporating well-vetted indices into stock assessments reduces uncertainty in model estimates (Haltuch et al. 2009; Uusitalo et al. 2015; Hill et al. 2002; Schirripa & Methot, 2002; Lindegren & Checkley, 2012).

In this thesis, I revisit the study by Field and Ralston (2005), which used spatially-explicit catch-at-age data to demonstrate that 72% of recruitment variability in Chilipepper Rockfish (*Sebastes goodei*) was shared along the coast between Morro Bay and Crescent City, though a considerable amount of variability was coherent over smaller scales. I expand on this work by quantifying spatial and temporal variability in recruitment deviations of Chilipepper Rockfish off the coast of California from 1973-2014 (thereby augmenting the data considered by Field and Ralston by 16 years), a period in which there was substantial rebuilding of the stock (Field et al. 2015) and variability in ocean conditions (Chavez et al. 2002; Barth et al. 2007; Barth et al. 2015; McClatchie, 2016). I then extend this analysis with an investigation of how recruitment variability and coherence are related to environmental drivers of productivity and transport in the California Current across several spatial scales.

Chilipepper Rockfish Early Life History

Chilipepper Rockfish are ovoviviparous (bear live young) winter-spawners (Love et al. 2002). Larvae are typically released into the plankton during the winter (in southern California from August to April, with peak parturition occurring between December and January; in northern California from November to June, peaking from January through February) (Wyllie-Echevarria, 1987; Love et al. 2002). Rockfish recruitment success is thought to be determined by survival of larvae and pelagic juveniles (which lasts 3-5 months), presumably a function of retention and enrichment during this winter and spring. Year-class strength is more or less established by the culmination of the juvenile stage as young-of-the-year settle on sandy-bottoms outside of kelp beds and eventually move to deeper waters (Love et al. 2002). Chilipepper Rockfish can live up to 35 years, fifty percent are mature at age 3, and they recruit to the fishery around age 4-5 (Field, 2007).

Stock Assessment and Fishery History of Chilipepper Rockfish

Chilipepper Rockfish are managed by the Pacific Fishery Management Council (PFMC) as a single stock ranging from the U.S.-Mexico to the U.S.-Canada border. The stock is concentrated between Point Conception and Cape Mendocino, with the greatest concentration of biomass (and landings) off north-central California (Field et al. 2015). Assessments for Chilipepper Rockfish are developed in Stock Synthesis 3 (SS3, Methot & Wetzel, 2013), the framework in which assessments are developed for most groundfish

stocks along the U.S. West Coast (Field et al. 2015). Chilipepper Rockfish have been an important commodity to the U.S. West Coast fishing industry since the 1880s. The hook-and-line fishery reported the largest landings (in metric tons) until the 1950s when the trawl fishery expanded. The trawl fishery still accounts for the largest landings of Chilipepper Rockfish. In the 1950s the population began to decline and dropped below 25% of unfished spawning biomass in the late 1990s (Field et al. 2015). In 2002 trip limits and area closures were implemented for the protection of Boccacio and Canary Rockfish (*S. paucispinis* and *S. pinniger*, respectively), two species that co-occur with Chilipepper. Combined with several strong year classes in the recent past (especially 1999), reduction in fishing has allowed the population to rebuild. As of 2015, stock biomass was estimated at ~70% of unfished spawning biomass (Field et al. 2015).

Conceptual Models of Recruitment

Studies of recruitment in different regions of the CCS have found significant correlations with seasonal oceanographic conditions, but the seasons of importance vary from north to south. Off north-central California, recruitment and characteristics of recruits have been found to correlate most strongly with sea level anomaly, sea surface temperature (Laidig et al. 2007; Ralston et al. 2013) and upwelling (Laidig, 2010; Ralston et al. 2013) during the winter and early spring. In contrast, recruitment in southern California has been explained by upwelling and alongshore transport (in part captured by sea level anomaly) during the summer (Caselle et al. 2010).

This difference in timing is (in part) described by a variety of interwoven processes including enrichment, foraging success, predation, and transport (Parrish et al. 1981; Rothschild & Osborn, 1988; Mackenzie et al. 1994; Botsford et al. 2003), that feed into a variety of recruitment hypotheses (e.g. critical period [Hjort, 1914]; optimal environmental window [Cury & Roy, 1989]; match-mismatch [Cushing, 1990]; size-spectra surfing [Pope et al. 1994]). For example, wind-driven upwelling presents a potential tradeoff between enrichment of the plankton ecosystem (nutrient supply) and physical processes that retain larvae near coastal habitats (Parrish et al. 1981) and affect accessibility of prey or foraging efficiency (Cury and Roy 1989, Rothschild & Osborn, 1988). Cury and Roy (1989) hypothesized that optimal Ekman-type upwelling occurs at moderate levels because of trade-offs with physical processes (offshore transport, turbulence) and biological processes (nutrient availability). In a parallel response to variability in wind forcing, optimal feeding success is thought to occur when small-scale turbulence is moderate (Rothschild & Osborn, 1988; MacKenzie et al. 1994), though the optimal surface transport conditions vary with latitude and shelf width (Botsford et al. 2003). Surface transport from wind-stress (and subsequently upwelling) and ocean fronts also drive recruitment variability through impacts on retention of larvae within favorable habitat (and the population) (Parrish et al. 1981), and link widely-dispersed populations through alongshore transport (Petersen et al 2010), although there is evidence that hydrographic structure might help to counter offshore transport and to structure settlement (Bjorkstedt et al, 2002, Woodson et al. 2012).

Several hypotheses attempt to link recruitment to the intensity or timing of key processes. Of particular interest here is a generalization and extension of the match-mismatch concept that links the degree of recruitment success to the degree of overlap between spawning intensity and the onset (and subsequent continuity) of favorable oceanographic conditions (Cushing, 1990; Pope et al. 1994; Kerby et al. 2012), and integrative frameworks that assess the cumulative effects of diverse factors that affect recruitment (e.g., prey availability, feeding success, growth rate and drift with currents to either favorable or unfavorable environments) on survival through the pre-recruit juvenile stage (Houde, 2008, Hare, 2014). Unfortunately, evaluating environment-recruitment relationships through the lens of specific recruitment hypotheses can be complicated, especially if the ocean conditions that more strongly affect survival shift over the course of early life history. Likewise, any attempt to apply a particular (suite of) recruitment hypotheses is likely to be further muddled by variations in phenology of both peak parturition and optimality of oceanographic conditions, such as upwelling, throughout the range of many rockfish (Figure 1).

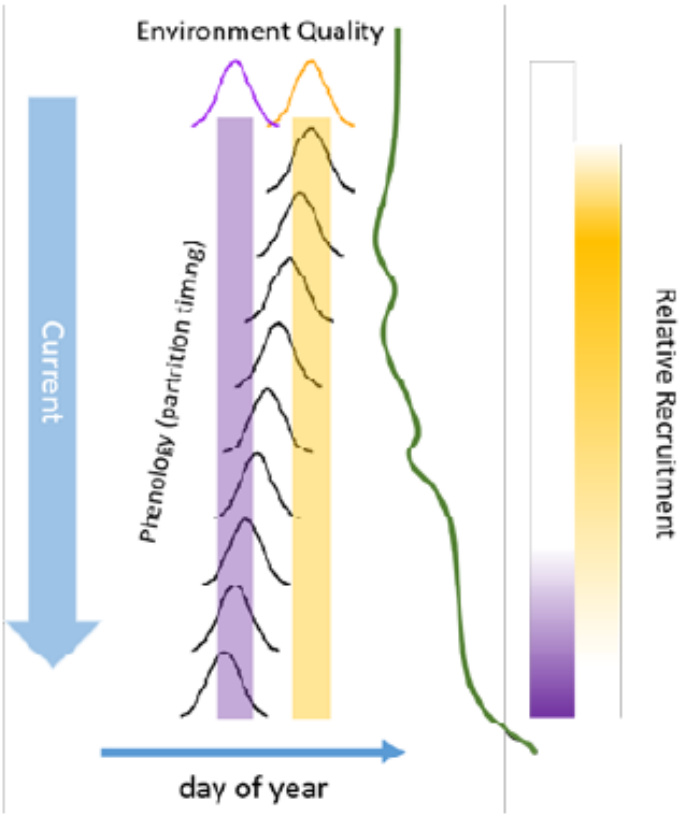

Figure 1: Conceptual diagram of the interaction between the match-mismatch hypothesis and spatial variability in the phenology of parturition in widely-distributed fisheries. The green line represents the outline of California. Purple and Yellow indicate two separate years where the peak of favorable environmental conditions occur at different time of the year. Black lines represent the gradient in timing of parturition throughout the coastline (northern areas spawning later than southern areas) and gradient on the right show where recruitment along the coast is most successful as predicted by overlap of phenology with favorable conditions.

Productivity and Transport in the California Current.

The California Current System (CCS) spans the U.S. West Coast, and it is broadly separated into three regions divided by Cape Mendocino and Point Conception (Figure 2;

Checkley & Barth, 2009). Nutrient enrichment processes in the CCS are dominated by energetic wind-driven upwelling along the coastal boundary and more diffuse but widespread curl-driven upwelling in offshore waters (Huyer, 1983). Winter and summer upwelling exhibit independent modes of variability with separate biological consequences. The winter mode (January to March), coincident with larval stages in Chilipepper Rockfish, is high-frequency (changes frequently in direction and strength), and has been positively related to growth in adult *Sebastes* spp. (Black et al. 2011). Winters marked by limited storm activity and mild upwelling allow early productivity that not only preconditions the ecosystem to respond robustly to subsequent upwelling, but also provides favorable conditions for larvae of winter-spawning rockfish, setting up conditions for young-of-the-year to survive through the duration of pre-recruit stages. The summer mode is low frequency and less correlated to growth of adult *Sebastes* spp., but captures the biologically critical spring transition (Black et al. 2011).

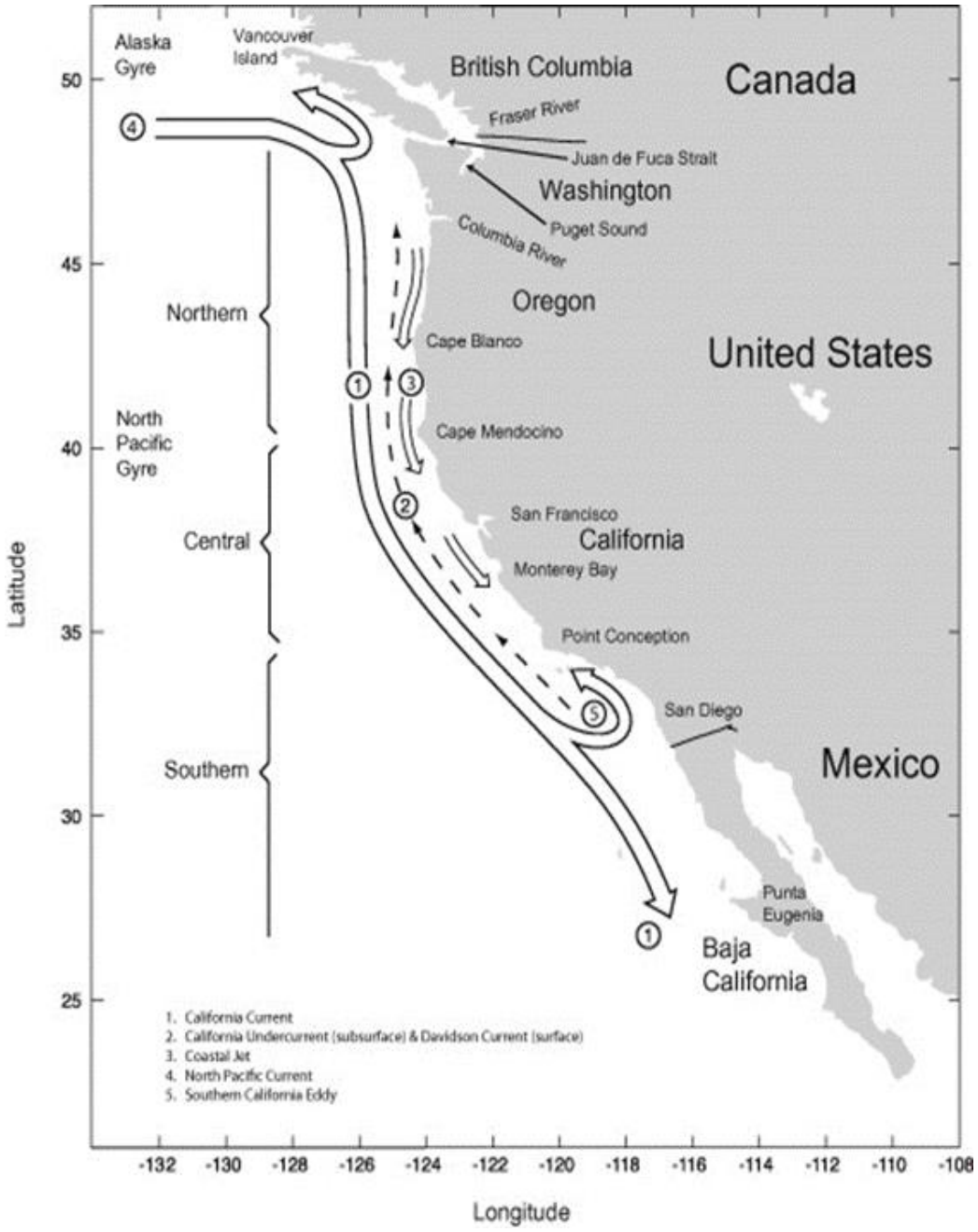

Figure 2: Characteristics of the California Current from Checkley & Barth, 2009.

The spring transition, which is the onset of the spring upwelling season, is a critical event in the CCS marked by a rapid shift from weak or pole-ward winds to strong, equator-ward, upwelling favorable winds. It is generally first observed in the southern California Current and progresses northward (Lynn et al. 2003). The spring transition is related to ecosystem productivity (or lack thereof), particularly in the northern CCS (Barth et al. 2007; Chenillat et al. 2012), though warm sea surface temperature anomalies and intense stratification in the water column can delay this productivity (Kosro et al. 2006). Relaxation events between upwelling pulses (rather than continual, strong upwelling) are necessary to prevent the offshore transport of upwelled nutrients and allow phytoplankton blooms to develop on the shelf (Botsfortd et al. 2003; Kudela et al. 2008). While upwelling is arguably the most important source of nutrients, its efficacy is (in part) mitigated by sea level, which can vary in response to remote forcing (e.g., variability in the tropics associated with El Niño). Sea level, an indicator of alongshore transport in the CCS, impacts the depth of the thermocline and subsequently the characteristics of water being upwelled (Chavez et al. 2002, Verdy et al. 2014).

Regional oceanographic conditions such as primary productivity, off- and along-shore transport are influenced by basin-scale modes of climate variability including the Pacific Decadal Oscillation (PDO), the North Pacific Gyre Oscillation (NPGO) and El Niño Southern Oscillation (ENSO). While these indices are basin-scale modes of variability, here I focus on how each manifests in the California Current System. The PDO and NPGO are the first and second modes of Sea Surface Temperature anomaly observations in the north Pacific, and are distinct from one another by definition, though

they can be correlated over short windows of time (Di Lorenzo et al. 2008). The PDO and NPGO are low-frequency, and fluctuate between positive (warm) and negative (cool) phases over multi-decadal time periods. The PDO captures variability in strength and of the California Current, supply of nutrient-rich waters from the north, and is significantly correlated with upwelling throughout the CCS, where upwelling is typically more intense during the cool phase of PDO (Hare et al. 1999; Chenillat et al. 2012; Di Lorenzo et al. 2013). While the NPGO also captures strength of flow in the California Current, it has a stronger regional expression in the central CCS where upwelling is generally stronger during a positive (strong flow) NPGO (Di Lorenzo et al. 2008; Chhak et al. 2009; Messie and Chavez, 2011; Chenillat et al. 2012). Variability in NPGO has also been related to a 1-2 month shift in the beginning of the spring transition, where positive phases of NPGO are associated with early onset of the upwelling season (Chenillat et al. 2012).

In contrast to the PDO and NPGO, ENSO originates in the tropics and varies at higher frequencies (e.g. 2-7 years) (Di Lorenzo et al. 2013). Atmospheric teleconnections can drive responses in the northern CCS in advance of any oceanic signals of ENSO, though ENSO events most strongly impact the CCS during winter, and stronger events can also persist through spring and summer (Bjorkstedt et al. 2010; Jacox et al. 2015). Of the ENSO modes, Eastern Pacific ENSO events have the most direct impact on the CCS. Such ENSO events trigger strong coastally-trapped Kelvin waves that result in persistent depression of the thermocline, which reduces the efficacy of upwelling, subsequently reducing primary productivity (Chavez et al. 2002; Bograd et al. 2009; Wolter & Timlin,

2011, Jacox et al. 2015). Time series of basin-scale indices between 1973 and 2015 are shown in Appendix A.

Questions to be Addressed

My analysis is structured around three questions that focus on understanding spatial scales in recruitment of Chilipepper Rockfish recruitment and whether variability in recruitment could be attributed to oceanographic dynamics at comparable spatial scales.

Q1. *How coherent are recruitment deviations in Chilipepper Rockfish along the coast of California, and at what scales are they coherent?*

Q2. *Are local recruitment deviations and coastwide-coherence in recruitment deviations linked to local or basin-scale oceanographic drivers?*

Q3. *Do spatial scales of recruitment variability correspond to spatial structure in oceanographic conditions along the coast?*

To address these questions, I constructed spatially discrete stock assessments (following Field and Ralston [2005]) to develop time series of recruitment deviations at scales of 50 to 200 km. Recruitment deviation time series from these assessments are the basis for subsequent analysis to assess modes of spatially-coherent variability along the coast, and for exploring links to oceanographic drivers of recruitment at regional to coastwide scales. Analysis of environment-recruitment relationships was motivated by hypotheses that transport and nutrient enrichment (and other ecological dynamics) during

the larval and juvenile stages impact survival of young-of-the-year and subsequent recruitment success. Specifically, I hypothesize that oceanographic conditions during winter (affecting larval stages) through spring-summer (affecting juvenile stages) govern recruitment success, assuming little additional variability in recruitment arises after settlement (but see Hobson et al. 2001 on post-settlement mortality).

The remainder of this thesis is organized into two major sections, each of which includes a Methods and Results section, followed by a synthetic Discussion. In the first section, Recruitment Deviations, I conduct regional stock assessments and then use results from these assessments to characterize spatial and temporal variability in Chilipepper Rockfish recruitment along the California coast. In the second, Oceanography, I explore spatially-explicit environment-recruitment relationships ranging from local scales to scales of coherent variability identified in the initial assessment-based analysis.

RECRUITMENT DEVIATIONS

Methods

Construction of assessment models

Stock Synthesis 3 (SS3; Methot & Wetzel, 2013) was used to develop independent stock assessment models for discrete regions along the California coast. These assessments were based on the model structure that underlies the coastwide assessment (Field et al. 2015). SS3 uses landings, CPUE, catch-at-length and catch-at-age data to develop estimates of virgin biomass, spawning biomass, and recruitment deviations in addition to many other biological parameters of interest to stock managers.

The California Commercial Fisheries Landings Database provides fishery-dependent landings, catch-at-length and catch-at-age data from four aggregated commercial fishing fleets (“trawl”, “hook and line”, “set-net” and “other”) from 1916 to 2015 (Figure 3). These data are parsed in a more spatially-explicit manner by the California Department of Fish and Wildlife which provides data on commercial fisheries from 2000 to 2015. Fishery-independent data are provided by the Northwest Fisheries Science Center (NWFSC) groundfish surveys which provide CPUE, catch-at-length and catch-at-age data.

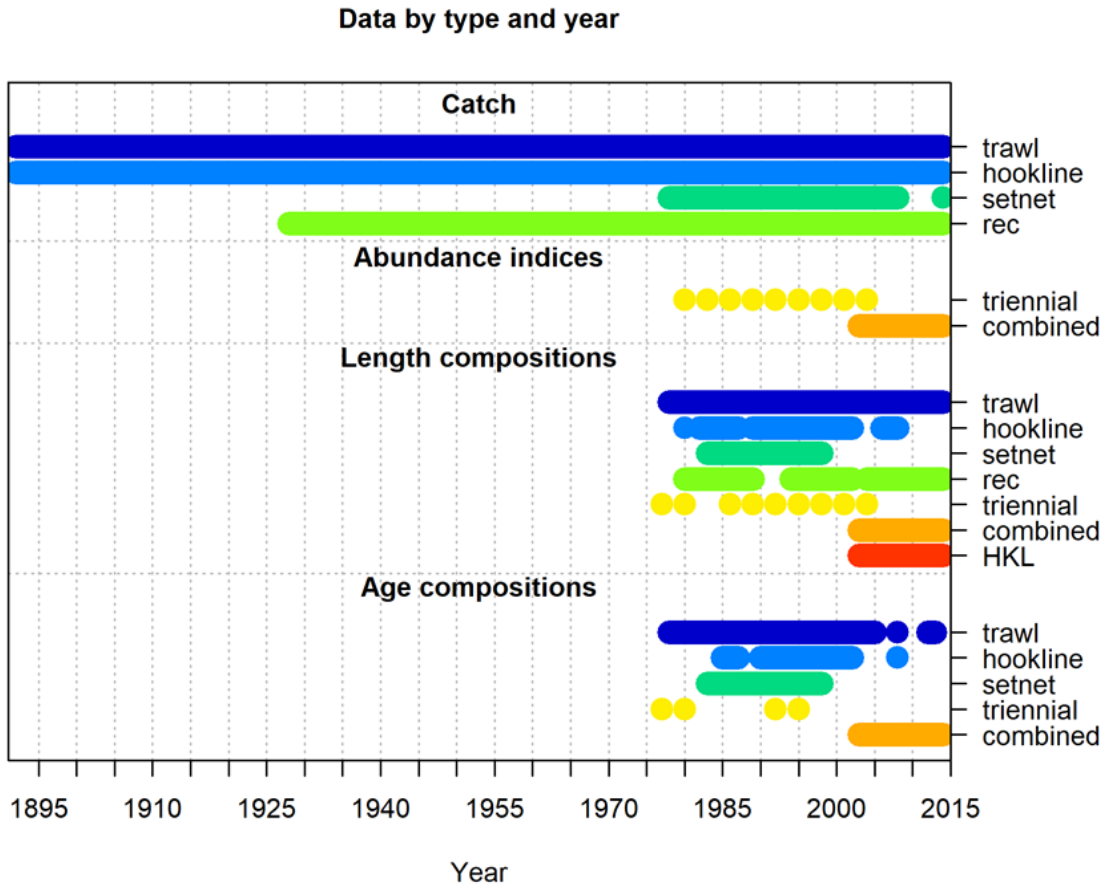

Figure 3: Data types and fleets which contributed to the 2015 stock assessment of Chilipepper Rockfish.

Selectivity curves are used to describe susceptibility of fish to capture as a function of length for each fleet or survey (Field et al. 2015). Selectivity in the "trawl" and "hook-and-line" fisheries were fit to a logistic curve to reflect a monotonic increase in susceptibility to the gear. Selectivity in the "set-net" and "recreational" were fit to a double normal curve that captures an initial increase in susceptibility and subsequent decline in susceptibility as the stock shifts out of the fisheries' range. Parameters for each

of these curves are estimated in the course of fitting the assessment model. The Triennial, Combined and Hook and Line surveys were assigned logistic selectivity curves to be estimated in the course of fitting the assessment.

The majority of fish for which age was estimated were drawn from those for which length had been measured. To ameliorate the issue of double-counting samples, I followed Field et al. (2015) and assigned length composition data 10% the weight of age composition data in the model fit. This weighting scheme also reflects the fact that age composition data are inherently more reliable at estimating year of recruitment.

Model diagnosis

Parameter and variance estimation is entirely internal to the SS framework, which employs maximum likelihood estimation to converge on parameter estimates, the inverse Hessian matrix to estimate variance around those estimates, and Monte Carlo Markov Chain to develop equilibrium and forecast results for each parameter (Methot & Wetzel, 2013). The full assessment was used as a general benchmark for determining that port-specific models were producing reliable results.

Comparison to coastwide assessment

To support the evaluation of the port-complex assessments, port-complex data were aggregated into a single assessment representing the whole of California. Recruitment deviations from this assessment output were compared to Field et al. 2015 to ensure that the span of my work sufficiently captured recruitment variability in Chilipepper Rockfish.

Focal results from assessments

Recruitment deviations were the main output of interest from stock assessment models. The Beverton-Holt stock-recruitment relationship (Beverton & Holt, 1957) was used to model recruitment and recruitment deviations:

$$1)\quad R_y = \frac{4hR_0SB_y}{SB_0(1-h)+SB_y(5h-1)}\, e^{-0.5b_y\sigma_R^2+\tilde{R}_y},\ \tilde{R}_y \sim N(0;\sigma_R^2)$$

where $R_y$is recruitment in year *y*, R_0 is the unfished equilibrium recruits, h is steepness of the curve (i.e., the ratio of the number of recruits produced at 20% virgin biomass to that produced at virgin biomass), SB_0 is the unfished spawning biomass, SB_y is the annual spawning biomass, b_y is the bias adjustment fraction in year *y*, σ_R^2 is the standard deviation of recruitment and $\tilde{R}_y$ is the lognormal recruitment deviation in year *y* (Methot, 2013). This relationship is generally accepted to represent U.S. West Coast *Sebastes* spp. (Dorn, 2002). SS3 estimates parameters of the stock recruitment (*S*-*R*) relationship, Equation (3), largely based on catch-at-age and catch-at-length data. Maximum likelihood is used to estimate recruitment deviations, and subsequently the annual number of recruits. Due in part to lack of data on recruitment success at low biomass, unconstrained estimates of steepness frequently converge to 1. This would indicate that equilibrium recruitment occurs even at small biomasses, which is unreasonable for most fishes. Thus, steepness was fixed to 0.57, based on conclusions drawn from a meta-analysis by Dorn (2002). Finally, a bias-adjustment factor, b_y, can be estimated to compensate for consistent underestimation of recruitment variability, in part because stronger recruitment years are better informed than weak year-classes (Methot & Taylor,

2011; Methot, 2013). A bias adjustment was not applied to the coastwide assessment, and thus was not used in this analysis.

Stock assessment data

The landings data and associated oceanographic indices were resolved or aggregated at different spatial scales that I define here for reference herein. The “port” scale refers to individual locations where fish were landed, represented by black dots in Figure 4. “Region” refers to areas designated by the California Department of Fish and Wildlife (CDFW) and California Commercial Fisheries Landings Database (CALCOM) within which landings from ports are aggregated (Figure 4). “Port-complex” refers to areas for which individual spatially-explicit stock assessments are developed from associated port- and region-specific data. Port-complexes are delineated with dashed red lines in Figure 4. “Station” refers to where oceanographic indices data were collected. “Core” refers to the area of Region 4, the approximate area of peak biomass for Chilipepper Rockfish.

Several sources of biological data from fishery-dependent and -independent sources are available to support development of stock assessments for Chilipepper Rockfish. Wherever possible, I have followed the formal coastwide assessment (Field et al. 2015) with respect to data sources and fishing fleet structure.

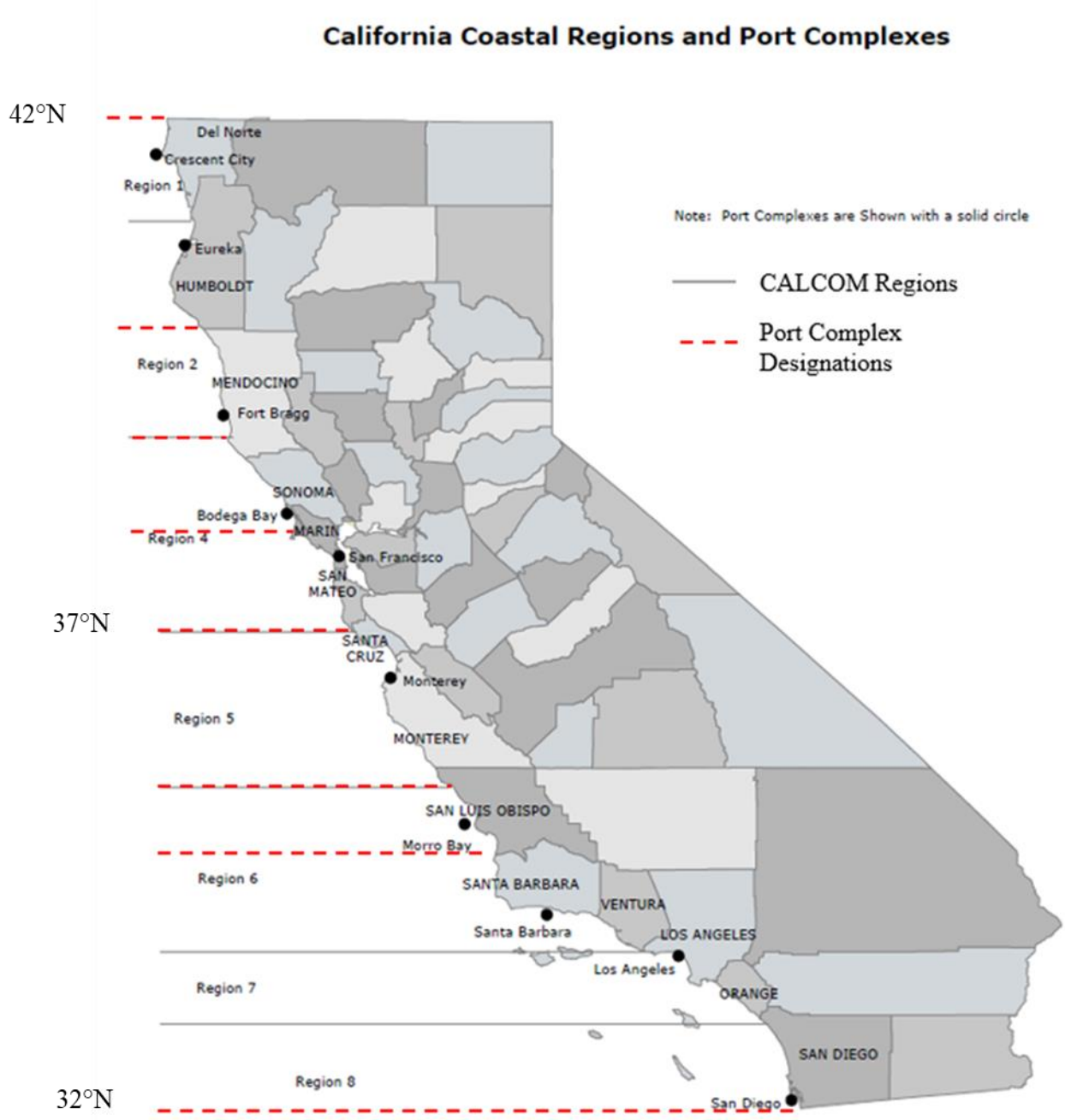

Figure 4: Region map provided by California Commercial Fisheries Landings Database for how landings were divided into regions. Black dots represent ports, grey lines represent region designations, and dashed red lines represented port-complex designations.

Port-complex designations

I partitioned the coast of California into seven regions that tradeoff geographic (latitudinal) extent and proportion of state-wide landings. Six regions match those designated by Field and Ralston (2005). I also define a southern region that spans ports from Santa Barbara to the U.S.-Mexico border (Table 1). This port-complex designation represents the smallest available area for which sufficient data were available to support a stock assessment model.

Table 1: Designation of port-complexes for California. Region landings were parsed between complexes by extrapolating recent port-complex-specific landings to historical region landings. This method is discussed further in text.

Port-complex	Latitude	Notes
Eureka	40°N-42°N	Apportioned 9.3% of landings from Region 2 and all landings from Region 1
Fort Bragg	39°N-40°N	Apportioned 90.7% of landings from Region 2
Bodega Bay	38°N-39°N	Apportioned 12.9% of landings from Region 4
San Francisco	37°N-38°N	Apportioned 87.1% of landings from Region 4
Monterey	36°N-37°N	All landings from Region 5
Morro Bay	35°N-36°N	Apportioned 95.0% of landings from Region 6; Hook and Line Survey information
Southern	32°N-35°N	Apportioned 5.0% of landings from Region 6 and all landings from Regions 7 and 8

Fishery-dependent data

Commercial fisheries data were obtained from two sources (California Commercial Fisheries Landings Database [CALCOM] and California Department of Fish and Wildlife [CDFW]) that parsed the same data in different manners. CALCOM includes data on commercial landings, lengths, and ages from 1916-2015, and is based in

part on the historical catch reconstruction of rockfish landings from 1916-1968 (Ralston et al. 2010). CALCOM parsed landings by region (Figure 4), and gear-type (on-bottom trawl, midwater trawl, hook and line, set-net, other, and unknown). The California Department of Fish and Wildlife (CDFW) parsed commercial landings data from 2000-2015 by port (Figure 4) with no consideration of gear type.

Landings: spatial distribution. Port-specific landings from 2000-2015 (CDFW) were used to apportion region-scale landings from the 1916-1999 (CALCOM) to port-complexes. Monterey Bay was the only port for which region and port-complex designations aligned with one another. For all other regions, landings were apportioned to port-complexes using the equation:

$$2) \quad L_{p_1 y} = \frac{{L^*}_{p_{1\,(2000-2015)}}}{{L^*}_{p_{1\,(2000-2015)}} + {L^*}_{p_{2\,(2000-2015)}}} * L_{ry}$$

where L^* represents port-complex landings, L represents region landings, y is year (ranging from 1916 to 1999) and p_1 and p_2 represent individual port-complexes within region r. Figure 5 demonstrates this process for Region 2 from which Eureka and Fort Bragg port-complex landings were generated. Eureka landings were generated by taking the proportion of Eureka landings to those of Eureka and Fort Bragg landings from CDFW between 2000 and 2015. Region 2 landings from 1916 to 1999 were then subset to the proportion generated from modern CDFW data to represent Eureka port-complex specific landings. The proportion of landings from each region apportioned to each port-complex (L_p) from this process are given in Table 1.

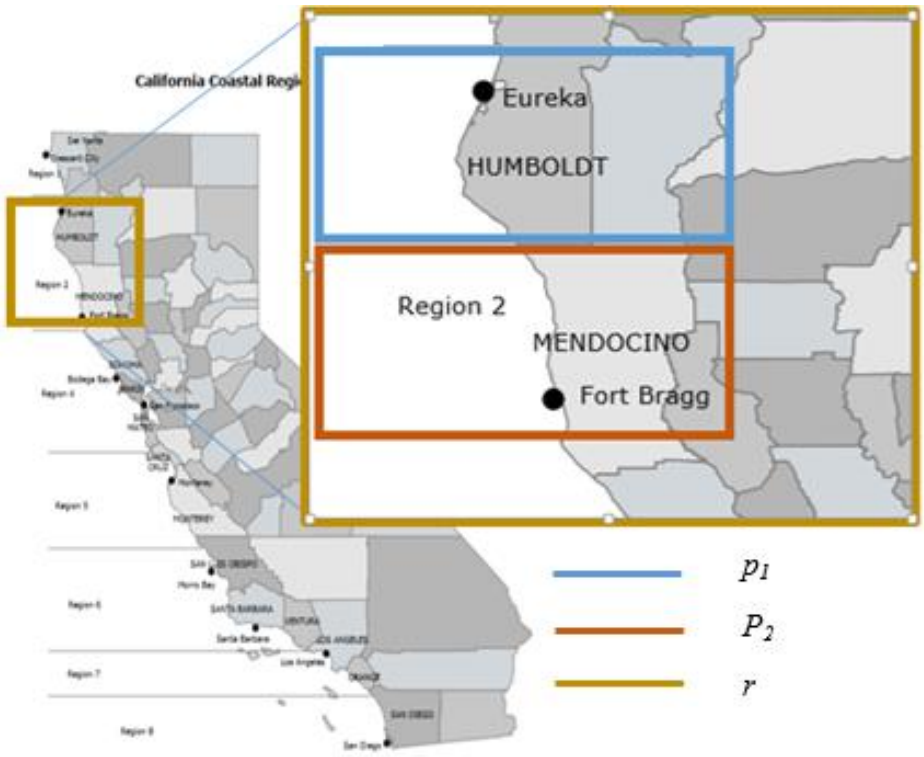

Figure 5: Separation of Region 2, *r*, into two ports, Eureka and Fort Bragg, which would represent p_1 and p_2 in equation 1.

This protocol does not account for historical shifts in how fishing pressure was distributed within and among CALCOM regions. A sensitivity analysis was used to assess the potential consequences of assumptions governing how landings were partitioned among regions for recruitment time series derived from port-complex-specific assessment models (Appendix B). These analyses demonstrated that recruitment deviation time series showed little response to differences in how historical fishing pressure was distributed, so I proceed with results based on my initial assumption.

Landings: fleet structure. In accordance with the coastwide assessment, landings data were partitioned among four fishing fleets: 1) “trawl”, which included both bottom and midwater trawls, 2) “hook-and-line”, primarily longline, 3) “set-net” (an anchored gill net), and 4) “recreational” (which included recreational, other, and unknown) (Field et al. 2015). Information on landings by fleet is necessary to account for differences in susceptibility to capture across gear types. The following equation demonstrates how port-complex-specific landings from equation (1) and region- and gear-specific landings from CALCOM were used in conjunction to develop port-complex- and gear- specific landings.

$$3) \qquad L^*_{pyg} = L^*_{py} * \frac{L^*_{\mathrm{ryg}}}{\sum_{\mathrm{i}=1}^{4} L^*_{\mathrm{ryg_i}}}$$

where L^* represents port-complex landings, y is year (ranging from 1916 to 2015), g is gear-type (on-bottom trawl, midwater trawl, hook and line, setnet, other, and unknown) and p is individual port within region r. The annual proportion of landings reported to each gear type in Region r was multiplied by annual port-complex-specific landings generated in equation (1) to produce port-complex- and gear- specific annual landings. Any violation of my assumption of consistent fleet structure over time is expected to have negligible effect on the recruitment deviation time series.

Length compositions. CALCOM provided port-specific catch-at-length and catch-at-age data collected since 1973 (Table 2). Unlike the landings data, CALCOM parses length- and age-data into individual ports, so these data were directly applied to port-complex assessments. To do so, catch-at-length data were first partitioned among ports.

From there, I used the same length composition method from Field et al. 2015, parsing catch-at-length data by fleet. Within fleet, fish were then classified by sex (male and female) and sorted into 2-cm length bins from 16-52 cm; fish larger than 52 cm are aggregated into a "plus" group. From these data, the relative proportion of fish of each sex, in each length bin, by year, and by fleet was obtained and applied to each port-complex stock assessments.

Table 2: Number (N) of commercial age and length observations contributing to each port-complex stock assessment. Note that subsamples were expanded to total landings by Ralston (2010). Fish used for age observations are also measured and are included in the length-observation count.

Port-complex	N length observations	N age observations
Eureka	1,634,235	930,360
Fort Bragg	5,525,875	3,561,574
Bodega Bay	3,365,359	2,205,435
San Francisco	7,993,761	4,072,145
Monterey	5,336,038	2,267,492
Morro Bay	2,822,203	1,366,339
Southern	806,559	41,204

Age compositions. Age compositions are based on the reading of annual increments of otoliths taken from a subset of the fish for which length data are collected (Field et al. 2015, Table 2). Age data were parsed in a manner similar to that of length data to develop age compositions for each port-complex, fleet, and sex. Fish were divided into 20 one-year age bins, and a "plus" group for fish 21 and older. Age- and sex- specific aging error matrices from Field et al. 2015 were applied to each of the port-complex assessments, under the assumption that such error did not exhibit any spatial pattern.

Fishery-independent data

The fisheries independent data sources considered here include the National Oceanic and Atmospheric Administration's (NOAA) Groundfish Triennial Shelf Survey (Triennial), Groundfish Combination Shelf and Slope Survey (Combined), and the Shelf Rockfish Hook and Line Survey (HKL). The Northwest Fisheries Science Center (NWFSC) conducted the Triennial survey from 1977 to 2004. Beginning in 2003, NOAA began sampling CCS groundfish on both the slope and shelf in the Combined survey. From both of these surveys, I included only those data associated with trawls deemed 'satisfactory' (i.e., the sampling gear functioned as intended) for analysis. The HKL survey occurred south of Monterey Bay annually from 2004 to the present. These three sources of fishery independent data are available through the NWFSC Fishery Resource Analysis and Monitoring Division (FRAM).

Catch per unit effort (CPUE). The Triennial and Combined surveys provide CPUE estimates that were divided into latitudinal bins to represent port-complex designations and then stratified by depth (55-150 meters and 150-400 meters) (Table 1).

Length and age compositions. Catch-at-length data were available from the Triennial, Combined and HKL surveys, and catch-at-age data were available from the Triennial and Combined surveys. Region-specific length and age compositions were then determined by the same method applied to respective data from fishery-dependent sources. Data were partitioned among port-complexes by latitude (Figure 4; see Table 3 for number and distribution of observations).

Table 3: Number (N) of length and age compositions from 1977 – 2015 from fishery-independent surveys contributing to port-complex stock assessments. Note that Morro Bay and Southern are the only port-complexes where the Hook and Line Survey operated, and consequently have elevated length observations.

Port-complex	N length observations	N age observations
Eureka	2,942	924
Fort Bragg	4,051	1,462
Bodega Bay	7,316	2,549
San Francisco	5,320	1,586
Monterey	2,969	1,000
Morro Bay	5,096	1,234
Southern	7,936	1,995

Retrospective analysis of recruitment deviations

Retrospective analysis is a method of examining how parameter estimates, such as recruitment deviations, change as recent data is sequentially removed from stock assessment models to mimic assessments conducted at earlier points in time. It is frequently used in stock assessments to examine if estimates of annual recruitment deviations change in a patterned manner with the addition of data from subsequent years (Szuwalski et al. 2017). Identifying a retrospective pattern in results can lead to concerns in the integrity of a model, so I used it as a tool to determine the reliability of port-complex-specific models and recruitment estimates. I sequentially truncated port-complex stock assessment models by one year such that seventeen stock assessment models were fit for each port-complex, ending between 1999 and 2015. Each regional assessment yielded an independent time series of recruitment deviations.

Diagnosis of pattern in recruitment variability

Time series of recruitment deviations were extracted from the results emerging from each assessment model. These represent port-complex-specific predicted recruitment deviations from 1973 to 2014. Error associated with these estimates is discussed in Appendix C, but in subsequent analysis they are used as true point estimates.

Two analyses were developed to quantify modes of shared variability in the set of recruitment deviation time series. First, following Field and Ralston (2005) I applied Principal Components Analysis (PCA) to the set of recruitment deviation time series, using prcomp from the "stats" package in R (R Core Team, 2017). PCA is a method of hierarchical dimension reduction for identifying shared patterns in a set of variables (Wold et al. 1987), which in this circumstance are port-complex-specific recruitment deviation time series. Recruitment deviation time series were arranged to estimate modes of temporal variability across port-complexes. Results from this analysis (specifically principal components 1, 2 and 3) were used to assess spatial and temporal patterns in recruitment deviations and formed the core of subsequent analysis in which variability in recruitment deviations (represented by PC1, PC2 and PC3) were modeled as functions of various oceanographic variables.

Second, as a complementary analysis, I applied Dynamic Factor Analysis (DFA). DFA is a method of dimension reduction that detects common patterns in a set of time series data (Zuur et al. 2003), accounting for the sequential nature of recruitment deviations that PCA does not. This was employed to compare with PCA results and

ensure that my conclusions were robust to analytical approaches. DFA produces common trends identified across time series, which are each associated with an error matrix. Each error matrix requires the estimation of additional parameters, thus DFA requires the specification of the number of common trends to identify in a set of time series. DFAs were run using the MARSS (Multivariate Autoregressive State-Space Modeling) function from the "MARSS" package in R (Holmes et al. 2014). There were six candidate DFA models with two types of error matrices (diagonal and equal, diagonal and unequal) and the model could specify one, two or three common trends. Models were ranked according to a small sample size corrected Akaike's Information Criterion (AICc) calculated internally to MARSS.

Results

Comparison to coastwide assessment

The time series of recruitment deviations from a California-wide assessment compared favorably to that derived from the coastwide assessment (Field et al. 2015) (Figure 6). This result is consistent with the observation that most of the Chilipepper stock is located (and landed) off California. Consistency in recruitment deviations between these two models allowed the further development of port-complex-specific stock assessment models derived from data used in the California-wide assessment.

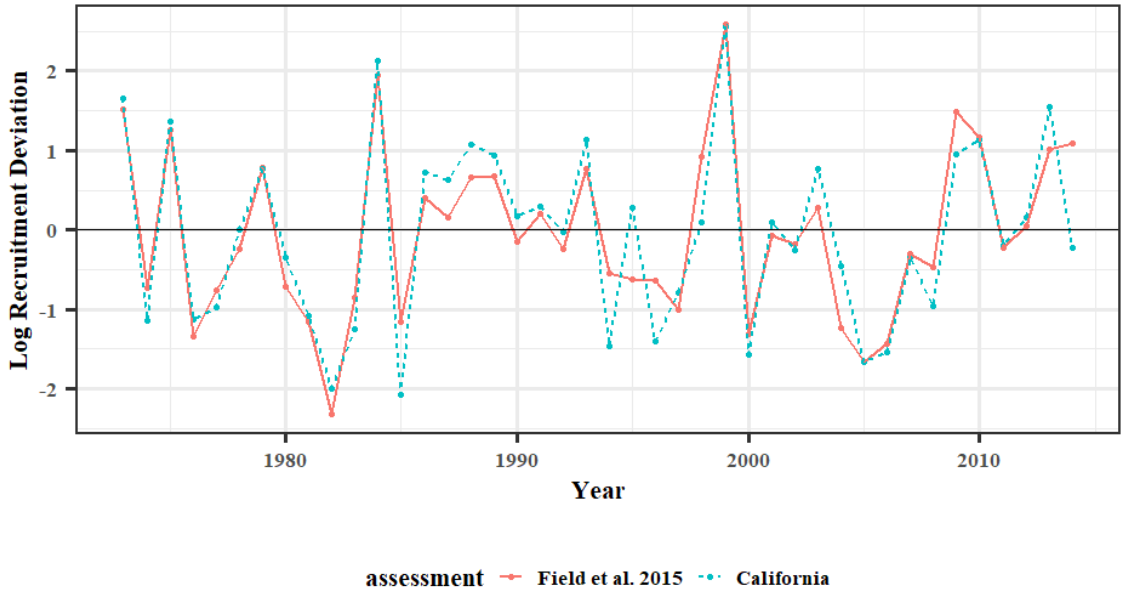

Figure 6: Comparison of recruitment deviations from the full assessment (Field et al. 2015) and an assessment based on California data.

Retrospective analysis of recruitment deviations

Results from the retrospective analysis (Figure 7) provide a basis for evaluating the reliability of recent estimates of recruitment. Each line in Figure 7 represents an individual year-class, or recruitment year. Each point represents the recruitment estimate for that year-class at a certain age (i.e., as additional years of data become available). Recruitment estimates at the beginning of year-classes are relatively poorly informed, but as the cohort ages, more data are available to inform the estimation of recruitment deviations. With the exception of the 1999 year-class (a product of both the magnitude of the year-class and unusual distribution of juveniles away from juvenile survey locations [ERIC SOURCE]), estimates of recruitment deviations stabilized between ages one and four for all year-classes in assessments for all port-complexes (Figure 7).

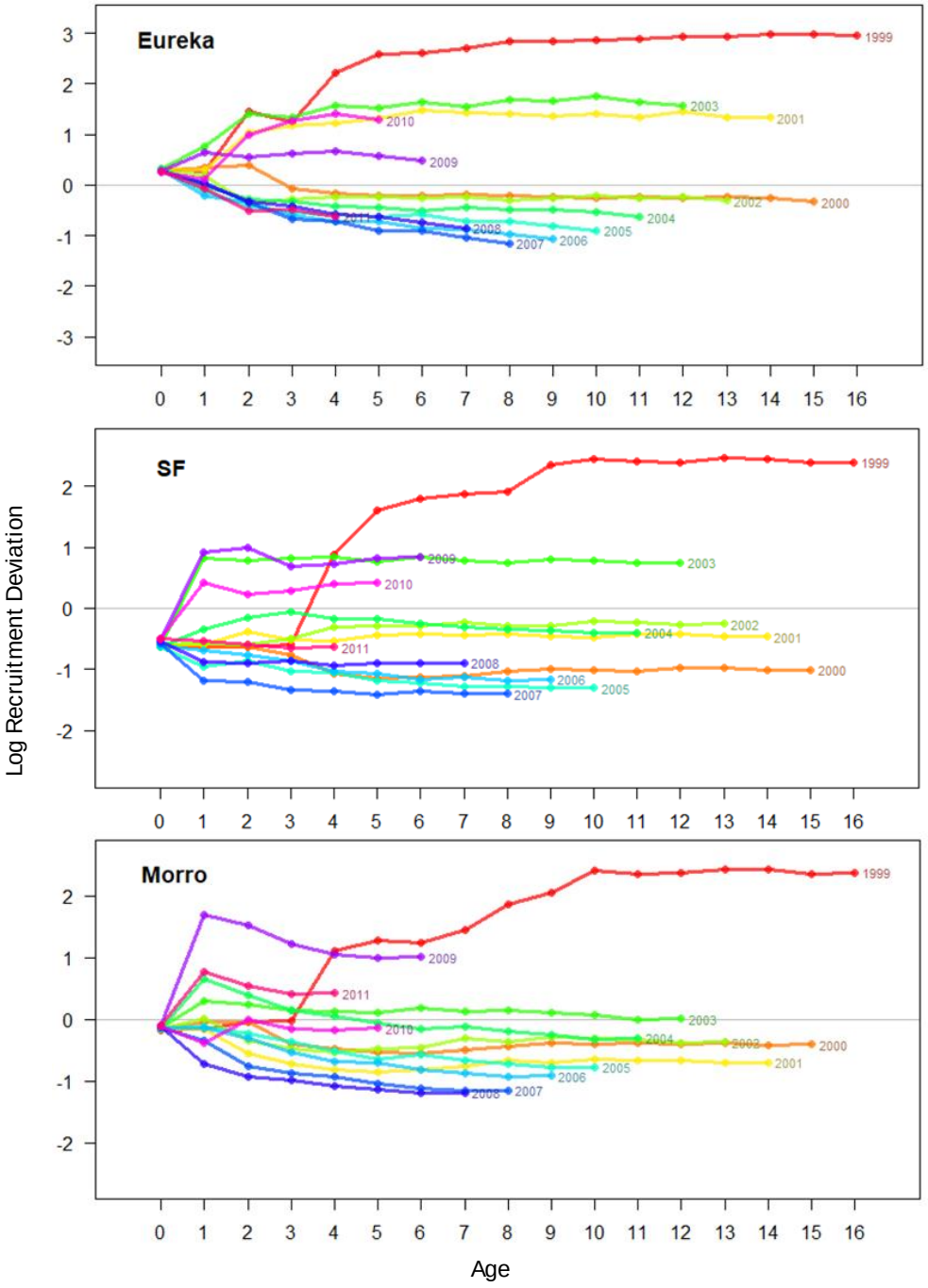

Figure 7: Retrospective analysis of recruitment deviations at Eureka, San Francisco (SF) and Morro Bay from 1999 to 2011. Each line represents a cohort from an individual year-class, and the x-axis, age, corresponds to the recruitment deviation estimate at that age.

Evolution of recruitment deviation estimates appear to exhibit geographic structure. While there was minimal retrospective pattern for strong year-classes, estimates of recruitment strength for northern port-complex recruitment typically showed a pattern of increasing from initial estimates until stable estimates were achieved around age 4. In contrast, southern port-complexes showed a slight overestimation during age 1 and subsequent declined to stable estimates over the following three years. This observation motivated examination of spatial patterns in distribution of young (age 0 to age 4) fish in the survey data, which suggest higher concentrations of young fish in southern regions (detailed in Appendix D). This may be responsible for the retrospective pattern observed. Recruitment deviation estimates through 2014 were used in this analysis as they were informed by age-one fish, and offer some estimate of recruitment deviations through the later period of this time series.

Port-complex recruitment deviations

Recruitment deviations exhibited a strong degree of synchrony along the California coast (Figure 8). Strong (e.g., 1984 and 1999) and weak year-classes (e.g., 1983, 1985, 2000, and 2005-2007) were observed across all port-complexes and coincided with those reported in the full assessment. Correlations in recruitment deviation time series across ports was high in general, but tended to progressively decline with increasing distance (Figure 8).

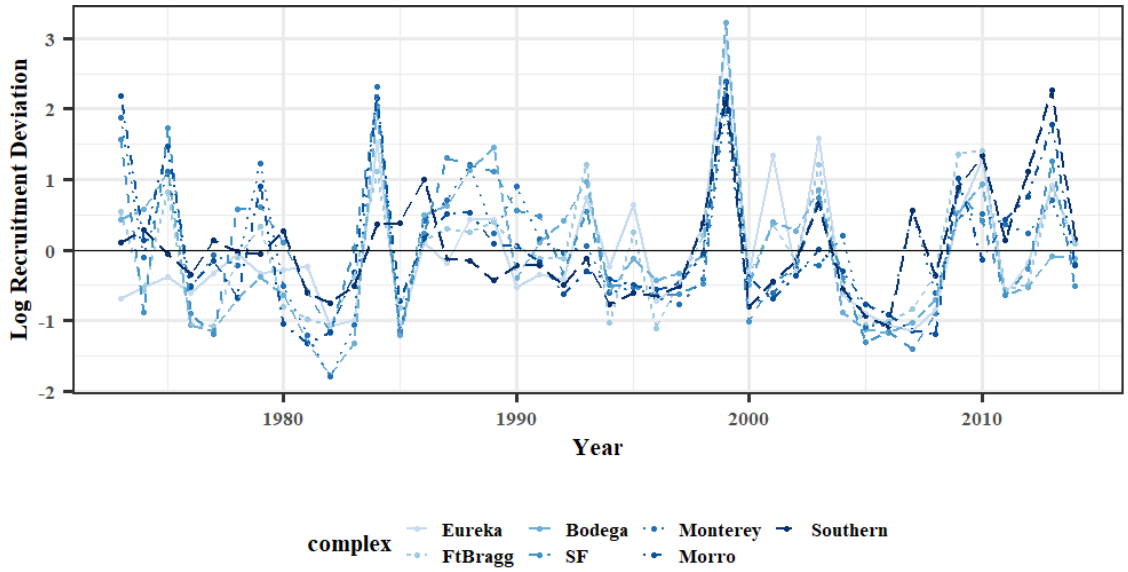

Figure 8: Recruitment deviations from port-complex assessments. North to south is light blue to dark blue.

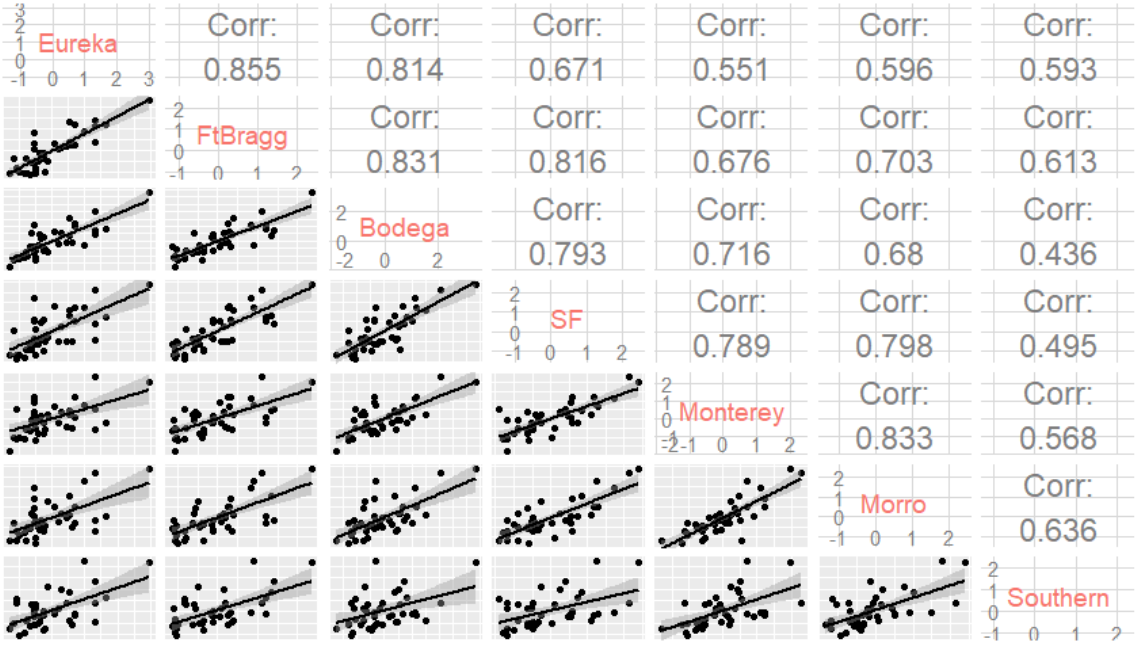

Figure 9: Scatterplot matrix of the seven port-complex time series of recruitment deviations. Corr stands for the Pearson correlation coefficient, R, from simple linear regression between port-complexes. All correlations are significant ($p < 0.05$).

Comparison among recruitment time series revealed substantial variability among port-complexes within the otherwise coherent recruitment pattern. Periods of moderate recruitment success typically exhibited spatially coherent patterns where the northern, central or southern regions performed relatively better or worse than other regions (Figure 10). Note that Southern was largely out of phase with other port-complexes during the 1980s, though confidence intervals for recruitment deviations are broad for Southern throughout this period (Appendix C). From 1987 through 1990, recruitment (relative to spawning stock biomass) was best in central California, diminishing as it spread from San Francisco. In 1993, 2001 and 2003 northern California experienced substantially better recruitment success than any of the ports south of San Francisco. In 1979 and 2011, ports south of San Francisco performed better than more northern ports.

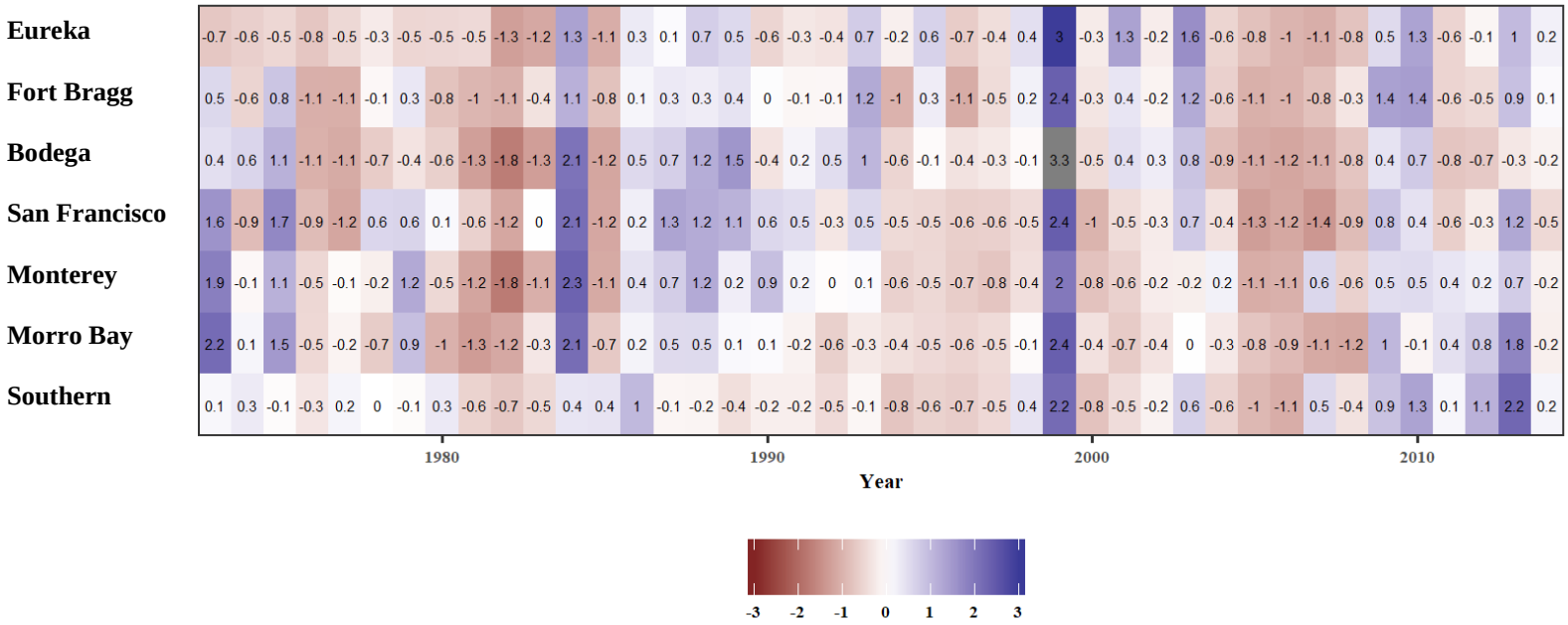

Figure 10: Heat map of recruitment from port-complex stock assessment models. Largely positive recruitment deviations are dark purple, and largely negative recruitment deviations are dark red. White indicates a recruitment deviation of zero.

Principal components analysis

A principal components analysis (PCA) identified three principal components that together explain >90% of the variability in the seven time series of port-complex-specific recruitment deviations (Figure 11). Loading (i.e., the directionality [positive or negative] and strength of associations between port-complexes and principal components) provide insight to how variability is shared or partitioned among port-complexes. All port-complexes loaded positively onto the first component (PC1), which describes 74% of the variability between port-complex recruitment deviations and represents coastwide coherence in recruitment deviations. Two clear peaks in PC1are the signature of strong 1984 and 1999 year-classes observed in most or all of the port-complex-specific assessments and in both coastwide and California-specific assessments (Figure 6; Figure 8; Figure 12). PC1 also captures moderate recruitment success throughout the late 1980s and early 1990s and followed a similar trajectory to the recruitment deviations from the port-complex-specific assessments (Figure 13).

a.

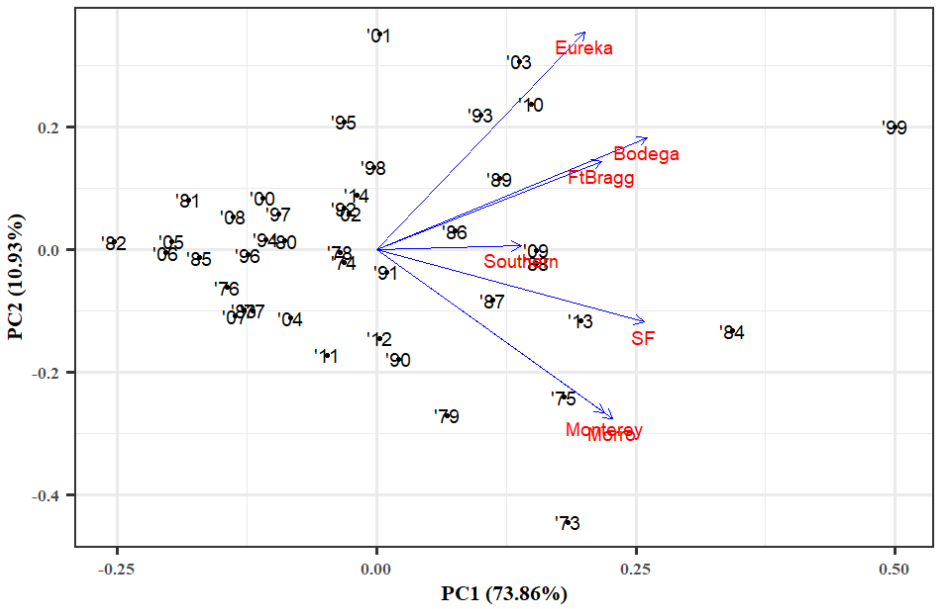

b.

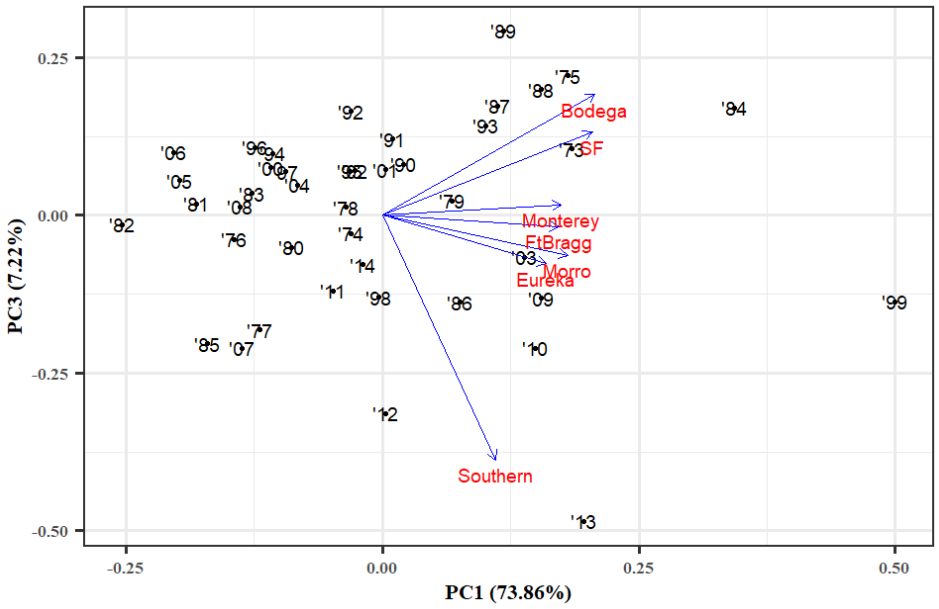

Figure 11: Principal components for port-specific recruitment deviations. (a) shows the first and second components, while (b) shows the first and third components. The first component explains 74% of the variability and groups all ports. The second component explains 11% of the variability and divides ports into north and south. The third component explains 7% of the variability and divides the core (Bodega and SF) from boundary regions to the north and south.

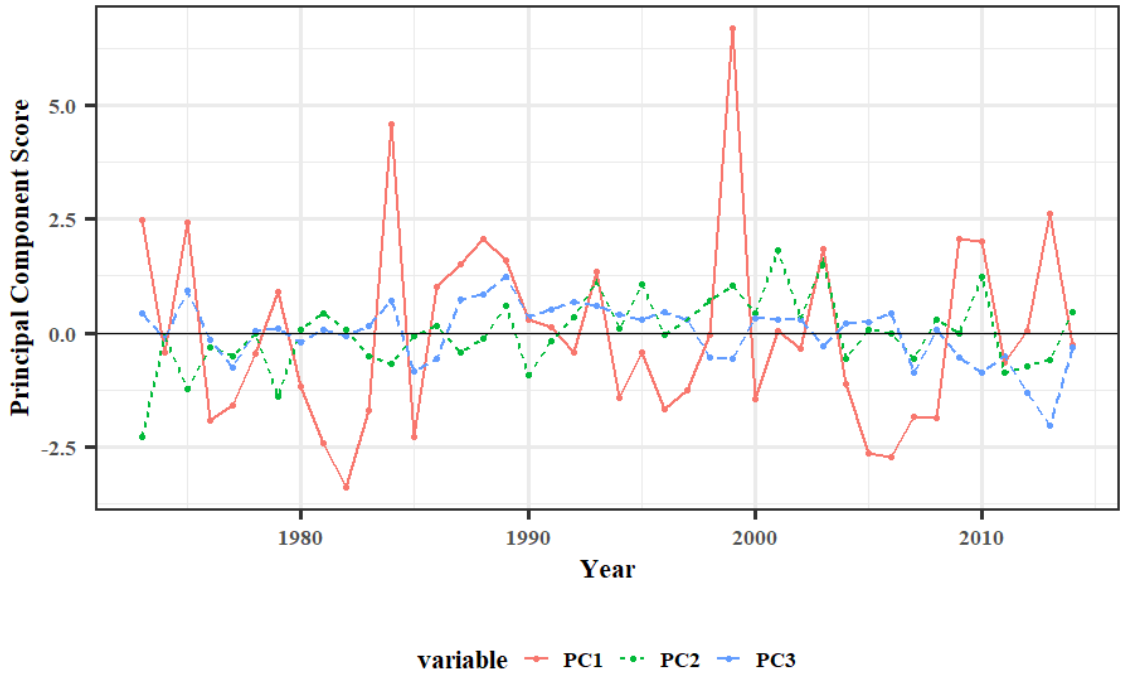

Figure 12: Principal component score over time for coastwide coherence in recruitment deviations and coherence at smaller spatial scales.

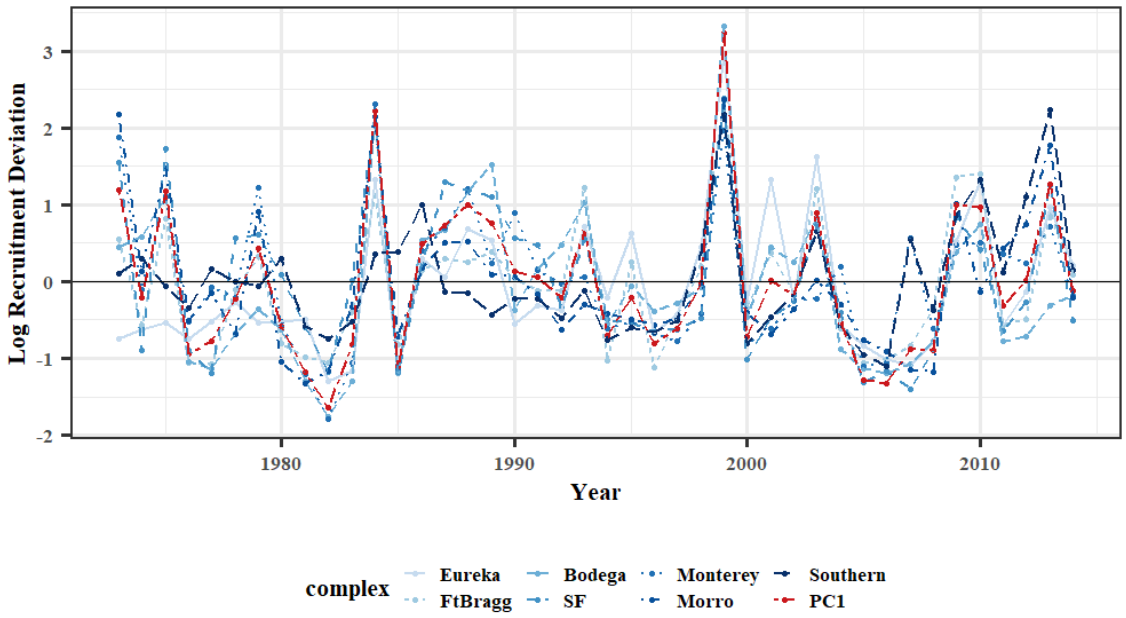

Figure 13: Port-complex-specific log recruitment deviations with PC1 overlaid. PC1 follows the trend in recruitment deviations.

The second principal component ($PC2_{rec}$) captures10.9% of the variability, and resolves a latitudinal gradient across regions, ranging from positive loadings in the north to negative loadings in the south while Southern loaded negligibly positive. PC2 captured subtle differences in recruitment deviations between northern (Eureka, Fort Bragg and Bodega Bay) and southern (San Francisco, Monterey Bay and Morro Bay) port-complexes (Figure 14). Based on loadings, a positive value of PC2 is an indication that recruitment success in northern regions is (relatively) better than in southern regions, and vice versa ($R^2 = 0.878$, $p < 0.001$). Such variability arises in years of moderate recruitment success along the coast. During years marked by strong or weak year-classes,

PC2 was nearly zero, reflecting the lack of spatial differentiation during these extreme events. There appeared to be two mean shifts in PC2 throughout the time series, though these may be superficial. The mean was slightly below zero from 1973 to 1984, indicating that southern port-complexes had relatively stronger recruitment. From 1984 to 1993, there was an increasingly positive trend in PC2, which remained positive from 1993 to 2003. PC2 shifted to a zero or slightly negative mean from 2004 to 2014 (except in 2010), the end of the time series.

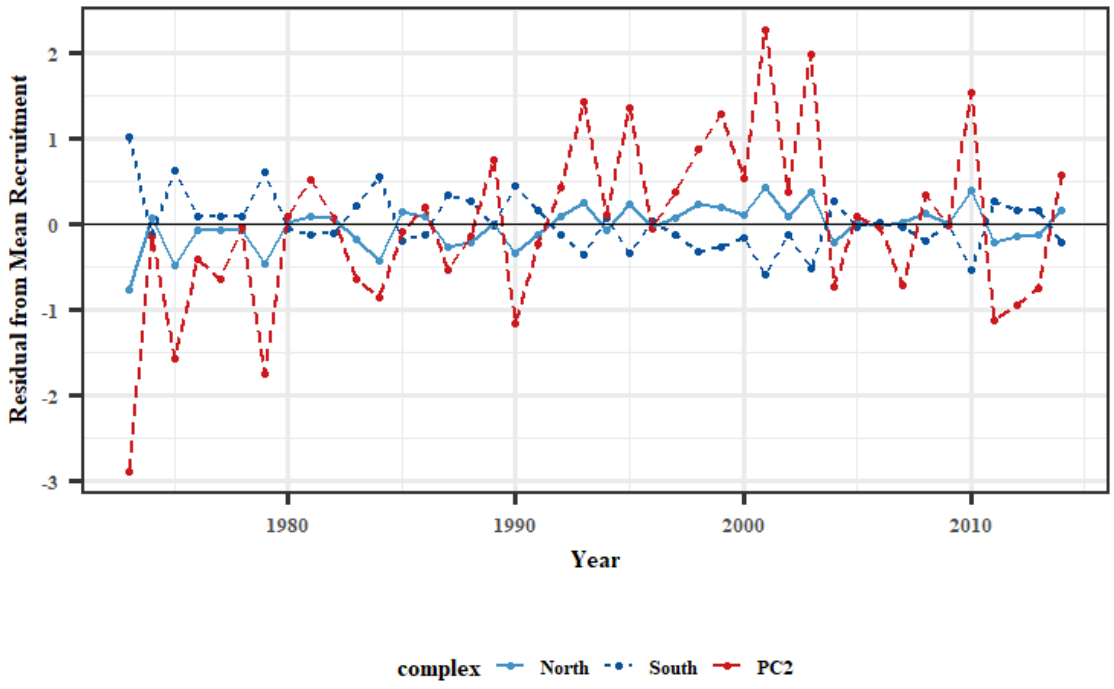

Figure 14: Residuals were calculated for northern (Eureka, Fort Bragg and Bodega) and southern (San Francisco, Monterey Bay, Morro Bay and Southern) port-complexes by first taking the average for these regions. That average was then subtracted from the average across all port-complexes, representing the residuals plotted. PC2 is displayed on the scale of log recruitment deviations.

The third principal component (PC3) captures 7% of the variability and differentiates the core of the population (Bodega Bay and San Francisco) from the boundary port-complexes to the north and south. To reiterate, "core" refers to the area of peak biomass for Chilipepper Rockfish. Southern loads strongly negative onto PC3, Bodega Bay and San Francisco load positively, and all other port-complexes load near zero or slightly negative (Figure 11). Positive PC3 indicates core port-complexes had relatively higher recruitment deviations than the northern and southern ranges of the stock, and vice versa. PC3 follows interannual variation in recruitment deviations through ports until 1985 (Figure 15). Between 1985 and 1998 PC3 captures the difference between central and southern California, though it slowly trends closer to zero as the relative recruitment success across port-complexes becomes more synchronous. The next strong signal occurs between 2008 and 2014 where northern or southern port-complexes consistently outperform the center of the stock, indicated by strongly negative PC3.

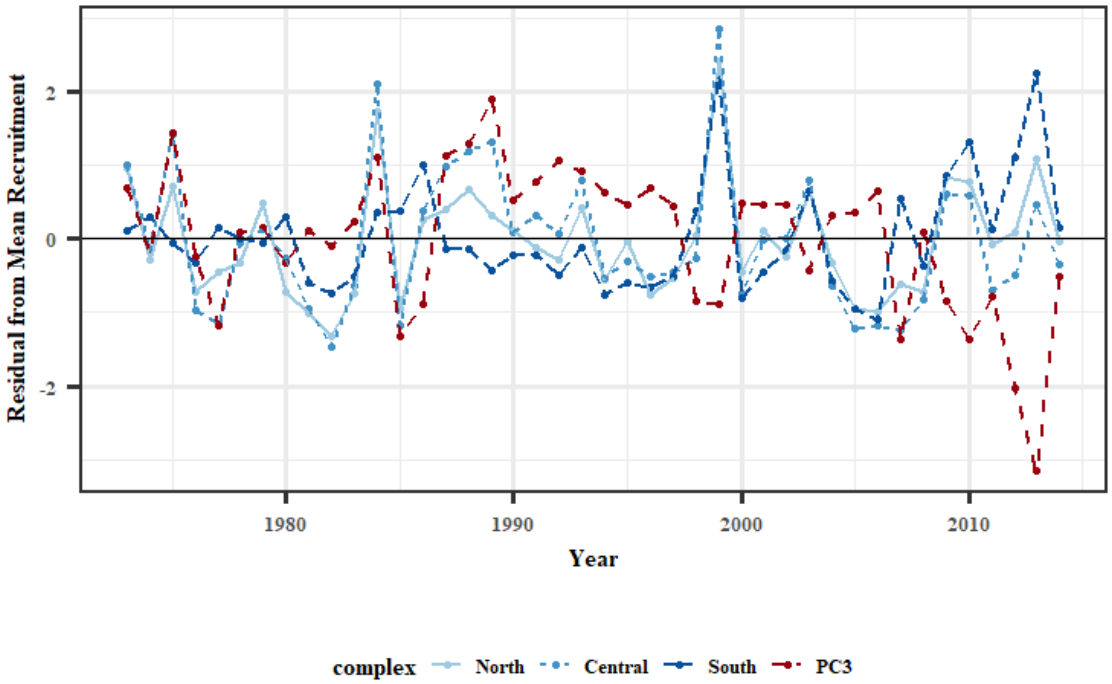

Figure 15: Third principal component (PC3) of port-complex-specific recruitment deviations plotted against the mean recruitment success in northern (Eureka and Fort Bragg), central (Bodega Bay and San Francisco) and southern California (Monterey, Morro Bay and Southern). Northern California loaded near zero onto PC3, central California port-complexes loaded positively and southern California loaded negatively. Southern loaded considerably more negatively onto PC3 than any other port-complex.

Dynamic factor analysis

The best dynamic factor analysis (DFA) model fit a diagonal and equal error matrix with three common trends (Table 4). Each trend represents a time series output of common patterns in recruitment deviations. All port-complexes loaded in the same direction across trends, reflecting that each trend captures some portion of the coherent pattern of observed recruitment variability (Figure 16). This shared variability reflects

structure captured in PC1 (Figure 11; Figure 13). Note that all three trends exhibit peaks corresponding to the 1984 and 1999 year-classes, though the magnitude of peaks varies across trends, further suggesting that variability captured in PC1 is distributed throughout DFA trends (Figure 16).

Table 4: Summary of top three models from dynamic factor analysis. Trends are the number of patterns onto which the dynamic factor analysis model can attribute deviations. N Parameters indicates the number of parameters the model fits, a function of the type of error matrix and number of trends.

Error Matrix	**Trends**	**N Parameters**	**ΔAICc**
Diagonal and Equal	3	19	0.000
Diagonal and unequal	3	25	2.754
Diagonal and unequal	2	20	15.087

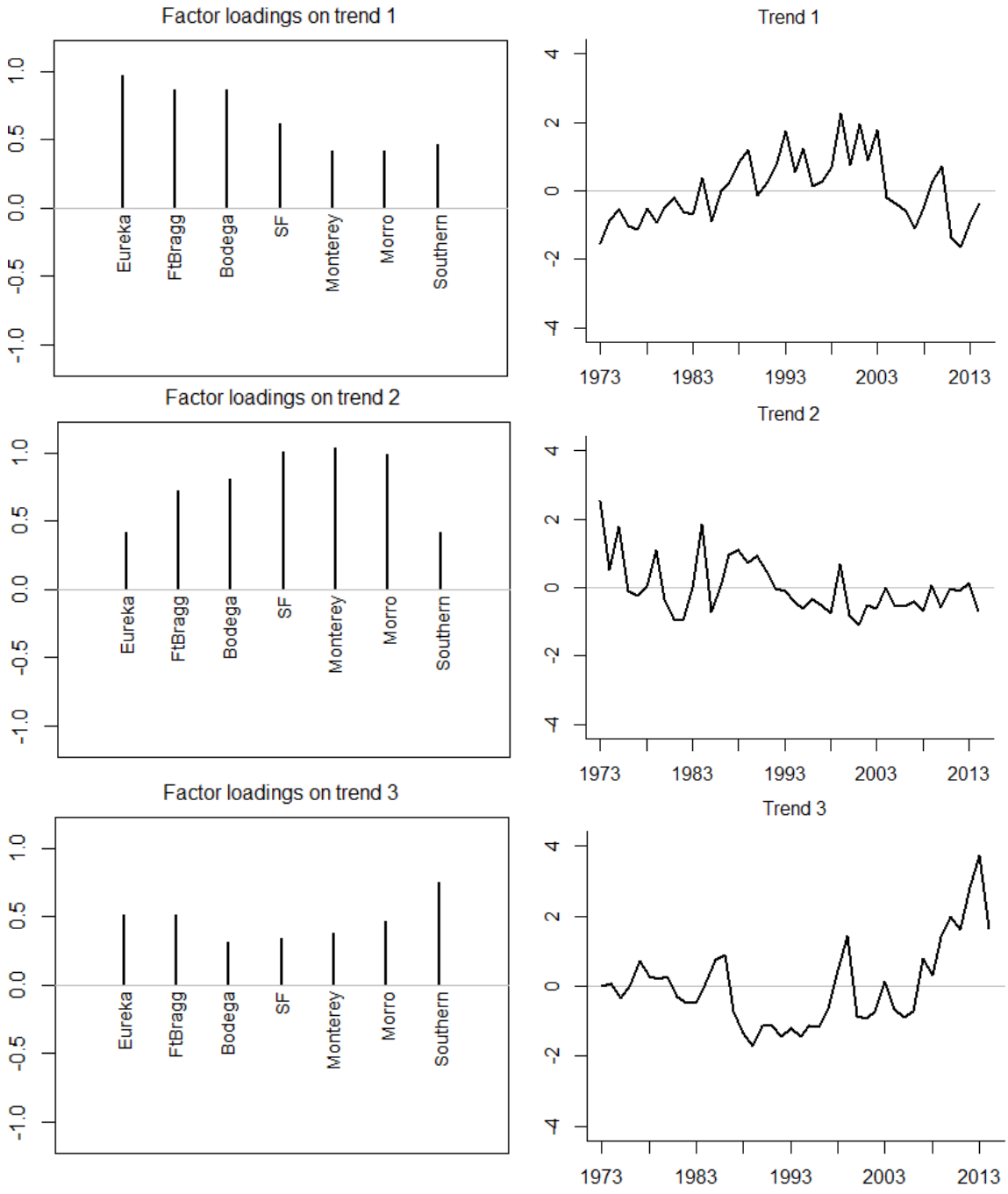

Figure 16: Factor loadings of port-complexes to each of three common trends identified by dynamic factor analysis model fit with three trends and a diagonal and unequal error matrix.

Regional differences are characterized by the strength of loadings onto the three DFA trends. While patterns manifest more strongly in one region over another, each trend is observed in all areas, differentiated by magnitude of loading. Eureka, Fort Bragg and Bodega loaded strongest onto Trend 1, while San Francisco, Monterey Bay and Morro Bay loaded most strongly onto Trend 2. Together these trends are somewhat analogous to PC2, which captured variability in recruitment between northern and southern port-complexes (Figure 11). These trends suggest that recruitment in the southern port-complexes, relative to other areas, were strongest between 1973 and 1985. In contrast, the northern port-complexes, relative to other areas, were strongest between 1985 and 2003.

Southern was the only port-complex to load strongly onto Trend 3. This trend strongly correlated with the inverse of PC3 ($R_2 = 0.078$, $p<0.001$) (Figure 17). This trend suggests that Southern, relative to other port-complexes, exhibited strong recruitment from 2005 to 2014. These modeled trends corroborate results from PCA analysis, and fit the time series of recruitment deviations well, capturing much of the variability in port-complex-specific recruitment deviations (Figure 18).

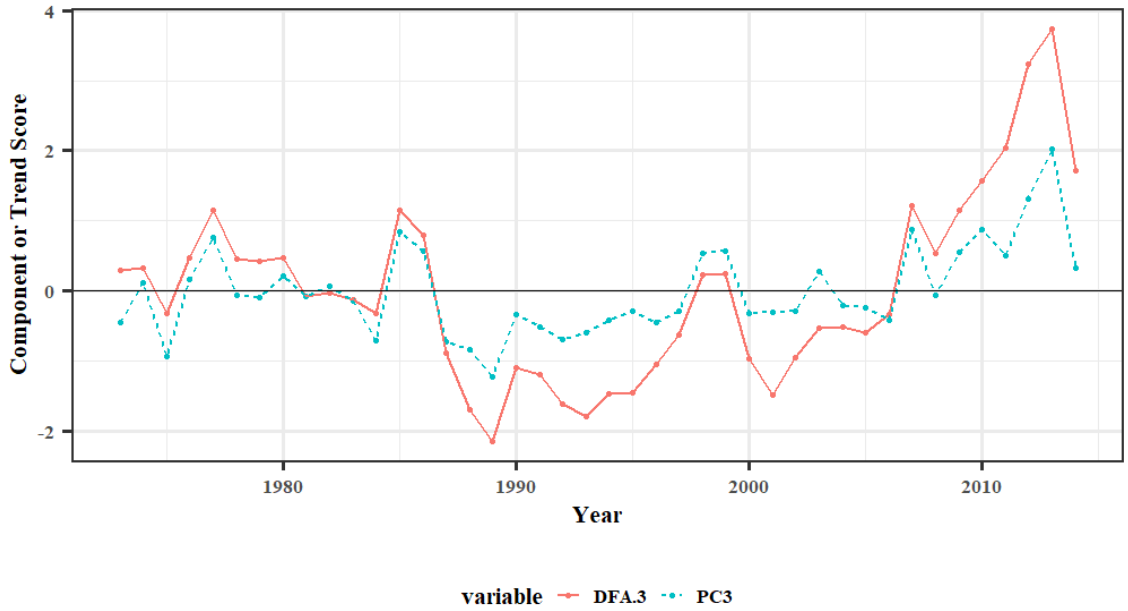

Figure 17: Comparison of the negative of PC3 from principal components analysis, and Trend 3 from dynamic factor analysis ($R^2 = 0.78$, $p < 0.001$).

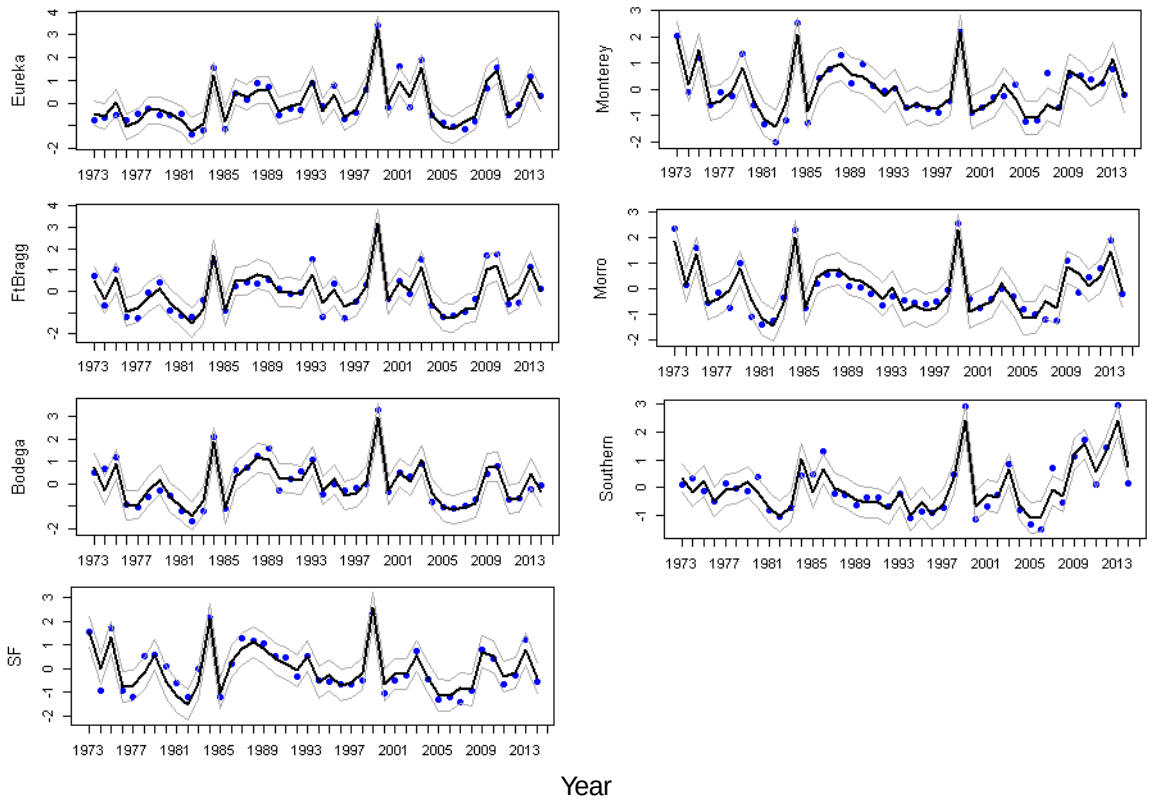

Figure 18: Fits to port-complex-specific recruitment deviations from dynamic factor analysis using three trends and a diagonal and equal error matrix.

OCEANOGRAPHY

Methods

Recruitment-environment models are structured around hypotheses that recruitment of Chilipepper Rockfish is strongly related to survival through the larval (winter) and juvenile (spring) stages, and that survival through these stages is driven (at least in part) by processes affecting productivity and retention. In this chapter, I use basin-scale indices (Pacific Decadal Oscillation [PDO], North Pacific Gyre Oscillation [NPGO], and Multivariate ENSO Index [MEI]) and local oceanographic variables (Sea Level anomaly [SLa], Upwelling Index anomaly [UIa], and Sea Surface Temperature [SST]) as proxies for productivity and retention in individual generalized additive models (GAMs) to predict each port-complex-specific recruitment deviations and coast-scale modes of recruitment variability (PC1, PC2, and PC3).

Linking recruitment variability and oceanographic conditions

Generalized additive models (GAM) (Wood, 2017) were used to identify relationships between metrics of oceanographic conditions and port-complex recruitment time series. I used GAMs because they can accommodate nonlinear relationship between recruitment and oceanographic indices (e.g. parabolic relationships where recruitment exhibits a maximum or minimum value relative to an oceanographic variable) (Cardinale & Arrhenius, 2000). To prevent overfitting of recruitment deviations GAMs were constrained to yield monotonic or unimodal (quasi-parabolic) relationships by limiting

the GAMs to three or fewer knots per covariate. Recruitment deviation-ocean relationships were explored by fitting GAMs that fit region-specific recruitment deviation time series as a function of corresponding regional oceanographic conditions. These oceanographic conditions were explored as (independent) monthly anomalies, as well as time windows of varying length to explore of oceanographic conditions during certain periods of rockfish early life history stages were particularly important in year-class survival. Consequently, we used four general structures of GAMs were used

4) $r_y = ti(cov_{m_1}) + ti(cov_{m_2})$

   e.g. $r_y = ti(UIa_{Jan}) + ti(UIa_{Apr})$,

5) $r_y = ti(mean(cov_{m_1 \ldots m_2}))$

   e.g. $r_y = ti(mean(UIa_{Jan,Feb,Mar,Apr}))$,

6) $r_y = ti(cov_{1m_1}) + ti(cov_{2m_1}) + ti(cov_{1m_2}) + ti(cov_{2m_2})$

   e.g. $r_y = ti(UIa_{Jan}) + ti(SLa_{Jan}) + ti(UIa_{Apr}) + ti(SLa_{Apr})$, and

7) $r_y = ti\left(mean(cov_{1_{m_1 \ldots m_2}})\right) + ti\left(mean(cov_{2_{m_1 \ldots m_2}})\right)$

   e.g. $r_y = ti(mean(UIa_{Jan,Feb,Mar,Apr})) + ti(mean(SLa_{Jan,Feb,Mar,Apri}))$

where r_y is recruitment deviation in year *y*, cov_1 represents any one of the environmental variables examined (e.g., UIa, SLa, SST, PDO, NPGO or MEI), cov_2 represents a separate environmental predictor than cov_1 (examined together within a single GAM), *m* is month (with m_1 and m_2 representing different months within a year), and *ti()* is the GAM smoothing function. Variables were modeled in different ways; when the mean of

the variable between m_1 and m_2 ($mean(var_{m1...m2})$) was used as a predictor, the mean of *var* (e.g., sea level anomaly) was taken across those months. For example, if m_1 is January and m_2 is April, the mean of January, February, March and April was used as the predictor for that model, offering a seasonal average of conditions for that variable. GAMs were fit with a Gaussian error distribution and an identity-link function using the package mgcv in R (Wood, 2017). All combinations of covariates used in the four model structures of GAMs are displayed in Table 5. Note that basin-scale indices (PDO, NPGO and MEI) and in-situ variables (UIa, SLa, and SST) were not examined within the same GAM structures due differences in spatial extent of indices.

Table 5: Summary of combinations of covariates (cov) considered in the analysis (upwelling index anomaly [UIa], sea level anomaly [SLa], sea surface temperature [SST], North Pacific Gyre Oscillation [NPGO], Pacific Decadal Oscillation [PDO], and Multivariate ENSO Index [MEI]). Italicized variables indicate covariates that were only examined as predictors of $PC1_{rec}$, $PC2_{rec}$ and $PC3_{rec}$. All combinations of candidate months, December through June, were examined in GAMs (e.g. mean[Dec-Jan], mean[Dec-Feb]).

Month 1 Cov 1	**Month 1 Cov 2**	**Month 2 Cov 1**	**Month 2 Cov 2**
UIa			
UIa		UIa	
SLa			
SLa		SLa	
SST			
SST		SST	
PDO			
PDO		*PDO*	
NPGO			
NPGO		*NPGO*	
MEI			
MEI		*MEI*	
UIa	SLa		
UIa	SLa	UIa	SLa
UIa	SST		
UIa	SST	UIa	SST
SLa	SST		
SLa	SST	SLa	SST
PDO	*NPGO*		
PDO	*NPGO*	*PDO*	*NPGO*
PDO	*MEI*		
PDO	*MEI*	*PDO*	*MEI*
NPGO	*MEI*		
NPGO	*MEI*	*NPGO*	*MEI*

Collinearity among candidate predictors was examined *a priori* by evaluating whether the variance inflation factor was greater than a threshold of five. Calculations were performed in R using the "vif" function in the package "HH" (Heiberger, 2018). *In situ* variables showed little collinearity (in part because they are expressed as monthly anomalies across years). Basin-scale variables (NPGO, MEI, PDO) frequently showed

strong collinearity between sequential months. Covariates identified as being collinear were not included together in any model. Corrected Akaike's Information Criterion (AICc) was used to rank models, and models within 2 AICc points of the 'best' model were retained to explore shape of relationships between oceanographic predictors and port-complex-specific recruitment deviations. In this exploratory analysis 420 models were run for each port-complex-specific recruitment deviation index.

Recruitment indices (PC1, PC2, and PC3). The four GAM model structures used to predict port-complex-specific recruitment deviations were also used to explore the relationship between oceanographic conditions and spatial modes of recruitment variability described by PC1, PC2 and PC3. Basin-scale indices (PDO, NPGO, and MEI) and *in situ* variables (all combinations of UIa, SLa and SST for each port-complex, discussed later) were used as predictors for these spatial modes of variability. As with port-complex recruitment deviations, models for principal components constructed using oceanographic conditions from paired months or longer-term means to represent conditions affecting survival during the larval and juvenile stage (Figure 1). The best model was selected based on AICc score, though models within 2 AICc points of the 'best' model were retained as strong candidate models. As these models were exploratory, 2,100 total GAMs were explored to link variability each principal component to oceanographic conditions.

Basin-scale indices

I selected three leading modes of low-frequency climate variability in the North Pacific for evaluation as potential predictors of recruitment success: MEI, PDO, and NPGO, all three of which have been shown to capture physical and ecological variability in the CCS (Mantua et al. 1997; Peterson & Schwing, 2003; Di Lorenzo et al. 2008; Bograd et al. 2009; Jacox et al. 2015). The PDO and NPGO are reported as monthly averages and MEI is reported as bimonthly averages. Monthly averages of PDO and NPGO (December [of the year prior to recruitment] through June [of recruitment year]) and bimonthly averages of MEI (December/January to June/July) were used as predictors for PC1 (mode representing coherence in coastwide recruitment deviations), PC2 north-south,, and PC3 (and north-central-south modes of recruitment variability) (Miller & Sydeman, 2004; Koslow et al. 2013; Ralston et al. 2013; Peterson et al. 2014).

In situ observational time series and indices

I selected three oceanographic variables measured at stations throughout California for evaluation as potential correlates of recruitment success: sea level anomaly (SLa), upwelling index anomaly (UIa) and sea surface temperature (SST). Previous work has connected these metrics of oceanographic conditions to indices of early life history survival in a variety of rockfishes (Laidig et al. 2007; Laidig, 2010; Ralston et al. 2013).

Sea level anomalies. Sea levels are recorded by tide gauge stations at San Diego (32°N), Monterey Bay (36°N) and Eureka (41°N) (Table 6). Sea level anomaly (SLa) is calculated from time series of daily average sea level measurements. The time series of

daily SLa is then aggregated into monthly average SLa. Anomalies are seasonally corrected such that a December anomaly is calculated by comparing it to only records from that month. These data were downloaded from (https://tidesandcurrents.noaa.gov/sltrends/sltrends.html).

Table 6: Spatially-explicit oceanographic variables and the latitudes of available data.

Oceanographic variable	**Station latitude**
Upwelling index anomaly (UIa)	33°N, 36°N, 39°N, 42°N
Sea level anomaly (SLa)	32°N, 36°N, 41°N
Sea surface temperature (SST)	32°N, 34°N, 36°N, 38°N, 40°N

Upwelling index anomalies. I obtained monthly averages of anomalies from the Bakun Upwelling Index (UIa) determined by atmospheric pressure fields and inferred geostrophic winds from four stations at Los Angeles (33°N), Monterey Bay (36°N), Fort Bragg (39°N) and Crescent City (42°N) (Table 6). Anomalies are calculated from the "raw" upwelling index to represent seasonally adjusted anomalies, such that a December anomaly in a given year represented the difference from the mean of all December observations in the time series. A positive upwelling index anomaly (UIa) indicates stronger upwelling than the climatological mean, and vice versa. These data were downloaded from http://www.pfeg.noaa.gov/products/las.

Sea surface temperature. Reconstructed SST data from ships, buoys and other platforms is made available by NOAA. SST is reported as daily averages at 2° resolution, and is available at five locations throughout California (32°N, 34°N, 36°N, 38°N, and 40°N) (Table 6), though 34°N was not used to represent SST at any port-complex in this

examination. Daily averages were then averaged over month for use in GAMs. These data were downloaded from https://www1.ncdc.noaa.gov/pub/data/cmb/ersst/v5/netcdf/.

Data preparation. While sea surface temperature wasn't converted into anomalies *a priori*, this was effectively done by standardizing all *in situ* time series before they were used as variables in GAMs. Time series were standardized (z-score was calculated) independently (i.e., not across space) to prevent bias towards variables or months with larger variance. When anomalies were calculated across months, for example mean[Dec-Feb], seasonally adjusted December, January and February upwelling anomalies were averaged across months.

Designation of oceanographic variables

Oceanographic variables were assigned to each port-complex on the basis of proximity within oceanographic region (Figure 2). As an example, although measurements of sea level at 32°N are closer to Morro Bay by distance than those taken at 36°N, conditions at 36°N are expected to more accurately describe conditions at Morro Bay because it is north of Point Conception.

In what follows, names of oceanographic parameters (e.g. UIa_32_Dec) indicate

(1) Variable (eg. UIa);

(2) Latitude of station, if applicable (e.g. 32); and

(3) Month (e.g. Dec)

Table 7: Summary of candidate variables to predict recruitment deviation indices. Variables are labeled first by variable (e.g. UIa is upwelling index anomaly) followed by the station latitude from which the variable was queried (e.g. 41 is 41°N).

Response	**Candidate Variables**
Eureka	UIa_42, SLa_41, SST_40
Fort Bragg	UIa_39, SLa_36, SST_38
Bodega	UIa_39, SLa_36, SST_38
San Francisco	UIa_39, SLa_36, SST_36
Monterey	UIa_36, SLa_36, SST_36
Morro Bay	UIa_36, SLa_36, SST_36
Southern	UIa_33, SLa_32, SST_32
PC1, PC2, PC3	NPGO PDO MEI UIa, SLa, SST (all stations listed above)

Results

Recruitment-oceanography relationships for port-specific recruitment deviations

There was substantial consistency in variables that contributed to top recruitment-oceanography models across port-complexes, though there was evidence for a north-south variability in the timing of ocean conditions that contributed to models (Figure 19). Across port-complexes, upwelling anomaly explained the most deviance in recruitment deviations. Upwelling in April, and frequently mean upwelling between April and June, contributed to top models for port-complexes between Eureka and Monterey Bay. Relationships between upwelling (both April and mean[April-June]) and port-complex recruitment deviations were consistent across port-complexes (Table 8). Recruitment deviations were more positive with higher upwelling in April (Figure 20), though this relationship shifted with mean[April-June] when recruitment deviations were strongest at either weak or strong upwelling.

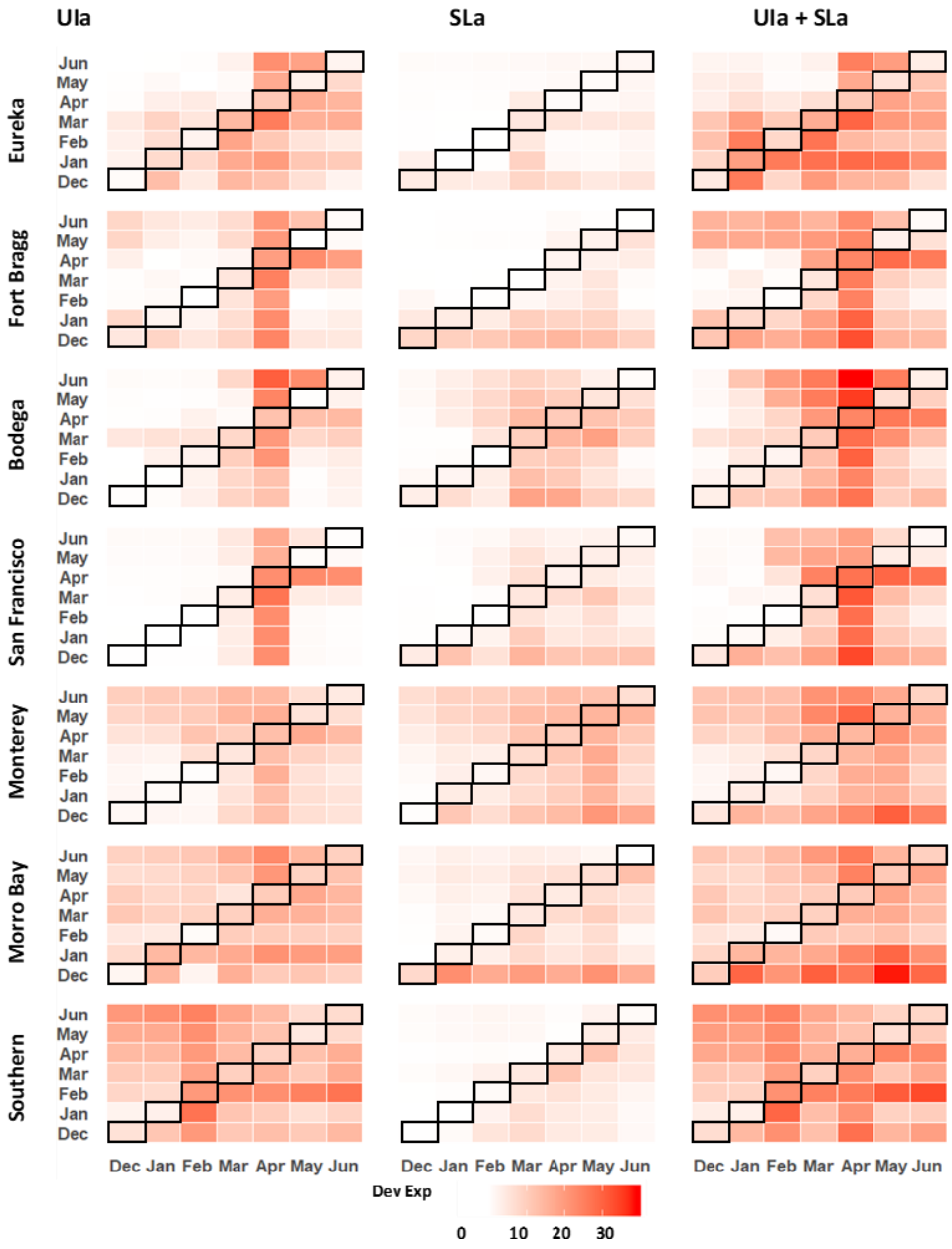

Figure 19: Heat map of deviance explained by GAMs using UIa and SLa to explain port-complex-specific recruitment deviations. The upper triangle represents predictors that were averaged across months (April/ June represents the average of an index across April, May and June), and the lower triangle represents when monthly predictors were used as individual predictors in a single GAM (April/June represents the index during April and June were both used as predictors within an individual GAM). Darker red values indicate higher deviance explained by that GAM. Refer to

Table 7 for interpretation of candidate variable names and location of oceanographic variable station.

Table 8: Decision table of top models (ΔAICc < 2) for port-complex-specific recruitment deviations. The direction of the relationship is shown whether it be positive (+), negative (-) or parabolic in some fashion (∪ or ∩). Refer to

Table 7 for interpretation of candidate variable names and location of oceanographic variable station.

	Port-complex	Model				Dev. Exp.	ΔAICc
1.	Eureka	**UIa**$_{Jan\_Feb}$	**(-)**	**SLa**$_{Jan\_Feb}$	**(-)**	25.8%	0.000
2.	Eureka	**UIa**$_{Apr\_Jun}$	**(∪)**			22.4%	0.677
3.	Eureka	**UIa**$_{Mar}$	**(∩)**	**UIa**$_{Apr}$	**(+)**	25.8%	1.799
1.	Fort Bragg	**UIa**$_{Apr\_Jun}$	**(∪)**			21.0%	0.000
2.	Fort Bragg	**UIa**$_{Apr\_May}$	**(∪)**			20.3%	0.354
3.	Fort Bragg	**UIa**$_{Apr}$	**(+)**			19.7%	0.458
4.	Fort Bragg	**UIa**$_{Jan}$	**(-)**	**UIa**$_{Apr}$	**(+)**	23.0%	1.182
5.	Fort Bragg	**UIa**$_{Apr}$	**(+)**	**UIa**$_{May}$	**(-)**	22.9%	1.43
6.	Fort Bragg	**UIa**$_{Mar}$	**(-)**	**UIa**$_{Apr}$	**(+)**	25.1%	1.45
7.	Fort Bragg	**UIa**$_{Apr\_May}$	**(∪)**	**SLa**$_{Apr\_May}$	**(-)**	23.8%	1.98
1.	Bodega	**UIa**$_{Apr\_Jun}$	**(∪)**	**SLa**$_{Apr\_Jun}$	**(-)**	39.2%	0.000
2.	Bodega	**UIa**$_{Apr\_Jun}$	**(∪)**			30.8%	1.077
1.	San Francisco	**UIa**$_{Apr}$	**(+)**			22.7%	0.000
2.	San Francisco	**UIa**$_{Mar}$	**(∩)**	**UIa**$_{Apr}$	**(+)**	27.2%	0.546
3.	San Francisco	**UIa**$_{Apr}$	**(+)**	**SLa**$_{Apr}$	**(∩)**	27.6%	1.512
1.	Monterey	**UIa**$_{Apr\_May}$	**(∪)**	**SLa**$_{Apr\_May}$	**(-)**	29.5%	0.000
2.	Monterey	**SST**$_{Jun}$	**(-)**			17.3%	0.666
3.	Monterey	**UIa**$_{Apr\_May}$	**(∪)**			16.2%	0.687
4.	Monterey	**UIa**$_{Apr\_Jun}$	**(∪)**	**SLa**$_{Apr\_Jun}$	**(-)**	23.4%	1.078
5.	Monterey	**SLa**$_{Dec}$	**(+)**	**SLa**$_{May}$	**(-)**	21.0%	1.17
6.	Monterey	**SLa**$_{May}$	**(-)**			15.1%	1.271
7.	Monterey	**UIa**$_{Mar\_May}$	**(+)**			15.0%	1.315
8.	Monterey	**SST**$_{May\_Jun}$	**(-)**			14.6%	1.513
9.	Monterey	**UIa**$_{Mar\_Jun}$	**(+)**			14.5%	1.562
10.	Monterey	**SST**$_{Mar}$	**(∩)**	**SST**$_{Jun}$	**(-)**	24.0%	1.797
11.	Monterey	**SLa**$_{Apr\_May}$	**(-)**			13.9%	1.84
12.	Monterey	**SLa**$_{Apr\_Jun}$	**(-)**			13.6%	1.997
1.	Morro Bay	**UIa**$_{Apr\_Jun}$	**(∪)**			23.4%	0.000
2.	Morro Bay	**UIa**$_{Apr\_May}$	**(∪)**			20.9%	0.797
3.	Morro Bay	**UIa**$_{Dec}$ **UIa**$_{May}$	**(+)** **(+)**	**SLa**$_{Dec}$ **SLa**$_{May}$	**(+)** **(∩)**	38.4%	0.889

	Port-complex	Model				Dev. Exp.	ΔAICc
1.	Southern	**UIa_{Feb_Jun}**	**(+)**			24.9%	0.000
2.	Southern	**UIa_{Feb}**	**(+)**	**UIa_{Jun}**	**(+)**	27.4%	1.042
3.	Southern	**UIa_{Feb_May}**	**(+)**			22.3%	1.455

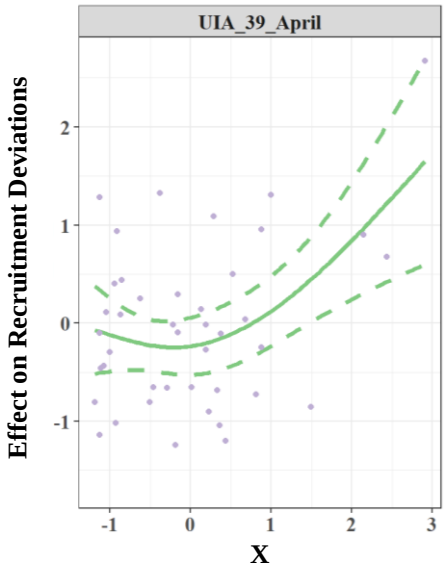

Figure 20: Smoothing function for relationship between upwelling in April and recruitment deviations at Fort Bragg. This relationship is representative of relationships between upwelling in April and all other port-complexes. Dashed lines indicate 95% confidence intervals.

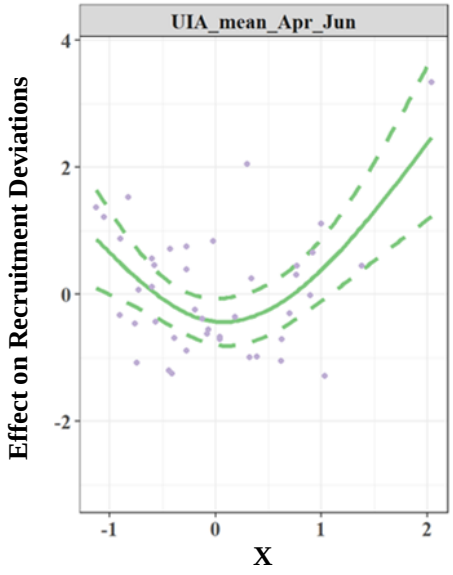

Figure 21: Smoothing function for relationship between mean[April-June] upwelling and recruitment deviations at Fort Bragg. This relationship is representative of relationships between upwelling in mean[April-June] and all other port-complexes. Dashed lines indicate 95% confidence intervals.

Morro Bay and Southern recruitment deviations were explained by upwelling throughout seasons, though winter upwelling, particularly February, described more deviance than at more northern port-complexes (Figure 19). Winter upwelling was consistently positively related to both Southern and Morro Bay recruitment deviations (Table 8; Figure 22), though relationships between Morro Bay recruitment deviations and mean[April-June] upwelling also mimic those of northern port-complexes.

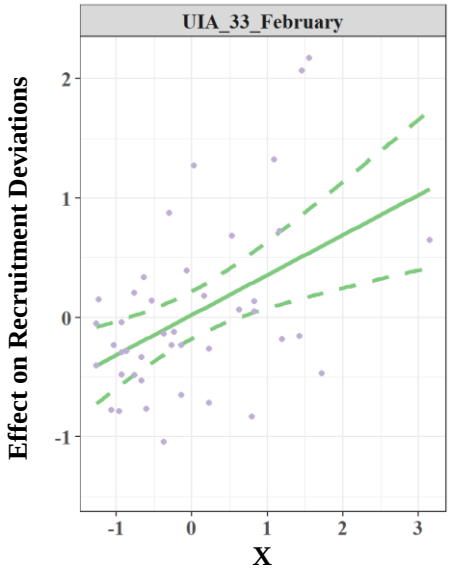

Figure 22: Smoothing function for relationship between February upwelling and recruitment deviations at Southern. This relationship is representative of relationships between upwelling in other winter months and Morro Bay. Dashed lines indicate 95% confidence intervals.

While sea level explains less deviance than upwelling (Figure 19), December sea level had a moderately positive relationship with all port-complexes (Figure 23), and explained more deviance than any other monthly or seasonal sea level. With the combination of upwelling and sea level, more deviance is explained, but there is less consistency in timing across port-complexes (Figure 19). Again, models incorporating April and December generally explained more deviance, though a greater variety of monthly and seasonal averages also explained some deviance. Sea surface temperature was only included in models for Monterey Bay (Table 8), where higher temperatures in March and June generally had a negative relationship with Monterey Bay recruitment deviations.

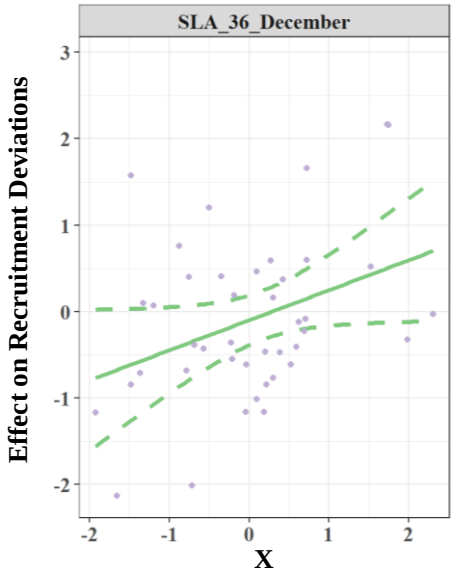

Figure 23: Smoothing function for relationship between December sea level and recruitment deviations at Morro Bay. This relationship is representative of relationships between December sea level and recruitment deviations at other port-complexes. Dashed lines indicate 95% confidence intervals.

Due to similarity across model fits and port-complexes, only those for Bodega Bay are explored here for the sake of brevity, though all other model fits can be found in Appendix E (Figure 24). Recruitment-ocean models across all port-complexes (except Southern) were driven by explaining the large recruitment deviation of the 1999 year-class. While comparably strong, the 1984 year-class was only captured at Morro Bay in a model using December and May upwelling and sea level, though this model did not fully capture the magnitude of the 1999 year-class. Throughout the rest of the time series, port-complex-specific models had minimal precision in estimating moderate interannual recruitment deviations. As recruitment-ocean models captured strong and weak year-classes but missed moderate interannual recruitment deviations, 1999, the year with

highest leverage, was removed and the models were re-examined to see if other variables captured moderate year-classes. While most models remained stable, and no model emerged with particularly better ability to predict moderate year-classes, sea level during winter did emerge as a more consequential variable. Winter sea level, which was initially noted in many port-complex-specific models, explained what little deviation was able to be captured in moderate recruitment years. In consequence, none of the models are robust at explaining recruitment deviations throughout the time series, though consistency between variables across port-complexes and reliability in predicting the strong 1999 year-class suggests these variables may also explain variability in coastwide recruitment deviation trends (PC1, PC2 and PC3).

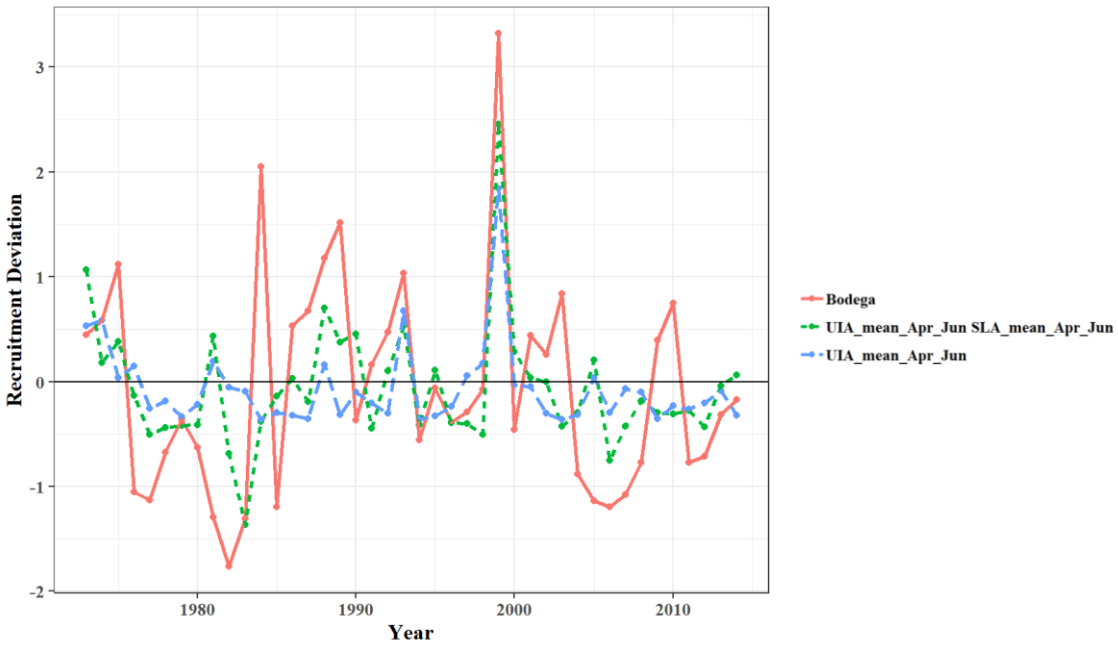

Figure 24: Model fits for two GAMs used to predict recruitment deviations at Bodega Bay. Model fits for all port-complexes can be found in Appendix E.

PC1rec

Models of the effect of oceanographic predictors on PC1 (coastwide coherence in recruitment deviations) strongly resembled those observed in port-complex-specific models (Figure 19). Here, I focus on models using upwelling anomaly at 42°N and sea level anomaly at 41°N because these conditions explained more deviance than those collected at any other station throughout the coast (though trends in timing and shape of relationships remained consistent across all stations) (Figure 25). Again, upwelling anomaly explained more deviance than sea level, and was most important later in the season between March and June, though April explained the most deviance. Sea level didn't capture as much deviance in PC1, although it did help explain some deviance when modeled in conjunction with late winter upwelling conditions.

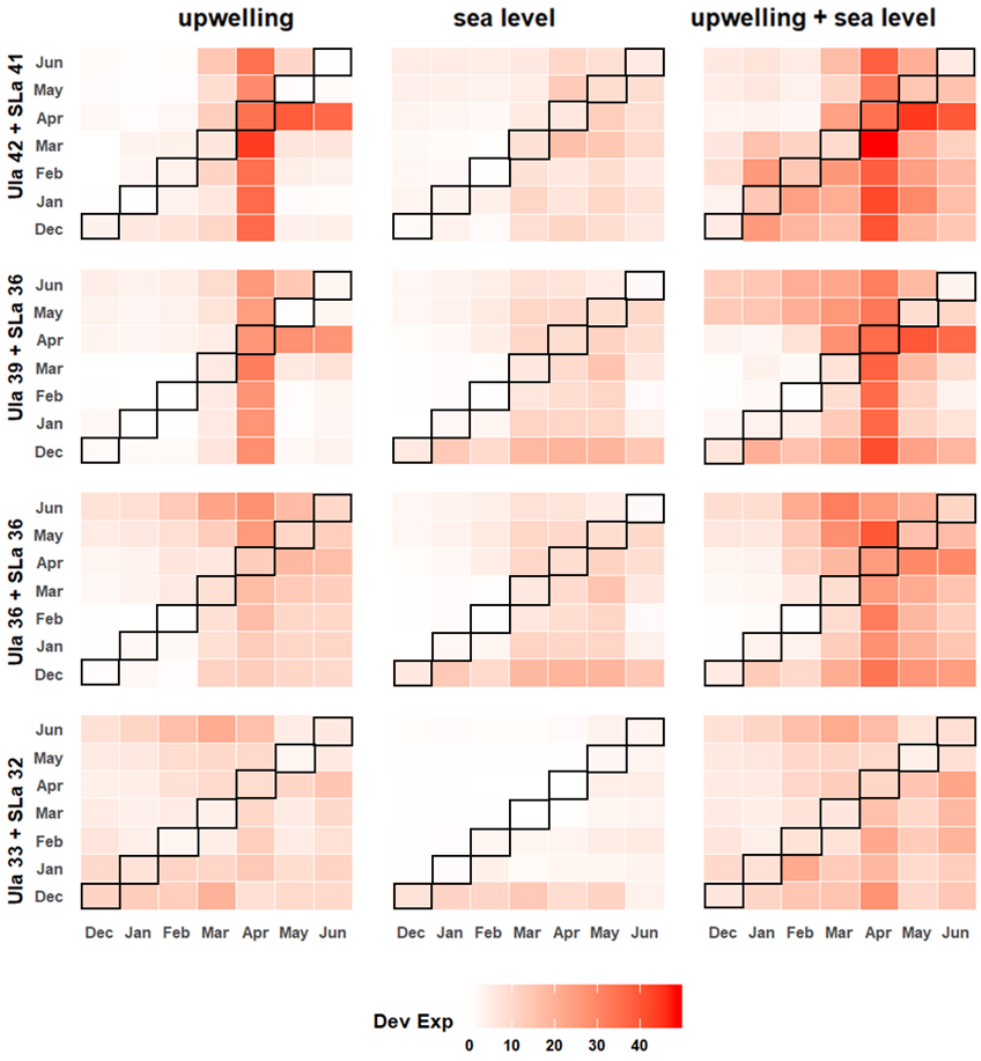

Figure 25: Heat map of deviance explained by GAMs using UIa and SLa to explain coastwide coherence in recruitment deviations, PC1. The upper triangle represents predictors that were averaged across months (April/ June represents the average of an index across April, May and June), and the lower triangle represents when monthly predictors were used as individual predictors in a single GAM (April/June represents the index during April and June were both used as predictors within an individual GAM). Darker red values indicate higher deviance explained by that GAM. Refer to

Table 7 for interpretation of candidate variable names and location of oceanographic variable station.

Coastwide coherence in recruitment deviations, captured by PC1, was best explained by upwelling anomalies in March, April and May (Table 9). This corroborates results from port-complex-specific models, which frequently included upwelling during April or mean[April-June]. PC1 was highest with strong upwelling anomalies in April (Figure 26), though high upwelling anomalies in March and May were associated with more negative PC1 values. These models capture the magnitude of the 1999 year-class, while again missing a strong year-class in 1984, and poorly predicting moderate interannual shifts in PC1 (Figure 27). All models were also examined with removal of the high-leverage 1999 year-class, and these two models still out-ranked all others. In essence, even without this high-leverage year, no model is able to capture moderate interannual changes in coherent coastwide recruitment deviations. This suggests that these oceanographic conditions may not be suited to capture moderate interannual shifts in coastwide recruitment deviations over the full course of the recruitment time series.

Table 9: Decision table of top models (ΔAICc < 2) for PC1 ($PC1_{rec}$) with the direction of the relationship whether it be positive (+), negative (-) or parabolic in some fashion (∪ or ∩). Refer to Table 10 for interpretation of candidate variable names.

Model					**Dev. Exp.**	**AICc**	**ΔAICc**
1.	$UIa_{\_42\_Mar}$	**(∩)**	**$UIa_{\_42\_Apr}$**	**(+)**	44.2%	167.777	0.000
2.	$UIa_{\_42\_Apr}$	**(+)**	**$UIa_{\_42\_May}$**	**(-)**	39.0%	169.644	1.867

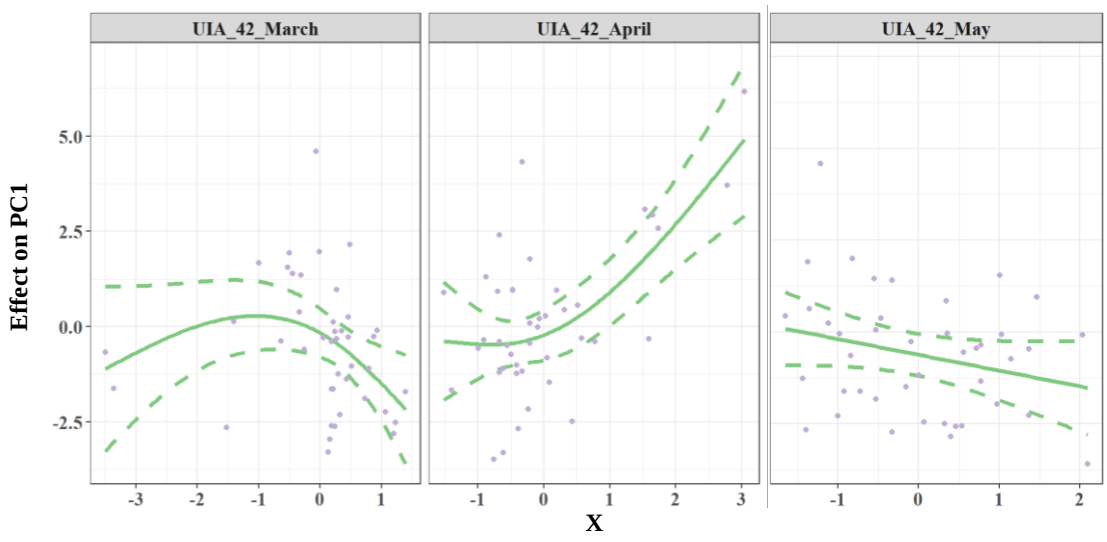

Figure 26: Smoothing function for relationship between upwelling at 42°N in March, April and May from three separate GAMs used to predict PC1, coastwide recruitment signal. Dashed lines indicate 95% confidence intervals.

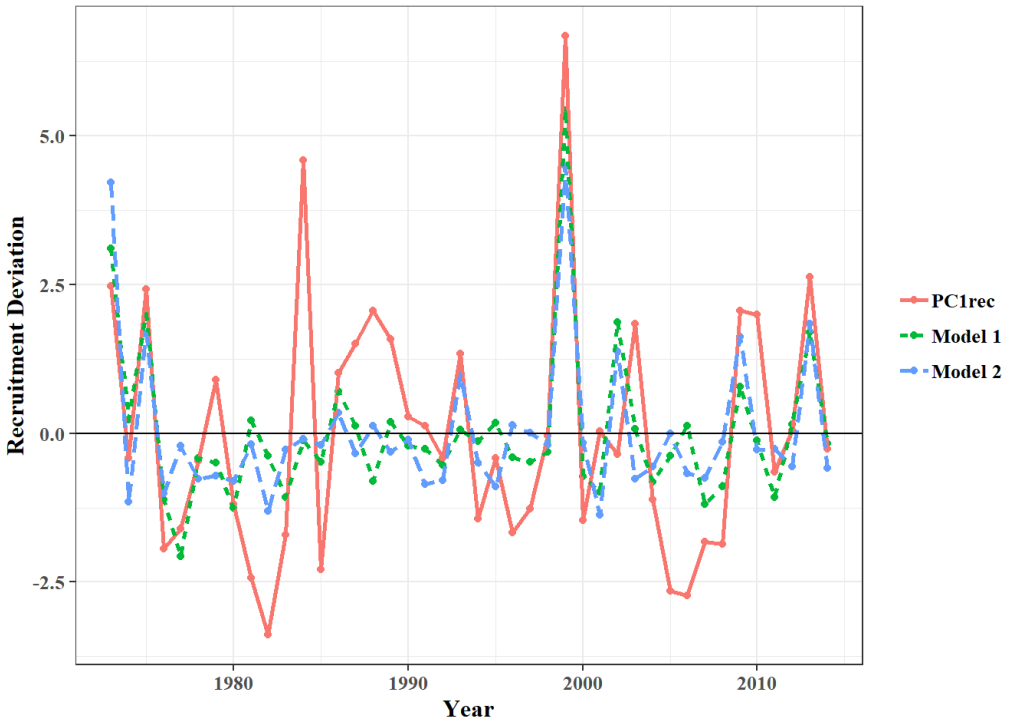

Figure 27: Model fits for $PC1_{rec}$ predicted by UIa at 42°N during March and April in Model 1 and April and May in Model 2.

PC2rec

The Pacific Decadal Oscillation and the North Pacific Gyre Oscillation explain the most deviance in PC2, which captured variability between northern (Eureka, Fort Bragg and Bodega Bay) and southern (San Francisco, Monterey Bay and Morro Bay) port-complexes (Figure 28). PDO did not have strong seasonal signals, though NPGO explained more deviance between winter and Spring. In combination, PDO and NPGO frequently explained more deviance than NPGO alone.

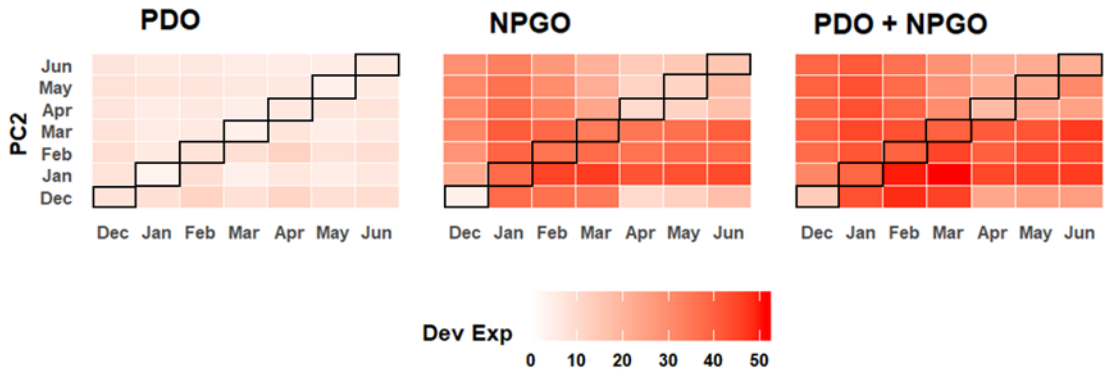

Figure 28: Heat map of deviance explained by GAMs using PDO and NPGO to explain variability between northern (Eureka, Fort Bragg and Bodega) and southern (San Francisco, Monterey Bay and Morro Bay) port-complexes, PC2. The upper triangle represents predictors that were averaged across months (April/ June represents the average of an index across April, May and June), and the lower triangle represents when monthly predictors were used as individual predictors in a single GAM (April/June represents the index during April and June were both used as predictors within an individual GAM). Darker red values indicate higher deviance explained by that GAM. Refer to

Table 7 for interpretation of candidate variable names and location of oceanographic variable station.

A variety of models fall within 2 AICc points of the best-ranked model for PC2, and NPGO is included in each (Table 10). Mean[Jan-Mar] NPGO was included most frequently in models, though many combinations of months in this range capture similar deviance. Recall that when PC2 is positive, northern port-complexes have relatively better recruitment than southern, and vice versa (Figure 11). Therefore, recruitment deviations were relatively better at southern port-complexes when mean[Jan-Mar] NPGO was moderate (Figure 29). This predictor captures varying relationships between January and March NPGO and PC2. When NPGO was strong in January, northern port-complexes had relatively stronger recruitment, while strong NPGO in March was associated with stronger recruitment deviations at southern port-complexes. Average NPGO across January and March captures these relationships in a parsimonious manner, while capturing 40.8% of the variability in PC2.

Table 10: Decision table of top models (ΔAICc < 2) for PC2 ($PC2_{rec}$) with the direction of the relationship whether it be positive (+), negative (-) or parabolic in some fashion (∪ or ∩). Refer to Table 10 for interpretation of candidate variable names.

Model					Dev. Exp.	AICc	ΔAICc
1.	**$PDO_{\_Jan\_Mar}$**	**(+)**	**$NPGO_{\_Jan\_Mar}$**	**(∪)**	44.6%	85.569	0.000
2.	**$NPGO_{\_Jan}$**	**(∪)**	**$NPGO_{\_Mar}$**	**(∪)**	46.4%	85.57	0.001
3.	**$NPGO_{\_Jan\_Mar}$**	**(∪)**			40.8%	85.764	0.195
4.	**$PDO_{\_Jan\_Apr}$**	**(+)**	**$NPGO_{\_Jan\_Apr}$**	**(∪)**	43.2%	86.545	0.976
5.	**$PDO_{\_Feb\_Mar}$**	**(+)**	**$NPGO_{\_Feb\_Mar}$**	**(∪)**	43.0%	86.748	1.179
6.	**$PDO_{\_Jan\_May}$**	**(+)**	**$NPGO_{\_Jan\_May}$**	**(∪)**	42.9%	86.787	1.218
7.	**$NPGO_{\_Jan\_Feb}$**	**(∪)**			39.0%	87.012	1.443
8.	**$PDO_{\_Jan\_Feb}$**	**(+)**	**$NPGO_{\_Jan\_Feb}$**	**(∪)**	42.0%	87.449	1.88
9.	**$NPGO_{\_Feb\_Mar}$**	**(∪)**			38.3%	87.475	1.906

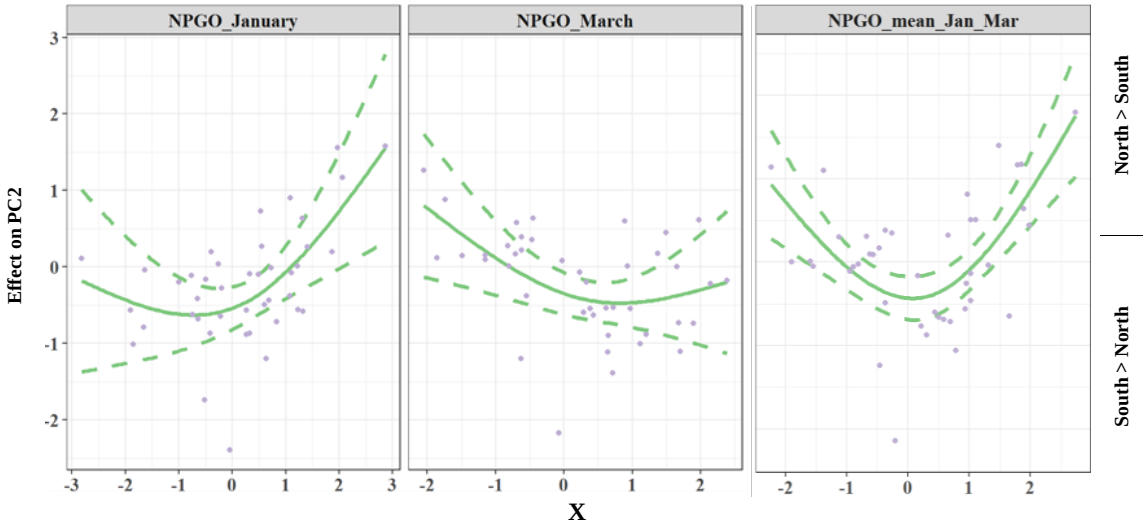

Figure 29: Smoothing functions of variables used to predict spatially-explicit recruitment deviations between northern (Eureka, Fort Bragg, and Bodega Bay) and southern (San Francisco, Monterey Bay and Morro Bay) port-complexes. Dashed lines indicate 95% confidence intervals.

All models captured approximately the same variability in PC2, each predicting mean shifts that were previously noted in PC2 (Figure 14; Figure 30). Models predict the zero-value of PC2 between 1975 and 1990 when northern and southern port-complex recruitment deviations were relatively equal. The models followed the positive mean shift in about 1991, which remained above zero until 2005. Finally, the models captured the negative mean shift through the end of the time series.

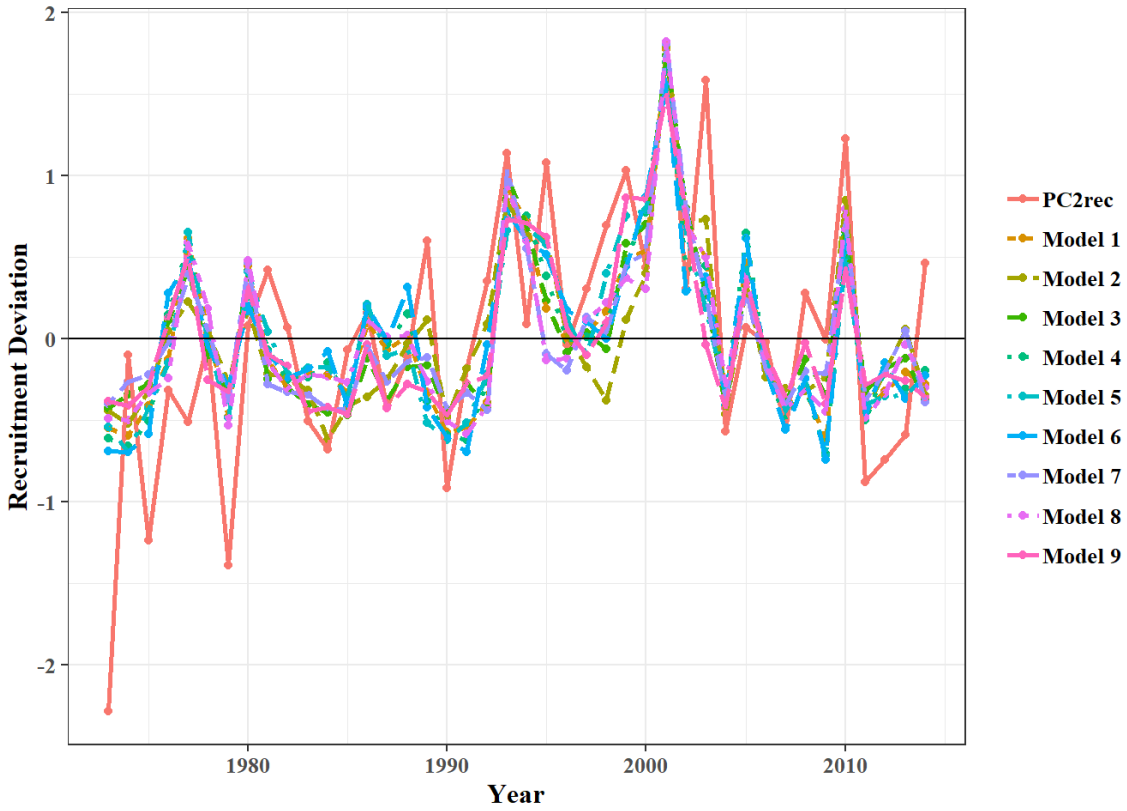

Figure 30: Model fits for $PC2_{rec}$ predicted by eleven models using a combination of NPGO and PDO across months and seasons. Refer to Table 10 for which predictors contribute to each model.

$PC3_{rec}$

PC3 captured the difference in recruitment deviations between core (San Francisco and Bodega Bay) and boundary (Eureka, Fort Bragg, Monterey Bay, Morro Bay and Southern) port-complexes. Upwelling anomaly at 39°N and sea level at 36°N explained more deviance in PC3 than any other station or oceanographic variable, including basin-scale indices (NPGO, PDO and MEI). Upwelling during February explained more deviance than any other month, though the deviance explained was

maximized by mean[Dec-Feb] (Figure 31). Sea level exhibited similar seasonality in deviance explained as upwelling, though it didn't explain as much deviance in PC3. In combination, sea level did not contribute much more deviance explained than upwelling alone, which was confirmed by ΔAICc (Table 11). No other model for PC3 fell within 2 AICc points of the best-ranked model, which included mean[Dec-Feb] upwelling anomaly as its only predictor.

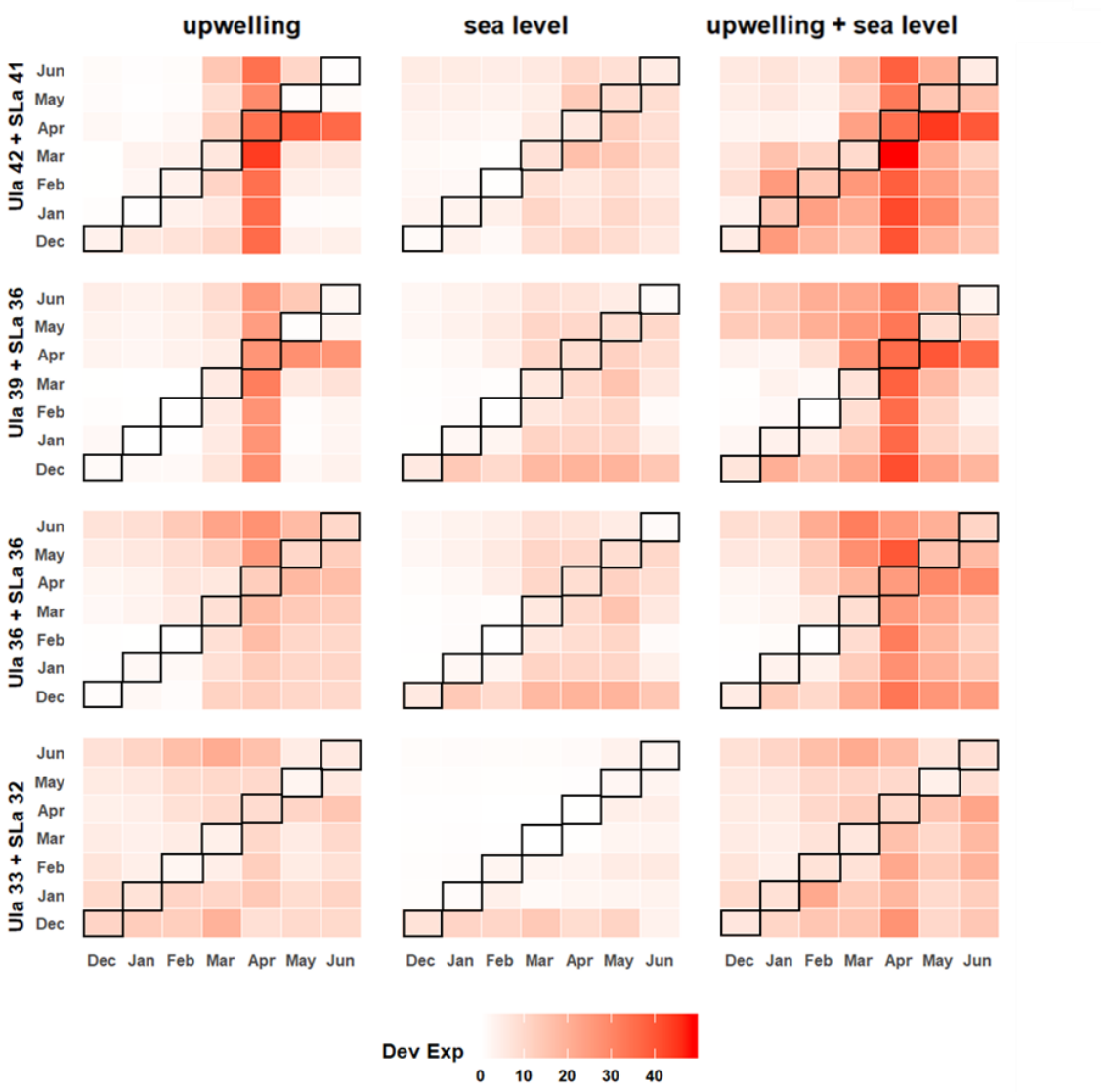

Figure 31: Heat map of deviance explained by GAMs using UIa and SLa to explain variability between core (Bodega Bay and San Francisco) and boundary (Eureka, Fort Bragg, Monterey Bay, Morro Bay and Southern) port-complexes, PC3. The upper triangle represents predictors that were averaged across months (April/ June represents the average of an index across April, May and June), and the lower triangle represents when monthly predictors were used as individual predictors in a single GAM (April/June represents the index during April and June were both used as predictors within an individual GAM). Darker red values indicate higher deviance explained by that GAM. Refer to

Table 7 for interpretation of candidate variable names and location of oceanographic variable station.

Table 11: Decision table of top models (ΔAICc < 2) for PC3 ($PC3_{rec}$) with the direction of the relationship whether it be positive (+), negative (-) or parabolic in some fashion (∪ or ∩). Refer to Table 10 for interpretation of candidate variable names.

Model	**Dev. Exp.**	**AICc**	**ΔAICc**
$UIa_{\_39\_Dec\_Feb}$ (∩)	38.6%	69.882	0.000

Recall that when PC3 is positive, core port-complexes have relatively stronger recruitment than boundary port-complexes, and vice-versa (Figure 11). When mean[Dec-Feb] upwelling anomaly was around zero, core port-complexes had relatively stronger recruitment, while boundary port-complexes outperformed core port-complexes when upwelling anomaly was higher or lower than average (Figure 32). This model poorly-resolved the period between 1988 and 1998 when PC3 was consistently above zero, though it did capture interannual shifts in PC3 from 2000 through 2014 (Figure 33).

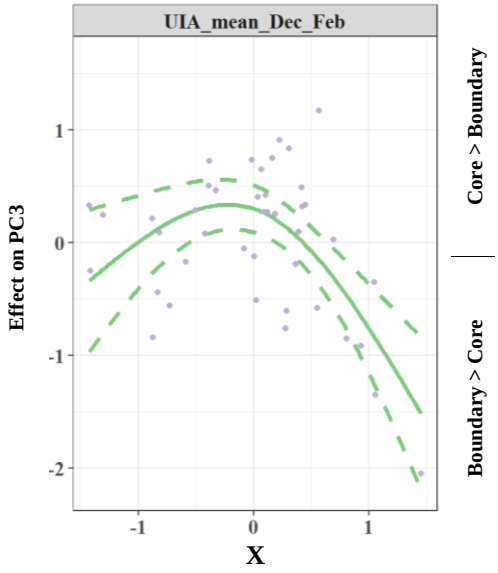

Figure 32: Smoothing function of variables used to explain variability between core (Bodega Bay and San Francisco) and boundary (Eureka, Fort Bragg, Monterey Bay, Morro Bay and Southern) port-complexes, PC3. Dashed lines indicate 95% confidence intervals.

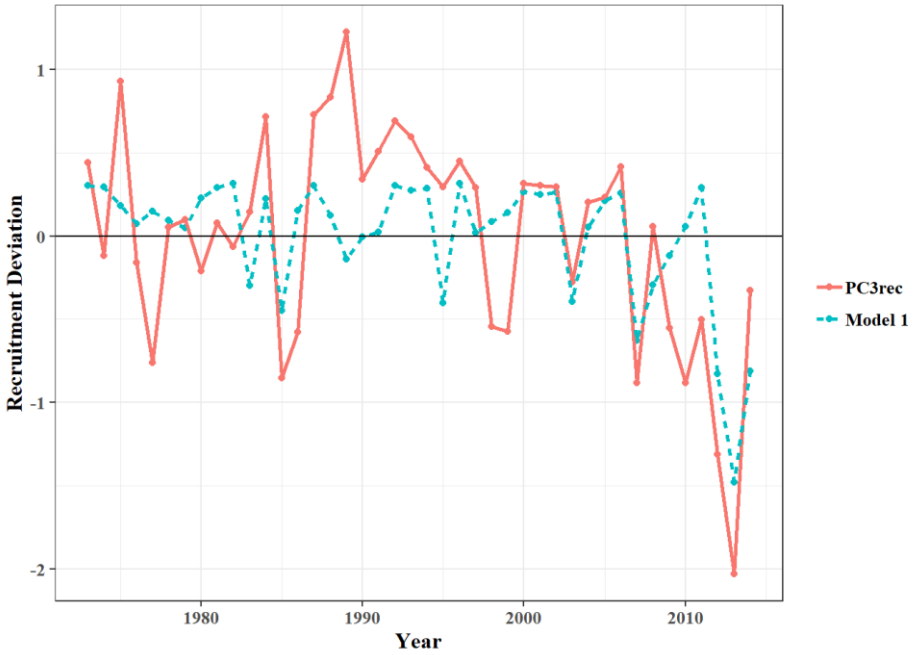

Figure 33: Model fits for $PC3_{rec}$ predicted by mean December to February upwelling anomaly at 39°N. Refer to Table 11 for model covariates.

DISCUSSION

This work demonstrates strong evidence for interannual coastwide coherence in recruitment deviations of Chilipepper Rockfish, thereby confirming patterns first identified by Field and Ralston (2005). Strong and weak year-classes manifested coastwide, while spatial variability and structure in recruitment deviations emerged during years of less extreme recruitment success or failure. Subsequent analysis of potential environmental drivers of recruitment variability suggest that upwelling and sea level might serve as useful indices for a suite of conditions (e.g., productivity, retention over the shelf, and alongshore transport) that influence survival of larval and juvenile rockfish and thus drive variability in recruitment success. In the following sections, I consider several aspects of this study and relevant caveats, then return to the broader implications of these results for integrating ecosystem conditions with stock assessments.

Port-complex-specific Assessments

Our assessment based on data aggregated along the California coast agreed well with the 2015 Chilipepper Rockfish stock assessment, which spans the continental U.S. West Coast (Field et al. 2015). This validated the model structure subsequently implemented in the development of port-complex-specific stock assessment models. Port-complex-specific stock assessment models were strongly coherent with one another, though there was a considerable amount of uncertainty at the beginning of the time series and during weak or moderate year-classes (Appendix C). Strong and weak year-classes

were shared coastwide, while gradients in recruitment success emerged at smaller-scales during years of moderate recruitment success. Of the seven port-complexes, Eureka (North of Cape Mendocino) and Southern (South of Point Conception) recruitment deviations were the most dissimilar from other port-complexes, suggesting that oceanographic structure associated with Cape Mendocino and Point Conception might structure such variability.

The first three principal components demonstrated both considerable spatial coherence and consistent spatial patterns across port-complexes that largely align with topography and oceanographic characteristics of the California coastline, in addition to the structure of the stock (majority of biomass is between Point Conception and Cape Mendocino). PC1 captured coherence in recruitment deviations across port-complexes, while PC2 and PC3 represented out-of-phase fluctuations, suggestive of north-south and core-boundary spatial patterns, respectively, around the coherent coastwide signal. The spatial extent of these models and recruitment indices suggest the potential to characterize interannual variation in recruitment success through space, which could contribute to recent advancements toward spatial stock assessments (Thorson & Wetzel, 2013).

Linking Recruitment Variability and Oceanographic Conditions

Generalized additive models (GAMs) were fit using recruitment deviation outputs from port-complex-specific stock assessment models as response variables. In doing so, I treat recruitment deviation outputs as true values of recruitment deviations, rather than

model output estimates with error (Appendix C, Brooks & Deroba, 2015). I did not explore methods of incorporating this error in this study. Measures of uncertainty in recruitment estimates could be used to frame a sensitivity analysis for evaluating whether environment-recruitment relationships are robust when accounting for that uncertainty.

Recruitment-environment models were developed with the underlying hypothesis that processes affecting productivity and retention, at least in part, impact survival during the larval (winter) and juvenile (spring) stages and thereby influence recruitment success of Chilipepper Rockfish. The models presented here do not capture all of the variables or spatio-temporal ranges that may impact recruitment success. In particular, ecological conditions (e.g., characteristics of prey or predator fields that larval and juvenile rockfish encounter) are absent from this analysis. Instead, models linking oceanographic conditions and recruitment deviation indices are exploratory in nature, and intended to support speculation regarding mechanistic drivers of these relationships. As such, this work is developed as a guide ongoing investigation of drivers of recruitment success in Chilipepper Rockfish and similar stocks.

Models relating port-complex recruitment deviations to oceanographic conditions at local (port-complex) scales commonly shared predictors. This is consistent with the strong correlation in recruitment deviations across port-complexes, coherence in oceanographic conditions throughout the California Current System (CCS) (Checkley & Barth, 2009), and an expectation of common phenology in Chilipepper Rockfish along the coast of California (Field et al. 2015). Across port-complexes, upwelling anomaly

explained the most deviance, corroborating conclusions drawn by Caselle et al. 2010 (though they focused on rockfish in southern California), with evidence for a spatial pattern in the timing of importance. A variety of monthly and seasonal averages explained substantial deviance at Morro Bay and Southern, though winter upwelling was more significant than at northern port-complexes. Furthermore, the shape of curves varied for winter upwelling based on location of port-complex. Between Eureka and San Francisco, winter upwelling was negatively related to recruitment success, while at Morro Bay and Southern, upwelling in winter was positively related to recruitment. These differences could be indicative of variability in how upwelling manifests between regions. While upwelling is more consistent across seasons in the southern CCS, upwelling varies substantially across seasons in the northern and central CCS (Checkley & Barth, 2009). Furthermore, the efficacy of upwelling at providing nutrients to surface waters during winter months might differ across space, having variable consequences for widely-distributed rockfishes. In addition, spatial variability in relationships between winter upwelling and recruitment could suggest difference in phenology of spawning between northern and southern port-complexes. Regional differences in the timing of parturition (release of larvae) (Love et al. 2002), and subsequent stage progression of young-of-the-year could lead to spatial variability in the ability of larval rockfish to take advantage of winter nutrient availability without being displaced by offshore transport of surface waters. All of these possible mechanisms might also act in concert to, at least in part, explain regional differences in relationships between upwelling and recruitment.

In contrast to relationships observed for winter conditions, the shape and direction of relationships between recruitment and upwelling during spring remained generally consistent across port-complexes. From Eureka through Monterey, April upwelling and mean[Apr-Jun] upwelling outperformed any other monthly or seasonal average. Across port-complexes, upwelling anomalies in April were positively related to recruitment deviations, suggesting that higher nutrient availability supported stronger recruitment success. The direction shifted with mean[Apr-Jun] where recruitment was weakest at average upwelling anomalies. This variable blends a positive relationship with April upwelling anomaly and a negative relationship between recruitment deviations and June upwelling anomaly. This may suggest that if upwelling during June is weak, what nutrients are in the water column remain available to rockfish without being forced offshore by upwelling.

Relationships with spring upwelling are echoed in models used to predict PC1, a mode for coastwide coherence in recruitment deviations. Upwelling anomalies during March, April and May from the northernmost station were best at predicting PC1. Again, upwelling in April had a strongly positive relationship with PC1, while March and May upwelling had negative relationships with recruitment success. It is not yet clear what might underpin the reversal of relationships between recruitment and seasonally adjusted upwelling anomaly through the spring. That these relationships are exhibited universally across port-complexes and the coast-scale index of recruitment suggests spring upwelling is an important determinant of year-class strength, though the relationship between PC1 and upwelling shifts throughout spring.

Spring correlations suggest that recruitment is defined later in life history than suggested by previous work by Laidig et al. (2007)which demonstrated that juvenile Blue Rockfish abundance in central California was associated with environmental conditions during the larval stage. While the majority of variability in year-class strength is thought to have occurred by the pelagic juvenile stage (Hjort, 1914; Ralston & Howard, 1996; Ralston et al. 2013), cumulative and integrated processes impacting pre-recruits are also likely to drive recruitment variability (Houde, 2008). Juvenile Chilipepper Rockfish are most abundant in the Southwest Fisheries Science Center Pelagic Juvenile Survey between March and April (Ralston et al. 2013), suggesting that settlement occurs soon-thereafter. Therefore, spring correlations suggest that upwelling between March and May could impact survival of Chilipepper Rockfish through the settlement stage and capture variability in factors that affect post-settlement processes, consequently driving year-class success.

A few lines of reasoning may explain the varying relationships between upwelling in March through May and recruitment success. Both Laidig (2010) and Caselle et al. (2010) found that time of settlement in rockfish was positively related to upwelling. If upwelling impacts the time of settlement and survival through settlement is important to eventual year-class strength, timing of upwelling may prove important for explaining some variability in recruitment success. This assertion feeds into the match-mismatch hypothesis to explain varying relationships between upwelling in March through May and recruitment success. While the classic match-mismatch hypothesis focuses on larval fish (Cushing, 1990), here I consider that it might also describe a bottleneck that occurs

during the juvenile stage. Favorable conditions, or higher upwelling, in April may have greater overlap with when the majority of juvenile rockfish are at the stage to take advantage of those favorable conditions, creating a “match”. This would allow for year-class success. When that high upwelling occurs either earlier or later, the proportion of individuals capable of using those nutrients while also being retained in the population is lower. In this situation, there is a “mis-match”, and relatively lower recruitment success.

However, spring oceanographic variables neglect the critical period hypothesis, which suggests that survival through larval stages is the most important period in defining interannual variability in recruitment (Hjort, 1914). In essence, for juvenile settlement to be important, young-of-the-year first have to survive the larval stage. No winter oceanographic variable (coincident with the larval stage) contributed to the best models for port-complexes or PC1, which is a critical distinction between these results and previous work (Laidig et al. 2007). Winter sea level, which was initially noted in many port-complex-specific models despite being outperformed by spring upwelling, explained what little deviation was able to be captured in moderate recruitment years. This distinction between spring upwelling and winter sea level may offer some insight to the critical period in larval Chilipepper Rockfish, suggesting that conditions associated with reduced alongshore transport are favorable for survival through larval stages and subsequent recruitment success during moderate year classes. However, during strong or weak year classes, pre-recruit juvenile survival drives recruitment variability, likely a result of cumulative effects (Houde, 2008) since parturition on young-of-the-year Chilipepper Rockfish.

The potential for variability in alongshore transport to affect the distribution and relative recruitment success of Chilipepper Rockfish is reinforced by relationships between basin-scale indices during winter and PC2 (which captured ~11% of the variability in recruitment deviations between northern and southern port-complexes). All models for PC2 included the North Pacific Gyre Oscillation (NPGO) between January and May, and several included the Pacific Decadal Oscillation (PDO), suggesting that variability in the strength of alongshore flow and efficacy of upwelling in the California Current influences recruitment dynamics and how recruitment is distributed along the coast. During moderate year-classes, the strength and direction of this current could impact where recruits are distributed, whether by survival or transport. Southern port-complexes had relatively stronger recruitment when NPGO was negative in January or positive in March. Positive NPGO is associated with an intensification of the subtropical gyre, driven by open-ocean wind stress curl anomalies. These create upwelling-favorable conditions in the California Current (Di Lorenzo et al. 2008). Therefore, models for PC2 suggest that if NPGO is positive in January, upwelling may force the offshore transport of larval rockfish. In contrast, if NPGO is positive in March, southward wind-stress not only favors upwelling that fish are large enough to utilize, but it may also drive southerly transport of larvae and juveniles. These dynamics represent subtle differences between northern and southern port-complex-specific recruitment deviations, and support conclusions from port-complex specific models that moderate recruitment years are positively related to winter sea level anomalies.

While PC3 only captured ~7% of the variability across port-complex recruitment deviations, it demonstrated spatial patterns that broadly align with regional distinctions along the California coastline defined by Cape Mendocino and Point Conception. Between Cape Mendocino and Point Conception, the San Francisco and Bodega Bay port-complexes were defined as the "core" of the stock- the area of peak biomass for Chilipepper Rockfish. Port-complexes to the north and south were defined as boundary regions. PC3 was best explained by winter upwelling anomaly collected at the core of the stock. The core of the stock has its strongest recruitment at moderate upwelling between December and February. In either high or low upwelling over this period, port-complexes to either the north or south experience relatively better recruitment. This is perhaps a signal that north- or south-ward larval transport during winter upwelling defines the difference between core and boundary recruitment success.

As a whole, these models suggest that port-complex, and subsequently coastwide, recruitment deviations are largely decided during late winter and spring. In contrast, the strength of recruitment success between one region and another is determined during winter, and appears to be driven in part by nutrient availability and low-frequency forcing on alongshore transport (indexed by NPGO and PDO). It is important to recognize that while these oceanographic variables were related to PC2 and PC3, these components together only account for ~ 17% of variability in port-complex recruitment, and might themselves be in part artefacts of how the principal components analysis is structured. Concordant results from PCA and DFA (which specifically accounts for the time series

structure of the data) lends credence to the patterns observed in recruitment indices and subsequent predictors.

Evidence for Spatially Explicit Population Dynamics

Development of spatially discrete assessments required the assumption that all port-complexes are independent of one another and there is no movement between them. It was understood that this assumption would not be satisfied, but was deemed acceptable because no investigation into the resolution of spatial variability in recruitment success could move forward while satisfying this assumption or without requiring assumptions regarding the spatial generation or distribution of recruitment (e.g. Thorson & Wetzel, 2015). An additional assumption in my analysis is that a single, constant rate of natural mortality applies to all port-complexes, regardless of latitude. This assumption is also made by the full assessment (consistent with assuming a single stock).

Two patterns emerge from my analysis that speak to how strongly these assumptions were violated. First, retrospective patterns in recruitment deviations varied in a patterned manner across port-complexes (Figure 7), suggesting either variable natural mortality or alongshore movement of individuals. Southern port-complexes show a slight retrospective pattern towards more moderate recruitment deviations than were initially estimated. In contrast, northern port-complexes initially underestimate recruitment success until the true magnitude is eventually realized between age 2-4. Second, empirical examination of age surveys (Appendix D) show there is also a latitudinal

gradient in age distribution of the population; Age-0 and age-1 fish are captured almost exclusively south of Monterey Bay.

Several plausible, non-exclusive mechanisms exist to explain observations of uneven distribution of age-0 and -1 Chilipepper Rockfish. For one, survey timing and gear may be biased towards greater capture rates for young-of-the-year in the south. Appendix F demonstrates that individuals from southern port-complexes have a faster growth rate, and thus may be susceptible to survey gear from an earlier age than northern individuals. This effect may be exacerbated by southward propagation of the NWFSC trawl surveys, which allows southern juveniles more time to grow (and to become susceptible to gear). In this scenario, we would expect a quick resolution to recruitment estimates by year 1, though the uneven distribution continues through age-1 individuals, andcontinues to develop for 2-4 years. The latitudinal gradient in growth rate does not account for why age-0 fish are captured at southern latitudes, but northern age-1 fish are not retained by the survey gear. Another explanation is that habitats occupied by northern juveniles are not sampled by survey gear.

Latitudinal variability in natural mortality may also explain the distribution of age-0 and -1 rockfish directly violating one of the assumptions of the underlying stock assessment models. To get the observed retrospective pattern in recruitment deviations, mortality rate would have to decrease with latitude (e.g. mortality lower in the north-consistent with ecosystem metabolism as function of temperature [Crane, 2014]). While this possibility wasn't inspected, it could be tested by examining the number of samples

for each age across size classes and fitting a mortality curve. This analysis, however, would also assume that there is no movement across port-complex designations, though the motivating hypothesis is not exclusionary.

Finally, unequal distribution of young rockfish is also consistent with equatorward transport of early life stages and subsequent poleward migration of age 0-4 fish. This hypothesis suggests that southward transport of younger fish, and consequently disproportionate capture of young fish at southern latitudes, causes an initial overestimation in recruitment deviations at these port-complexes. Recruitment deviations at northern latitudes reflect an initial deficit of young individuals, until compensatory migration of young rockfish occurs over the following 1-3 years. This process could result in the observed retrospective patterns and disproportionate representation of young fish at southern latitudes.

If real, dynamics driving unequal distribution of young rockfish might underlie interpretation of recruitment-ocean models for PC2 and PC3. Rather than capturing variability arising primarily from differential survival (and eventual recruitment success) between regions, these indices may instead be describing regional distribution of recruits as a function of transport. This could also explain why recruitment deviations at Eureka (north of Cape Mendocino) and Southern (south of Point Conception) are the least correlated with other port-complexes. Perhaps these geographic landmarks hinder connectivity and transport of young fish (though differences in production may also exist outside of these boundaries). Such transport and migration would result in strong mixing

over broad spatial scales within the stock, and would be consistent with evidence that Chilipepper rockfish exhibit remarkably low genetic variation relative to their broad range (Wishard 1980).

Next Steps

PCA and DFA results were largely coherent with and one another and supported the idea of a north - central - south designation in Chilipepper Rockfish recruitment deviations, in accordance with the oceanographic regions defined by Checkley and Barth (2009). Future work should examine whether three stock assessment models based on these geographic boundaries, serve as a better framework than the seven-region configuration used here for understanding spatial variability in recruitment.

However, the higher resolution approach used here is justified for several reasons. For one, the data for Chilipepper Rockfish are relatively rich in comparison to data for other West Coast groundfish, and Chilipepper Rockfish are one of the few species for which spatially divided data suffice to support satisfactory model fits. Second, the vast majority of Chilipepper Rockfish biomass exists between Cape Mendocino and Point Conception (explored in Appendix G). By merging this area into a single model, a considerable amount of the variability that might exist between these landmarks would be lost. By developing seven port-complex-specific assessments, I determined that a substantial amount of variability was shared coastwide but also that variability existed at smaller scales (including within the geographic central region) as well.

In my examination of oceanographic drivers as predictors of recruitment deviations, I found that oceanographic indices for retention and nutrient enrichment during winter and spring consistently predicted both coherent-coastwide and spatially-explicit recruitment success (though a considerable amount of variability in the data still remains unexplained). The relatability of these results to what is known about rockfish early life history further reinforces their potential applicability to future stock assessments of this and other winter-spawning rockfishes, though I emphasize these models and predictors were purely exploratory. Furthermore, this work ignores interactions between upwelling and sea level, which are known to interact both in origin and consequence. Future work should evaluate the robustness of these results through changes in the spatial extent of port-complex stock assessment models, consider integrated measures of sea level and upwelling (e.g. Coastal Upwelling Transport Index [CUTI], Biologically Effective Upwelling Transport Index [BEUTI]) (Jacox et al. 2018) that might yield greater insight into recruitment-ocean dynamics, and finally evaluate shifts in these relationships based on duration of time series. This could be accomplished by taking advantage of the capacity for DFA to include time series of environmental indices alongside recruitment time series.

Concluding Remarks

This work sets the stage for more detailed analysis of oceanographic variables as drivers of recruitment deviations, assessment of potential shifts in dominant environmental controls over recruitment, and the potential for inclusion of variables in

future formal stock assessments. While Myers (1998) demonstrated that environment-recruitment relationships rarely hold over time, the present study spans a period of considerable oceanographic variation, including regime shifts in the Pacific Decadal Oscillation and North Pacific Gyre Oscillation. Furthermore, the coherence in recruitment deviations remained consistent over time, evidenced by the comparability with results from Field and Ralston (2005). The corroboration of their results through analysis of an additional 17 years of data and the incorporation of the area south of Point Conception reinforces the evidence for coherence in coastwide Chilipepper Rockfish year-classes. In addition, I extended the analysis of Field and Ralston (2005) to identify potential drivers of recruitment variability that might serve to advance development of future stock assessments for Chilipepper Rockfish and other important West Coast groundfish. This has even stronger consequences when multiple species covary, as in many winter-spawning West Coast rockfish (Ralston et al. 2013; Thorson et al. 2013), suggesting that these results could also help inform models for data-poor species (Schirippa et al. 2009).

Perhaps most immediately, this work complements advancements from Thorson & Wetzel (2015) which incorporated spatial structure to the Canary Rockfish stock assessment model but requires strong *a priori* assumptions regarding the spatial distribution (and drivers of interannual variability in the distribution) of both recruitment and magnitude of recruitment success. My work approaches this question by attempting to empirically estimate variability in recruitment deviations over space, and thus contributes to the broad effort to use environmental covariates to reduce uncertainty of

biological outputs from stock assessment models and subsequent management reference points (e.g. Acceptable Biological Catch) (Shelton et al. 2014).

REFERENCES

Allain, G., Petitgas, P., & Lazure, P. (2001). The influence of mesoscale ocean processes on anchovy (Engraui encrasicolus) recruitment in the Bay of Biscay estimated with a three-dimensional hydrodynamic mode. *Fisheries Oceanography, 10*(2), 151-163.

Barth, J. A., Menge, B. A., Lubchenco, J., Chan, F., Bane, J. M., Kirincich, A. R., ... & Washburn, L. (2007). Delayed upwelling alters nearshore coastal ocean ecosystems in the northern California current. *Proceedings of the National Academy of Sciences*, *104*(10), 3719-3724.

Bates, D. M. and Chambers, J. M. (1992) *Nonlinear models.* Chapter 10 of *Statistical Models in S* eds J. M. Chambers and T. J. Hastie, Wadsworth & Brooks/Cole.

Berkeley, S. A., Hixon, M. A., Larson, R. J., & Love, M. S. (2004). Fisheries sustainability via protection of age structure and spatial distribution of fish populations. *Fisheries*, *29*(8), 23-32.

Beverton, R. J. H., & Holt, S. J. (1957). On the dynamics of exploited fish populations. Fisheries Investigation Series 2, volume 19, UK Ministry of Agriculture. *Fisheries, and Food, London, UK*.

Beyer, S. G., Sogard, S. M., Harvey, C. J., & Field, J. C. (2015). Variability in Rockfish (Sebastes spp.) fecundity: species contrasts, maternal size effects, and spatial differences. *Environmental biology of fishes*, *98*(1), 81-100.

Bjorkstedt, E. P., Goericke, R., McClatchie, S., Weber, E., Watson, W., Lo, N., ... & Gaxiola-Castro, G. (2010). State of the California Current 2009-2010: Regional variation persists through transition from La Niña to El Niño (and back?).

Black, B. A., Schroeder, I. D., Sydeman, W. J., Bograd, S. J., Wells, B. K., & Schwing, F. B. (2011). Winter and summer upwelling modes and their biological importance in the California Current Ecosystem. *Global Change Biology*, *17*(8), 2536-2545.

Bograd, S. J., Schroeder, I., Sarkar, N., Qiu, X., Sydeman, W. J., & Schwing, F. B. (2009). Phenology of coastal upwelling in the California Current. *Geophysical Research Letters*, *36*(1).

Botsford, L. W., Lawrence, C. A., Dever, E. P., Hastings, A., & Largier, J. (2003). Wind strength and biological productivity in upwelling systems: an idealized study. *Fisheries Oceanography*, *12*(4-5), 245-259.

Brooks, E. N., & Deroba, J. J. (2015). When "data" are not data: the pitfalls of post hoc analyses that use stock assessment model output. *Canadian Journal of Fisheries and Aquatic Sciences*, *72*(4), 634-641.

Cardinale, M., & Arrhenius, F. (2000). The influence of stock structure and environmental conditions on the recruitment process of Baltic cod estimated using a generalized additive model. *Canadian Journal of Fisheries and Aquatic Sciences*, *57*(12), 2402-2409.

Caselle, J. E., Wilson, J. R., Carr, M. H., Malone, D. P., & Wendt, D. E. (2010) Can we predict interannual and regional variation in delivery of pelagic juveniles to nearshore populations of Rockfishes (genus Sebastes) using simple proxies of ocean conditions?. *Reports of California Cooperative Oceanic Fisheries Investigations*, *51*, 91-105.

Charles, A. T. (1998). Living with uncertainty in fisheries: analytical methods, management priorities and the Canadian groundfishery experience. *Fisheries Research*, *37*(1), 37-50.

Chavez, F. P., Pennington, J. T., Castro, C. G., Ryan, J. P., Michisaki, R. P., Schlining, B., ... & Collins, C. A. (2002). Biological and chemical consequences of the 1997–1998 El Niño in central California waters. *Progress in Oceanography*, *54*(1-4), 205-232.

Checkley, D. M., & Barth, J. A. (2009). Patterns and processes in the California Current System. *Progress in Oceanography*, *83*(1), 49-64.

Chenillat, F., Rivière, P., Capet, X., Di Lorenzo, E., & Blanke, B. (2012). North Pacific Gyre Oscillation modulates seasonal timing and ecosystem functioning in the California Current upwelling system. *Geophysical Research Letters*, *39*(1).

Chhak, K., & Di Lorenzo, E. (2007). Decadal variations in the California Current upwelling cells. *Geophysical Research Letters*, *34*(14).

Colton, A. R., Wilberg, M. J., Coles, V. J., & Miller, T. J. (2014). An evaluation of the synchronization in the dynamics of blue crab (Callinectes sapidus) populations in the western A tlantic. *Fisheries Oceanography*, *23*(2), 132-146.

Crane, K. E. (2014). Environmental effects on growth of early life history stages of rockfishes (Sebastes) off Central California based on analysis of otolith growth patterns.

Cury, P., & Roy, C. (1989). Optimal environmental window and pelagic fish recruitment success in upwelling areas. *Canadian Journal of Fisheries and Aquatic Sciences*, *46*(4), 670-680.

Cushing, D.H., 1990. Plankton production and year-class strength in fish populations: an update of the match/mismatch hypothesis. Advances in marine biology, 26, pp.249293.

Di Lorenzo, E., Combes, V., Keister, J. E., Strub, P. T., Thomas, A. C., Franks, P. J., ... & Peterson, W. T. (2013). Synthesis of Pacific Ocean climate and ecosystem dynamics. *Oceanography*, *26*(4), 68-81.

Di Lorenzo, E., Schneider, N., Cobb, K. M., Franks, P. J. S., Chhak, K., Miller, A. J., ... & Powell, T. M. (2008). North Pacific Gyre Oscillation links ocean climate and ecosystem change. *Geophysical Research Letters*, *35*(8).

Dorn, M. W. (2002). Advice on West Coast Rockfish harvest rates from Bayesian meta-analysis of stock− recruit relationships. *North American Journal of Fisheries Management*, *22*(1), 280-300.

Echeverria, T. W. (1987). Thirty-four species of California rockfishes: maturity and seasonality of reproduction. *Fishery Bulletin*, *85*(2), 229-250.

Field, J. C. (2007). Status of the Chilipepper Rockfish, Sebastes goodei, in 2007. *Status of the Pacific Coast groundfish fishery through*.

Field, J. C, Beyer, S. G, & He, X. (2015). Status of the Chilipepper Rockfish, Sebastes goodie, in the California Current for 2015. *Pacific Fishery Management Council*.

Field, J. C, & Ralston, S. (2005). Spatial variability in Rockfish (sebastes spp.) recruitment events in the california current system. Canadian Journal of Fisheries and Aquatic Sciences, 62(10), 2199-2210.

Fogarty, M. J., & Botsford, L. W. (2007). Population connectivity and spatial management of marine fisheries. *Oceanography*, *20*(3), 112-123.

Galindo-Cortes, G. , De Anda-Montañez, J. , Arreguín-Sánchez, F. , Salas, S. , & Balart, E. (2010). How do environmental factors affect the stock–recruitment relationship? the case of the pacific sardine (sardinops sagax) of the northeastern pacific ocean. Fisheries Research, 102(1/2), 173-183.

Goethel, D. R., Quinn, T. J., & Cadrin, S. X. (2011). Incorporating spatial structure in stock assessment: movement modeling in marine fish population dynamics. *Reviews in Fisheries Science*, *19*(2), 119-136.

Green, K. M., & Starr, R. M. (2011). Movements of small adult black rockfish: implications for the design of MPAs. *Marine Ecology Progress Series*, *436*, 219-230.

Haltuch, M. A., Punt, A. E., & Dorn, M. W. (2009). Evaluating the estimation of fishery management reference points in a variable environment. *Fisheries Research*, *100*(1), 42-56.

Hare, J. A. (2014). The future of fisheries oceanography lies in the pursuit of multiple hypotheses. *ICES Journal of Marine Science*, *71*(8), 2343-2356.

Hare, S. R., Mantua, N. J., & Francis, R. C. (1999). Inverse production regimes: Alaska and West Coast Pacific salmon. *Fisheries*, *24*(1), 6-14.

Heiberger, R. M. (2018). HH: Statistical Analysis and Data Display: Heiberger and Holland. R package version 3.1-35. URL https://CRAN.R-project.org/package=HH

Hill, K. T., Dorval, E., Lo, N. C., Macewicz, B. J., Show, C., & Felix-Uraga, R. (2007). Assessment of the Pacific sardine resource in 2007 for US management in 2008. *NOAA Technical Memorandum NMFS. National Oceanic and Atmospheric Administration, National Marine Fisheries Service Southwest Fisheries Science Center*.

Hjort, J. (1914). Fluctuations in the great fisheries of northern Europe viewed in the light of biological research. ICES.

Hobson, E. S., Chess, J. R., & Howard, D. F. (2001). Interannual variation in predation on first-year Sebastes spp. by three northern California predators. *Fishery Bulletin*, *99*(2), 292-292.

Holmes, E. E., Ward, E. J., & Scheuerell, M. D. (2014). Analysis of multivariate time-series using the MARSS package. *NOAA Fisheries, Northwest Fisheries Science Center*, *2725*, 98112.

Houde, E. D. (2008). Emerging from Hjort's shadow. *Journal of Northwest Atlantic Fishery Science*, *41*, 53-70.

Jacox, M. G., Edwards, C. A., Hazen, E. L., & Bograd, S. J. (2018). Coastal upwelling revisited: Ekman, Bakun, and improved upwelling indices for the US west coast. *Journal of Geophysical Research: Oceans*, *123*(10), 7332-7350.

Jacox, M. G., Fiechter, J., Moore, A. M., & Edwards, C. A. (2015). ENSO and the California Current coastal upwelling response. *Journal of Geophysical Research: Oceans*, *120*(3), 1691-1702.

Kerby, J. T., Wilmers, C. C., & Post, E. R (2012). Climate change, phenology, and the nature of consumer–resource interactions: advancing the match/mismatch

hypothesis. *Trait-mediated indirect interactions: ecological and evolutionary perspectives*, 508-25.

Kilduff, D., Botsford, L., & Teo, S. (2014). Spatial and temporal covariability in earlyocean survival of chinook salmon (oncorhynchus tshawytscha) along the West Coast of north america. ICES Journal of Marine Science, 71(7), 1671-1682.

King, J. R., McFarlane, G. A., & Beamish, R. J. (2001). Incorporating the dynamics of marine systems into the stock assessment and management of sablefish. *Progress in Oceanography*, *49*(1), 619-639.

King, J. R., & McFarlane, G. A. (2006). A framework for incorporating climate regime shifts into the management of marine resources. *Fisheries Management and Ecology*, *13*(2), 93-102.

Koslow, J., Goericke, R., & Watson, W. (2013). Fish assemblages in the southern California Current: relationships with climate, 1951–2008. *Fisheries Oceanography*, *22*(3), 207-219.

Kosro, P. M., Peterson, W. T., Hickey, B. M., Shearman, R. K., & Pierce, S. D. (2006). Physical versus biological spring transition: 2005. *Geophysical Research Letters*, *33*(22).

Kudela, R. M., Banas, N. S., Barth, J. A., Frame, E. R., Jay, D. A., Largier, J. L., ... & Vander Woude, A. J. (2008). New insights into the controls and mechanisms of plankton productivity in coastal upwelling waters of the northern California Current System. *Oceanography*, *21*(4), 46-59.

Laidig, T. E., Chess, J. R., & Howard, D. F. (2007). Relationship between abundance of juvenile Rockfishes (Sebastes spp.) and environmental variables documented off northern California and potential mechanisms for the covariation. *Fishery Bulletin*, *105*(1), 39-49.

Laidig, T. (2010). Influence of ocean conditions on the timing of early lifehistory events for blue Rockfish [sebastes mystinus] off california. Fishery Bulletin, 108(4), 442.

Lindegren, M., & Checkley Jr, D. M. (2012). Temperature dependence of Pacific sardine (Sardinops sagax) recruitment in the California Current Ecosystem revisited and revised. *Canadian Journal of Fisheries and Aquatic Sciences*, *70*(2), 245-252.

Love, M.S., M. Yolkavich and L. Thorsteinson. 2002. The Rockfishes of the Northeast Pacific. University of California Press: Berkeley.

Lynn, R. J., Bograd, S. J., Chereskin, T. K., & Huyer, A. (2003). Seasonal renewal of the California Current: The spring transition off California. *Journal of Geophysical Research: Oceans*, *108*(C8).

Mantua, N. J., & Hare, S. R. (2002). The Pacific decadal oscillation. *Journal of oceanography*, *58*(1), 35-44.

Maunder, M. N., & Watters, G. M. (2003). A general framework for integrating environmental time series into stock assessment models: model description, simulation testing, and example. *Fishery Bulletin*, 101(1), 89-99.

McClatchie, S. (2016). State of the California Current 2015–16: Comparisons with the 1997–98 El Niño. *California cooperative oceanic fisheries investigations. Data report*, *57*.

Messié, M., & Chavez, F. (2011). Global modes of sea surface temperature variability in relation to regional climate indices. *Journal of Climate*, *24*(16), 4314-4331.

Methot, R. D. (2013). User manual for Stock Synthesis model version 3.24 s, updated November 21, 2013. NOAA Fisheries, Seattle, WA.

Methot Jr, R. D., & Taylor, I. G. (2011). Adjusting for bias due to variability of estimated recruitments in fishery assessment models. *Canadian Journal of Fisheries and Aquatic Sciences*, *68*(10), 1744-1760.

Methot, R. D., & Wetzel, C. R. (2013). Stock synthesis: a biological and statistical framework for fish stock assessment and fishery management. *Fisheries Research*, *142*, 86-99.

Miller, A. K., & Sydeman, W. J. (2004). Rockfish response to low-frequency ocean climate change as revealed by the diet of a marine bird over multiple time scales. *Marine Ecology Progress Series*, *281*, 207-216.

NWFSC (2018). Temperature Anomaly. https://www.nwfsc.noaa.gov/research/divisions/fe/estuarine/oeip/da-sea-surface-temp.cfm#TA-01

Petersen, C. H., Drake, P. T., Edwards, C. A., & Ralston, S. (2010). A numerical study of inferred Rockfish (Sebastes spp.) larval dispersal along the central California coast. *Fisheries Oceanography*, *19*(1), 21-41.

Peterson, W. T., Fisher, J. L., Peterson, J. O., Morgan, C. A., Burke, B. J., & Fresh, K. L. (2014). Applied fisheries oceanography: Ecosystem indicators of ocean conditions inform fisheries management in the California Current. *Oceanography*, *27*(4), 80-89.

Peterson, W. T., & Schwing, F. B. (2003). A new climate regime in northeast Pacific ecosystems. *Geophysical research letters*, *30*(17).

Pope, J. G., Shepherd, J. G., & Webb, J. (1994). Successful surf-riding on size spectra: the secret of survival in the sea. *Phil. Trans. R. Soc. Lond. B, 343*(1303), 41-49.

R Core Team (2017). R: A language and environment for statistical computing. R Foundation for Statistical Computing, Vienna, Austria. URL https://www.R-project.org/.

Ralston, S., & Howard, D. F. (1996). On the development of year-class strength and cohort variability in two northern California Rockfishes. *Oceanographic Literature Review*, *9*(43), 929.

Ralston, S., Pearson, D. E., Field, J. C., & Key, M. (2010). *Documentation of the California catch reconstruction project*. US Department of Commerce, National Oceanic and Atmospheric Administration, National Marine Fisheries Service, Southwest Fisheries Science Center.

Ralston, S., Sakuma, K. M., & Field, J. C. (2013). Interannual variation in pelagic juvenile Rockfish (Sebastes spp.) abundance–going with the flow. *Fisheries Oceanography*, *22*(4), 288-308.

Sakuma, K. M., Ralston, S., & Wespestad, V. G. (2006). Interannual and spatial variation in the distribution of young-of-the-year Rockfish (Sebastes spp.): expanding and coordinating a survey sampling frame. *California Cooperative Oceanic Fisheries Investigations Report*, *47*, 127.

Secor, D. H. (2007). The year-class phenomenon and the storage effect in marine fishes. *Journal of Sea Research, 57*(2-3), 91-103.

Schirripa &, M., & Colbert, J. (2006). Interannual changes in sablefish (anoplopoma fimbria) recruitment in relation to oceanographic conditions within the california current system. Fisheries Oceanography, 15(1), 25-36.

Schirripa, M. J., Goodyear, C. P., & Methot, R. M. (2009). Testing different methods of incorporating climate data into the assessment of US West Coast sablefish. *ICES Journal of Marine Science*, *66*(7), 1605-1613.

Schirripa, M. J., & Methot, R. D. (2002). Status of the sablefish resource off the US Pacific coast in 2002. *Pacific Fishery Management Council*.

Shelton, A. O., Thorson, J. T., Ward, E. J., & Feist, B. E. (2014). Spatial semiparametric models improve estimates of species abundance and distribution. *Canadian Journal of Fisheries and Aquatic Sciences*, *71*(11), 1655-1666.

Szuwalski, C. S., Ianelli, J. N., Punt, A. E., & Handling editor: Jan Jaap Poos. (2017). Reducing retrospective patterns in stock assessment and impacts on management performance. *ICES Journal of Marine Science*, *75*(2), 596-609.

Thorson, J. T., Stewart, I. J., Taylor, I. G., & Punt, A. E. (2013). Using a recruitment-linked multispecies stock assessment model to estimate common trends in recruitment for US West Coast groundfishes. *Marine Ecology Progress Series*, *483*, 245-256.

Thorson, J. T., & Wetzel, C. (2015). The status of canary rockfish (Sebastes pinniger) in the California Current in. *Availble at http://www. cio. noaa. gov/services_programs/prplans/pdfs/ID308_FinalProduct_CanaryRockfish_2016. pdf*.

Uusitalo, L., Lehikoinen, A., Helle, I., & Myrberg, K. (2015). An overview of methods to evaluate uncertainty of deterministic models in decision support. *Environmental Modelling & Software*, *63*, 24-31.

Verdy, A., Mazloff, M. R., Cornuelle, B. D., & Kim, S. Y. (2014). Wind-driven sea level variability on the california coast: An adjoint sensitivity analysis. *Journal of Physical Oceanography*, *44*(1), 297-318.

Wilderbuer, T. K., Hollowed, A. B., Ingraham, W. J., Spencer, P. D., Conners, M. E., Bond, N. A., & Walters, G. E. (2002). Flatfish recruitment response to decadal climatic variability and ocean conditions in the eastern Bering Sea. *Progress in Oceanography*, *55*(1), 235-247.

Wishard, L. N., Utter, F. M., & Gunderson, D. R. (1980). Stock separation of five Rockfish species using naturally occurring biochemical genetic markers. *Mar. Fish. Rev*, *42*(3-4), 64-73.

Wold, S., Esbensen, K., & Geladi, P. (1987). Principal component analysis. *Chemometrics and intelligent laboratory systems*, *2*(1-3), 37-52.

Wolter, K., & Timlin, M. S. (2011). El Niño/Southern Oscillation behaviour since 1871 as diagnosed in an extended multivariate ENSO index (MEI. ext). *International Journal of Climatology*, *31*(7), 1074-1087.

Wood, S.N. (2017) *Generalized Additive Models: an introduction with R (2nd edition)*, CRC

Woodson, C. B., McManus, M. A., Tyburczy, J. A., Barth, J. A., Washburn, L., Caselle, J. E., ... & Palumbi, S. R. (2012). Coastal fronts set recruitment and connectivity patterns across multiple taxa. *Limnology and Oceanography*, *57*(2), 582-596.

Zuur, A. F., Tuck, I. D., & Bailey, N. (2003). Dynamic factor analysis to estimate common trends in fisheries time series. *Canadian journal of fisheries and aquatic sciences*, *60*(5), 542-552.

APPENDIX A

Appendix A: Here I present time series of environmental variables used to model port-complex-specific recruitment deviations and modes of recruitment variability time series. Local indices are shown first, Upwelling Index Anomaly (UIa), Sea Level Anomaly (SLa), Sea Surface Temperature (SST) and are ordered from north to south. Finally, time series are displayed for basin-scale indices of North Pacific Gyre Oscillation (NPGO), Pacific Decadal Oscillation (PDO) and Multivariate ENSO Index (MEI). Recall that December of the year prior to recruitment was used to predict recruitment, so in the following graphs of UIa, SLa or SST in December, they will be shown for the recruitment year, rather than the year of collection. For example, December UIa shown for 2009 was actually collected from December in 2008 because it has consequences for and is used to predict the 2009 recruitment year.

(A)

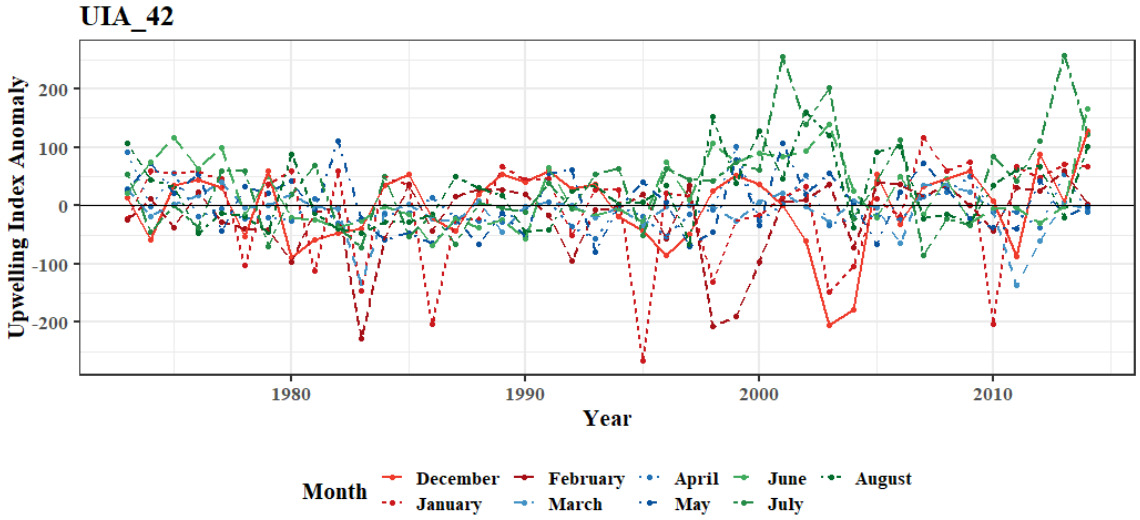

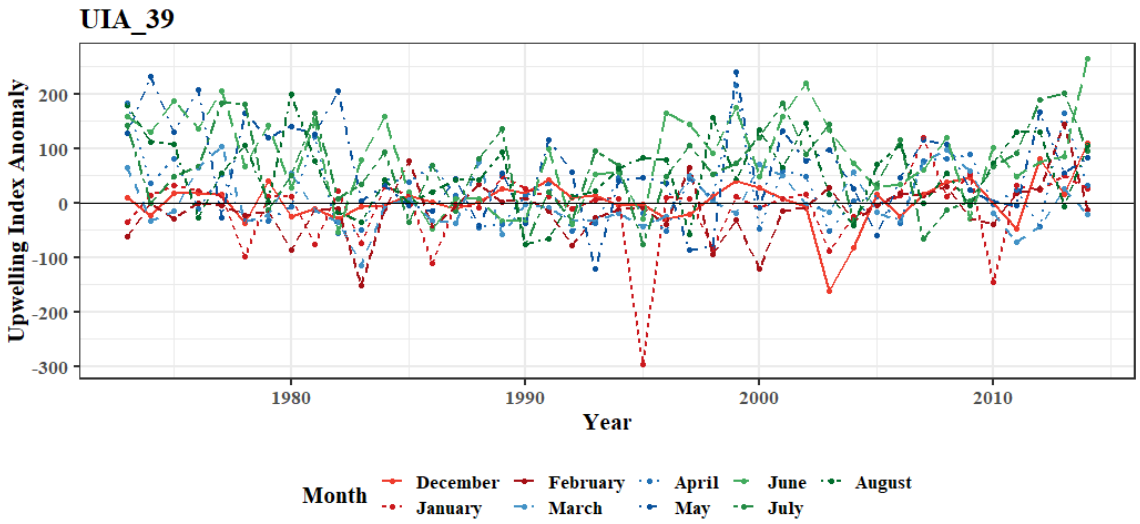
UIA_39
Upwelling Index Anomaly
200
100
0
-100
-200
-300
1980
1990
2000
2010
Year
Month
December
January
February
March
April
May
June
July
August

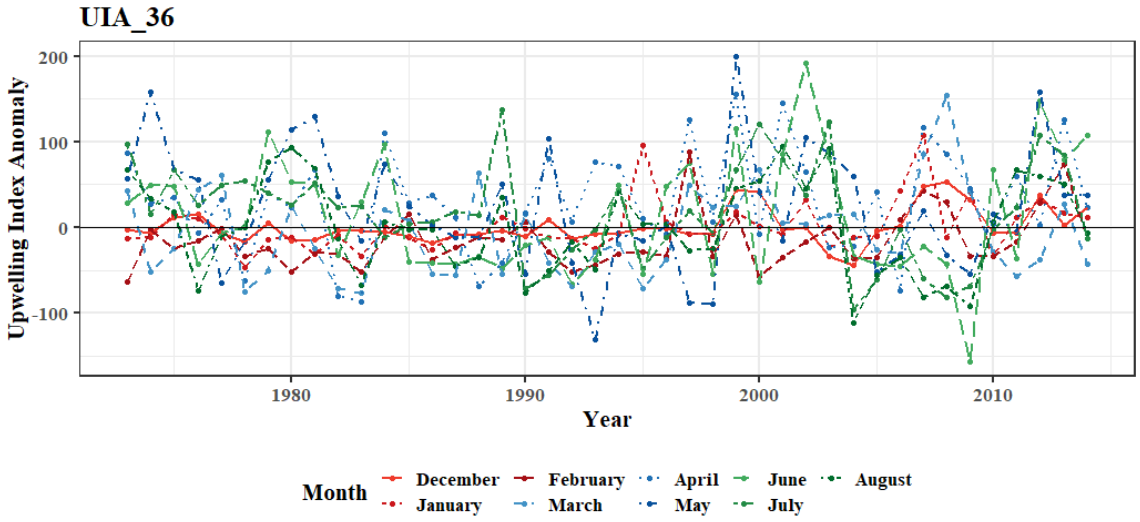
UIA_36
Upwelling Index Anomaly
200
100
0
-100
1980
1990
2000
2010
Year
Month
December
January
February
March
April
May
June
July
August

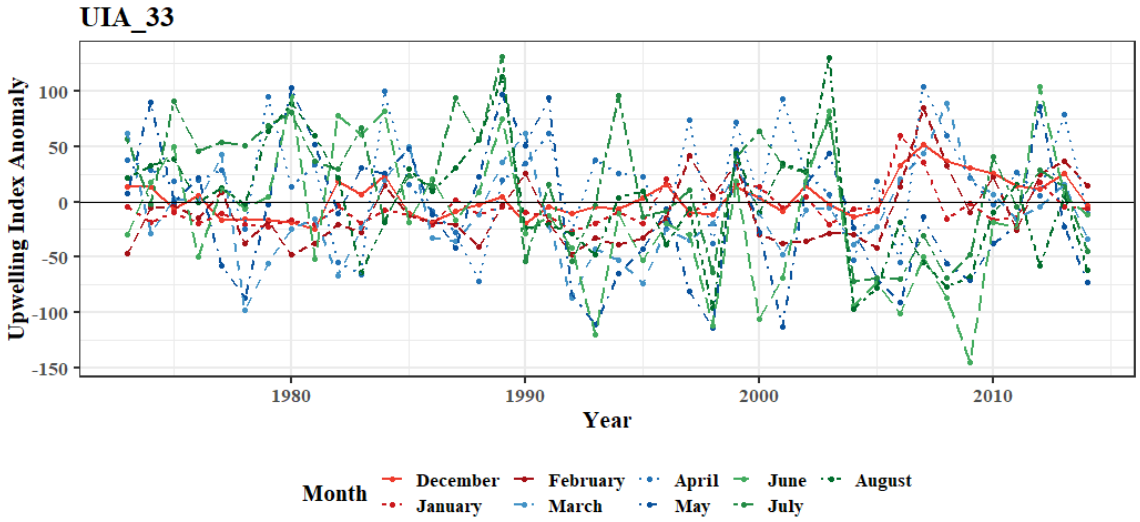
UIA_33
Upwelling Index Anomaly
100
50
0
-50
-100
-150
1980
1990
2000
2010
Year
Month
December
January
February
March
April
May
June
July
August

(B)

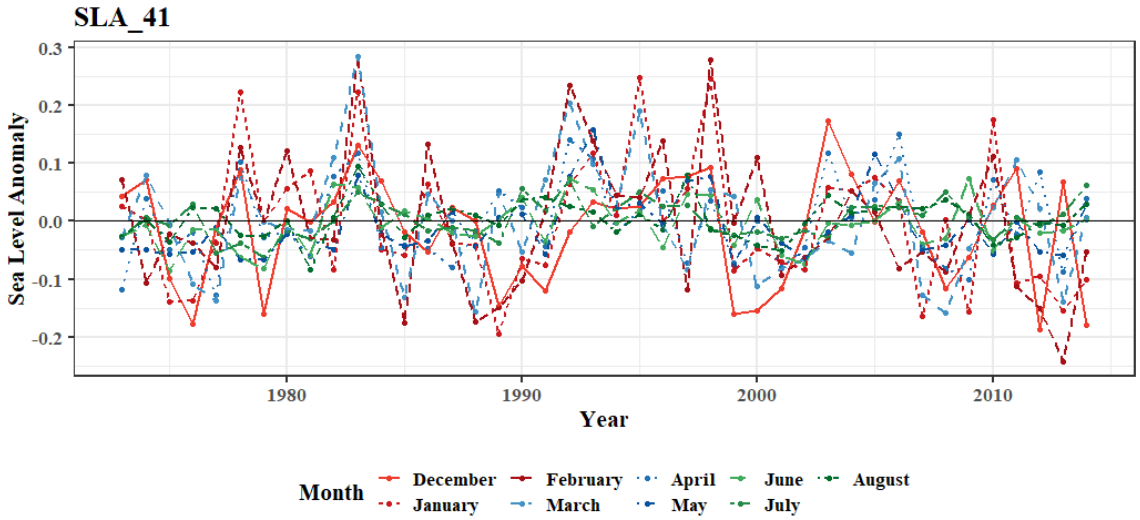
SLA_41
Sea Level Anomaly
0.3
0.2
0.1
0.0
-0.1
-0.2
1980
1990
2000
2010
Year
Month
December
January
February
March
April
May
June
July
August

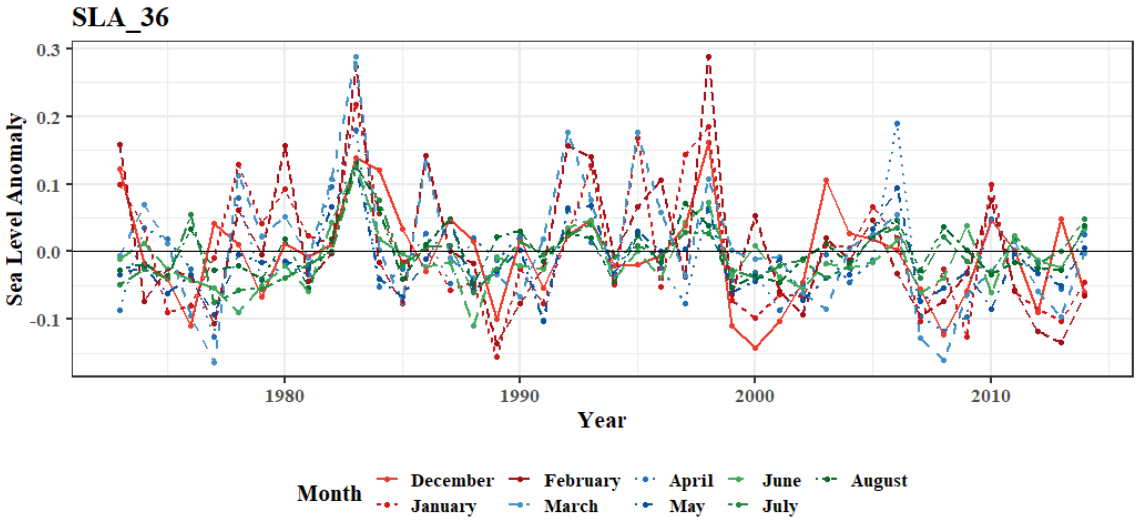
SLA_36
Sea Level Anomaly
0.3
0.2
0.1
0.0
-0.1
1980
1990
2000
2010
Year
Month
December
January
February
March
April
May
June
July
August

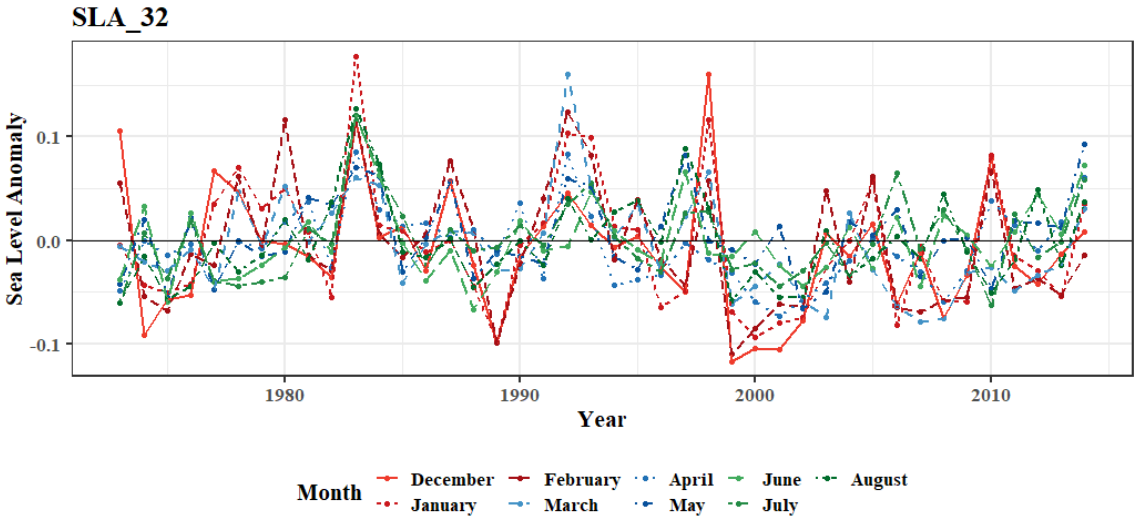
SLA_32
Sea Level Anomaly
0.1
0.0
-0.1
1980
1990
2000
2010
Year
Month
December
January
February
March
April
May
June
July
August

(C)

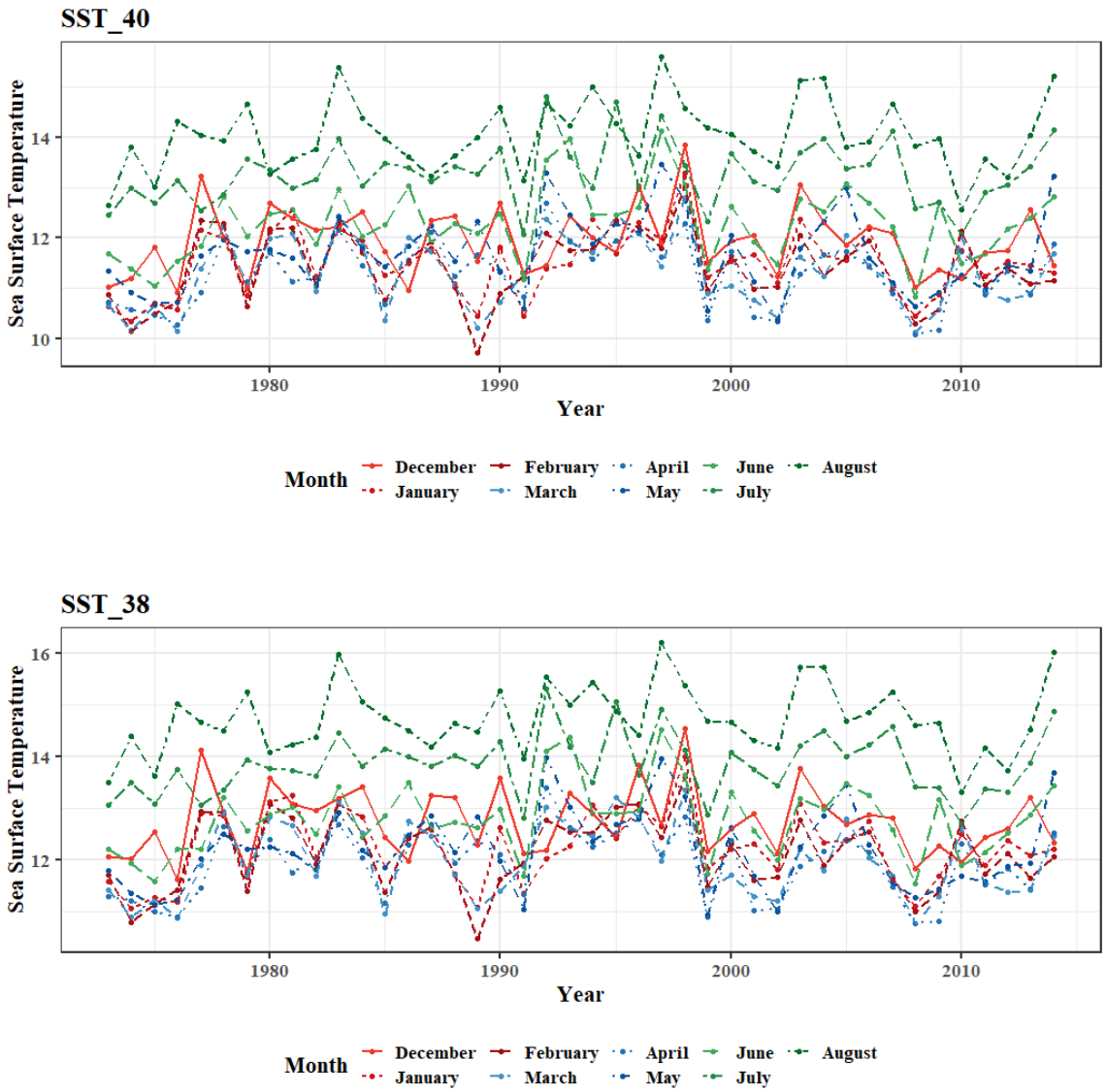
SST_40
Sea Surface Temperature
14
12
10
1980
1990
2000
2010
Year
Month
December
January
February
March
April
May
June
July
August
SST_38
Sea Surface Temperature
16
14
12
1980
1990
2000
2010
Year
Month
December
January
February
March
April
May
June
July
August

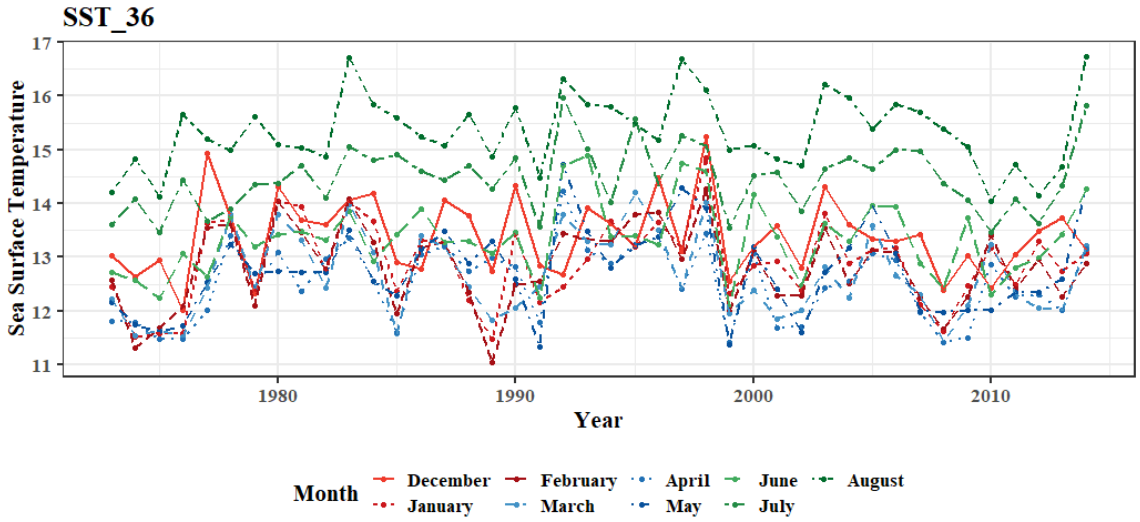
SST_36
Sea Surface Temperature
17
16
15
14
13
12
11
1980
1990
2000
2010
Year
Month
December
January
February
March
April
May
June
July
August

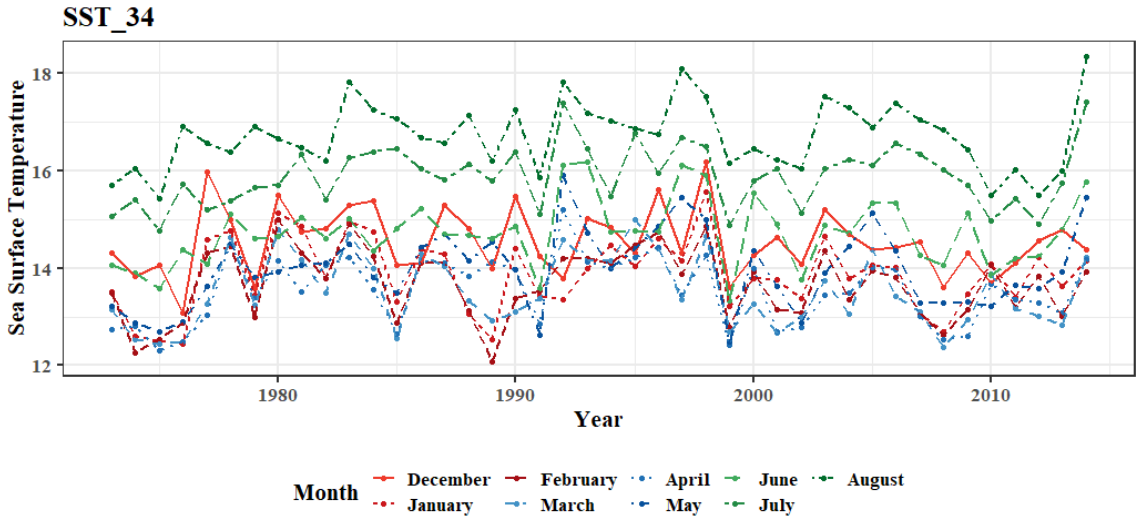
SST_34
Sea Surface Temperature
18
16
14
12
1980
1990
2000
2010
Year
Month
December
January
February
March
April
May
June
July
August

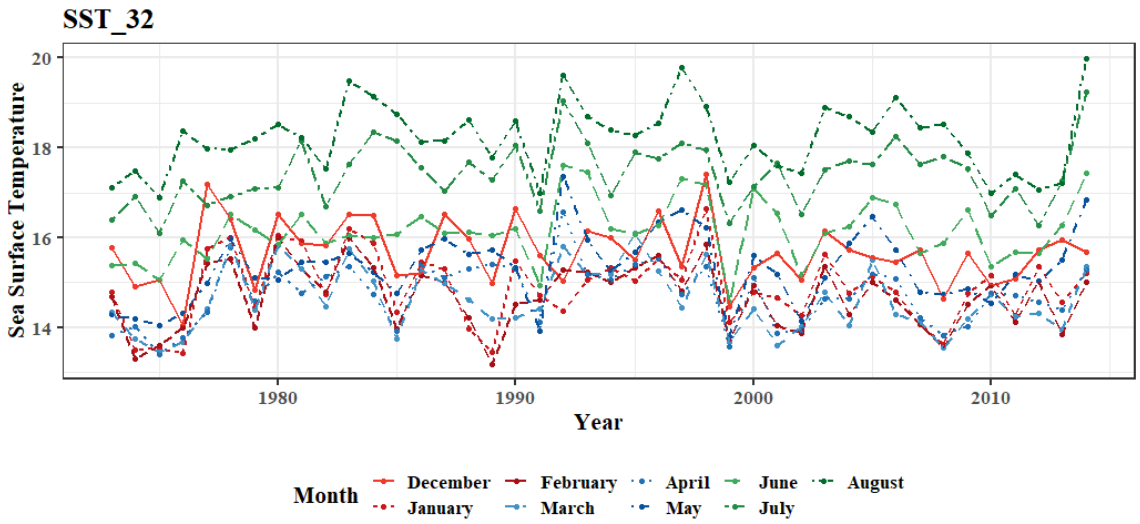
SST_32
Sea Surface Temperature
20
18
16
14
1980
1990
2000
2010
Year
Month
December
January
February
March
April
May
June
July
August

(D)

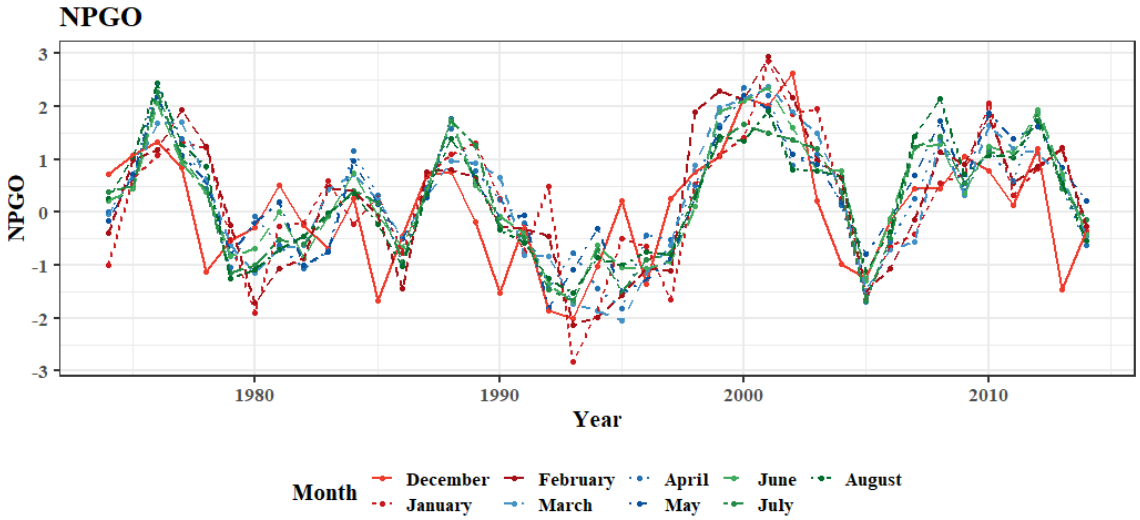
NPGO
NPGO
3
2
1
0
-1
-2
-3
1980
1990
2000
2010
Year
Month
December
January
February
March
April
May
June
July
August

(E)

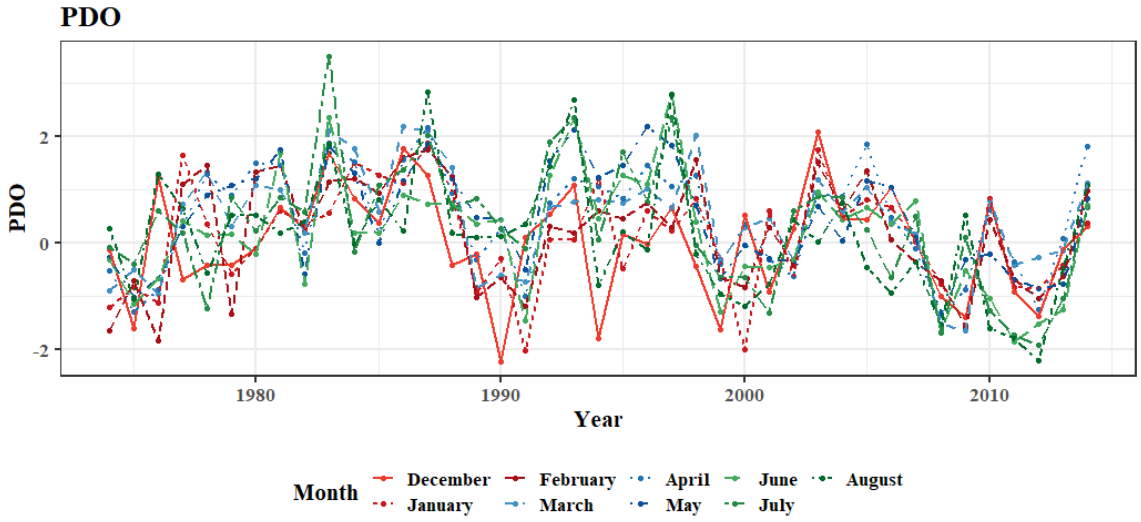
PDO
PDO
2
0
-2
1980
1990
2000
2010
Year
Month
December
January
February
March
April
May
June
July
August

(F)

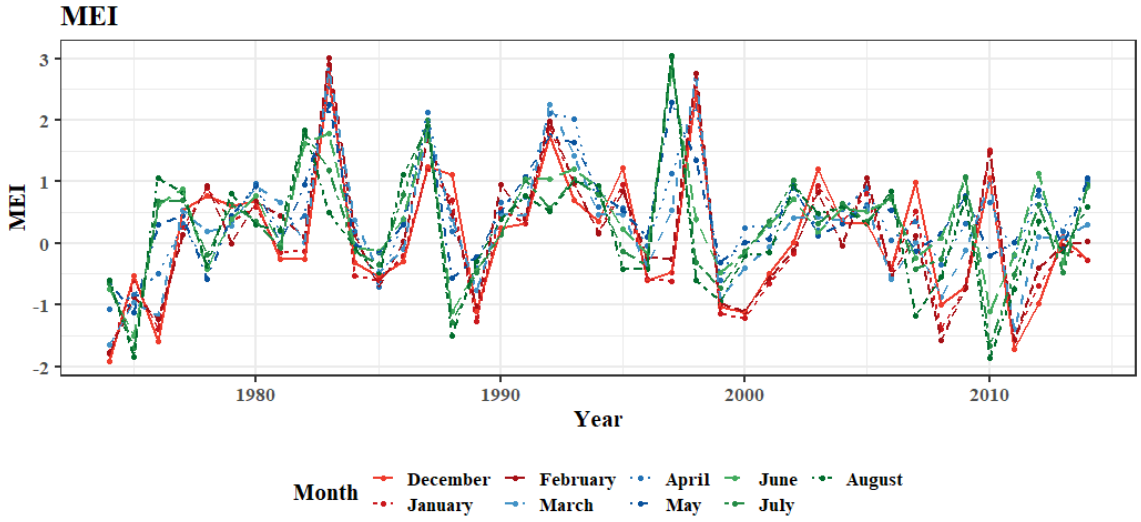
MEI
MEI
3
2
1
0
-1
-2
1980
1990
2000
2010
Year
Month
December
January
February
March
April
May
June
July
August

APPENDIX B

Appendix B: Correlation are presented between final models and sensitivity runs for the six stock assessments which underwent landings apportioning. The bottom shows simple linear regression between all models, and the top shows the correlation coefficient and p-value ($\alpha = 0.05$). The figures are shown from north to south- (A) Eureka, (B) Ft Bragg, (C) Bodega, (D) San Francisco, (E) Morro, (F) Southern. Monterey was the only port-complex that did not undergo sensitivity analysis for landing proportion because the CALCOM region designation matches our latitudinal boundaries for port-complex (Figure 4). Of the other six port-complexes, Eureka and Southern showed the greatest change in recruitment deviations with adjustments to landings. As these two port-complexes are the farthest from the center of the population and therefore are the most data-limited, it is unsurprising that they are the most sensitive to change. Even so, there was a substantial amount of agreement with less than 2% difference between any sensitivity scenario and the final models. Due to the stability of recruitment deviations through a variety of landings proportions, I decided that there was justification to continue with the degree of spatial discretion between our models.

(A)

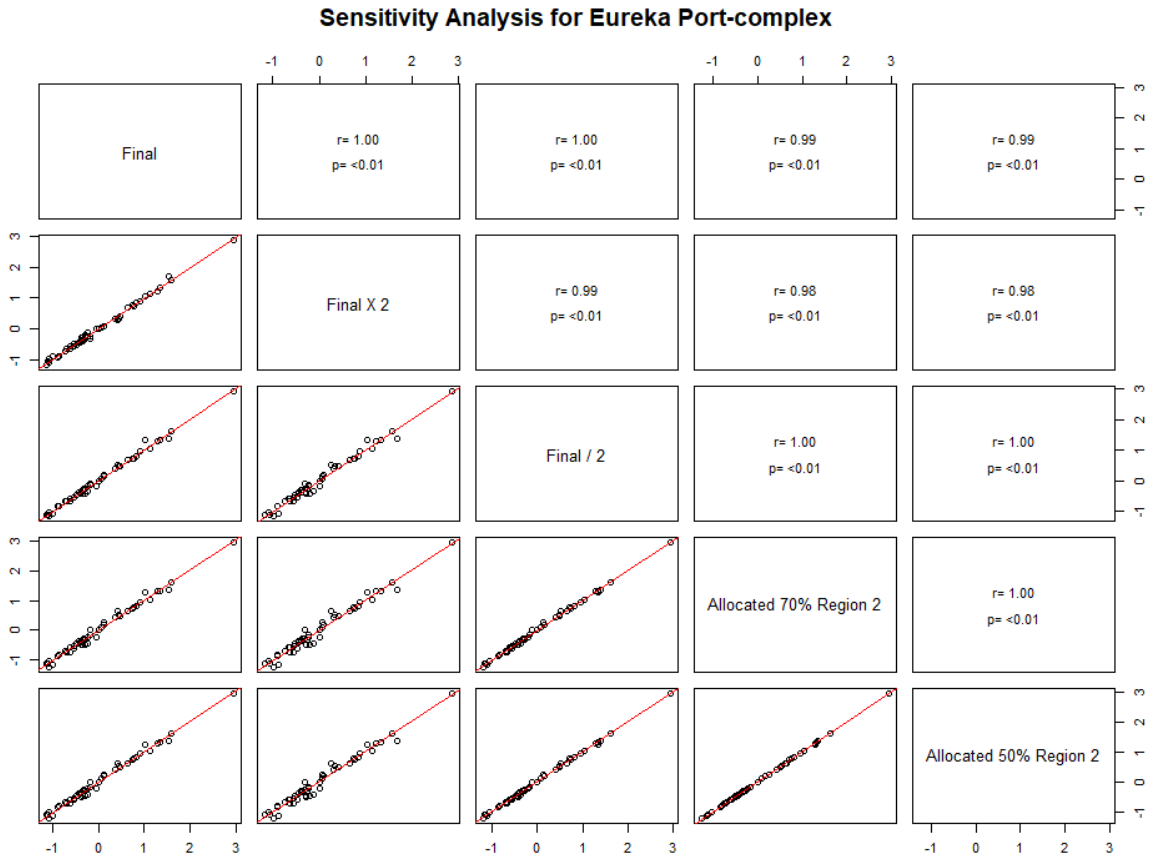
Sensitivity Analysis for Eureka Port-complex
Final
r= 1.00
p= <0.01
r= 1.00
p= <0.01
r= 0.99
p= <0.01
r= 0.99
p= <0.01
Final X 2
r= 0.99
p= <0.01
r= 0.98
p= <0.01
r= 0.98
p= <0.01
Final / 2
r= 1.00
p= <0.01
r= 1.00
p= <0.01
Allocated 70% Region 2
r= 1.00
p= <0.01
Allocated 50% Region 2
-1
0
1
2
3

(B)

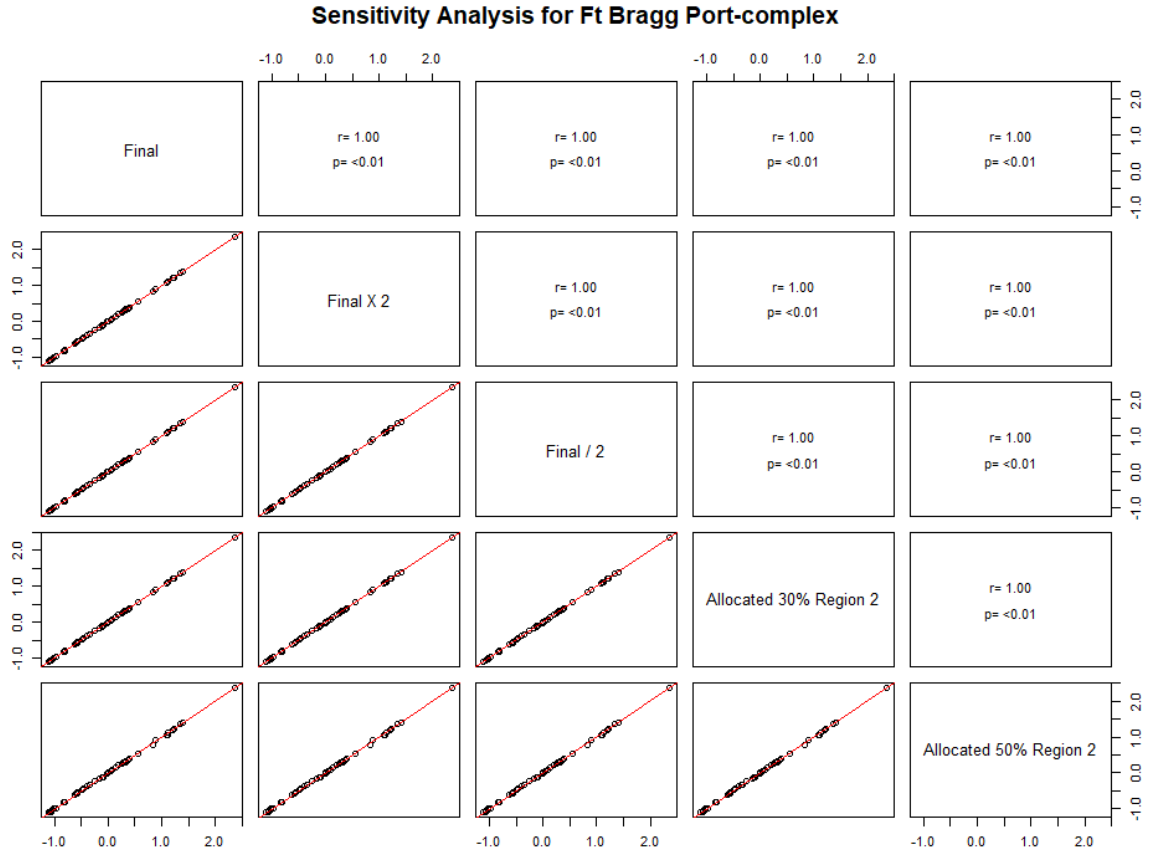
Sensitivity Analysis for Ft Bragg Port-complex
Final
Final X 2
Final / 2
Allocated 30% Region 2
Allocated 50% Region 2
r= 1.00
p= <0.01
-1.0
0.0
1.0
2.0

(C)

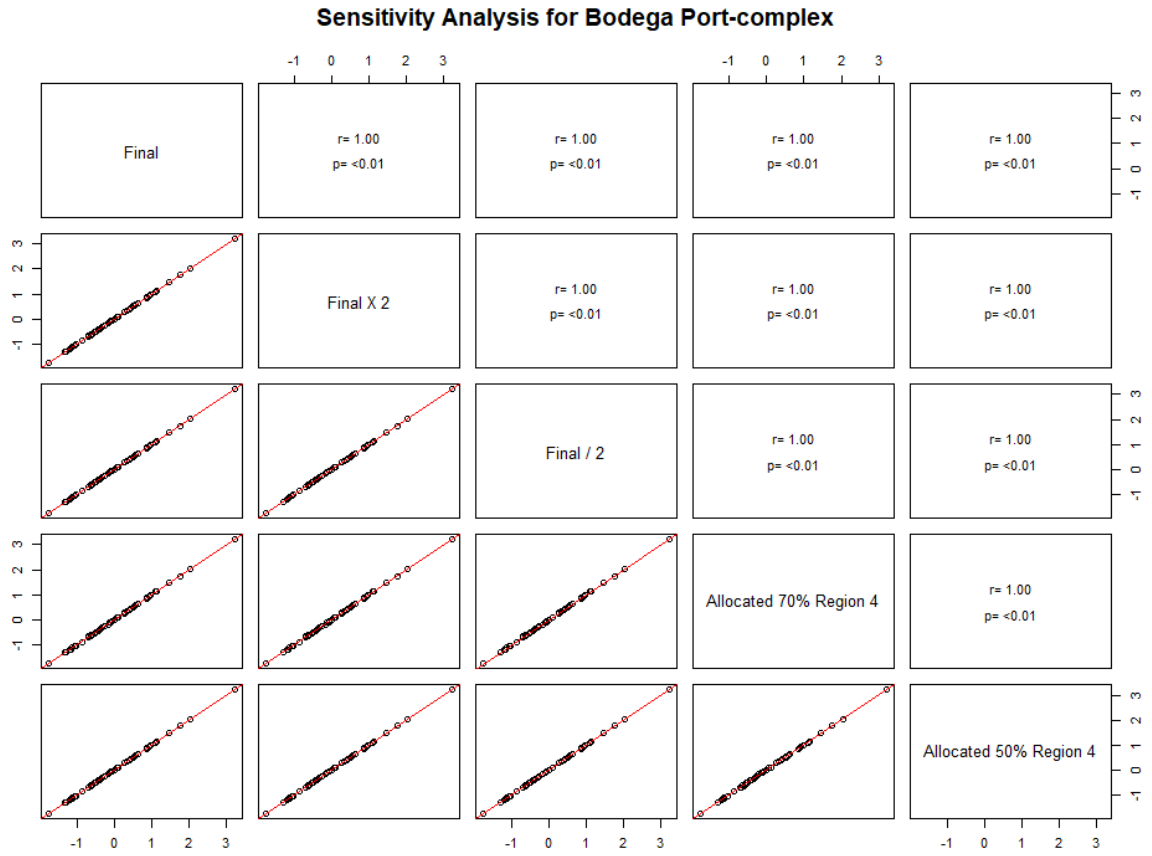
Sensitivity Analysis for Bodega Port-complex
Final
Final X 2
Final / 2
Allocated 70% Region 4
Allocated 50% Region 4
r= 1.00
p= <0.01

(D)

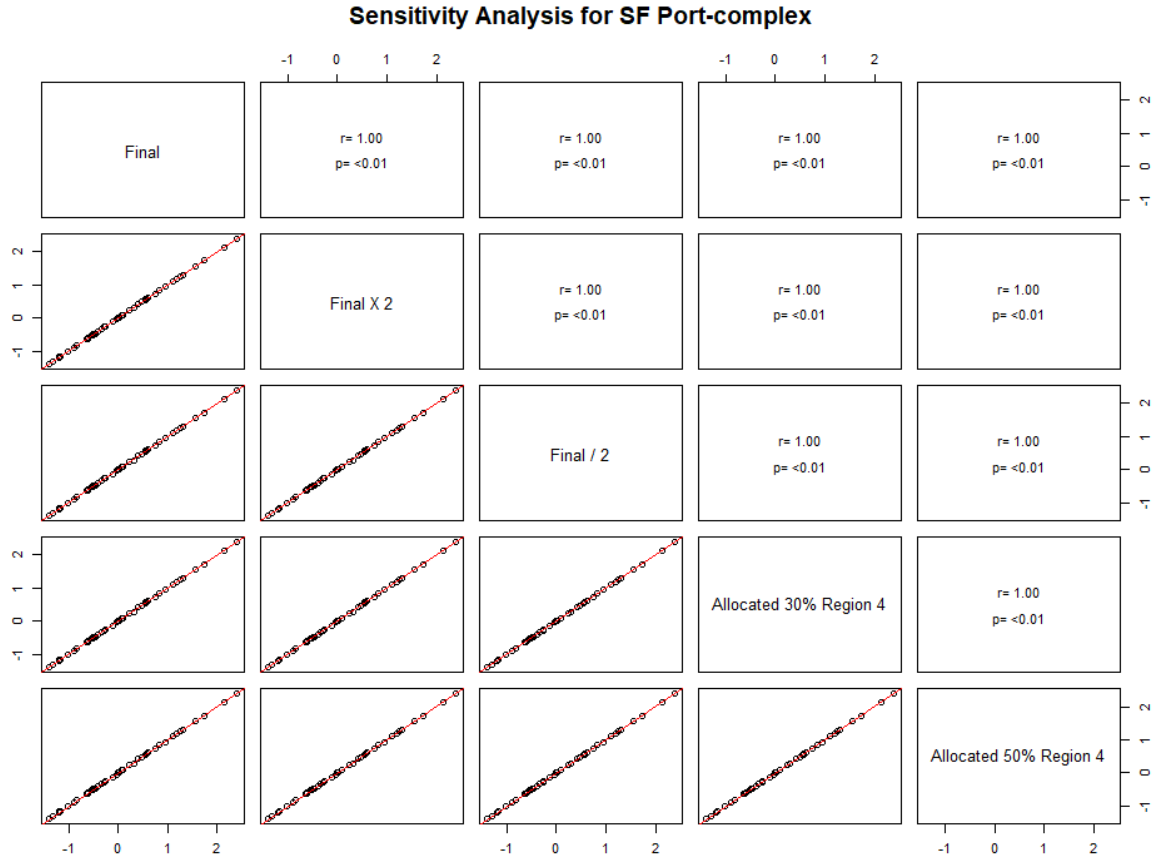
Sensitivity Analysis for SF Port-complex
Final
Final X 2
Final / 2
Allocated 30% Region 4
Allocated 50% Region 4
r= 1.00
p= <0.01

(E)

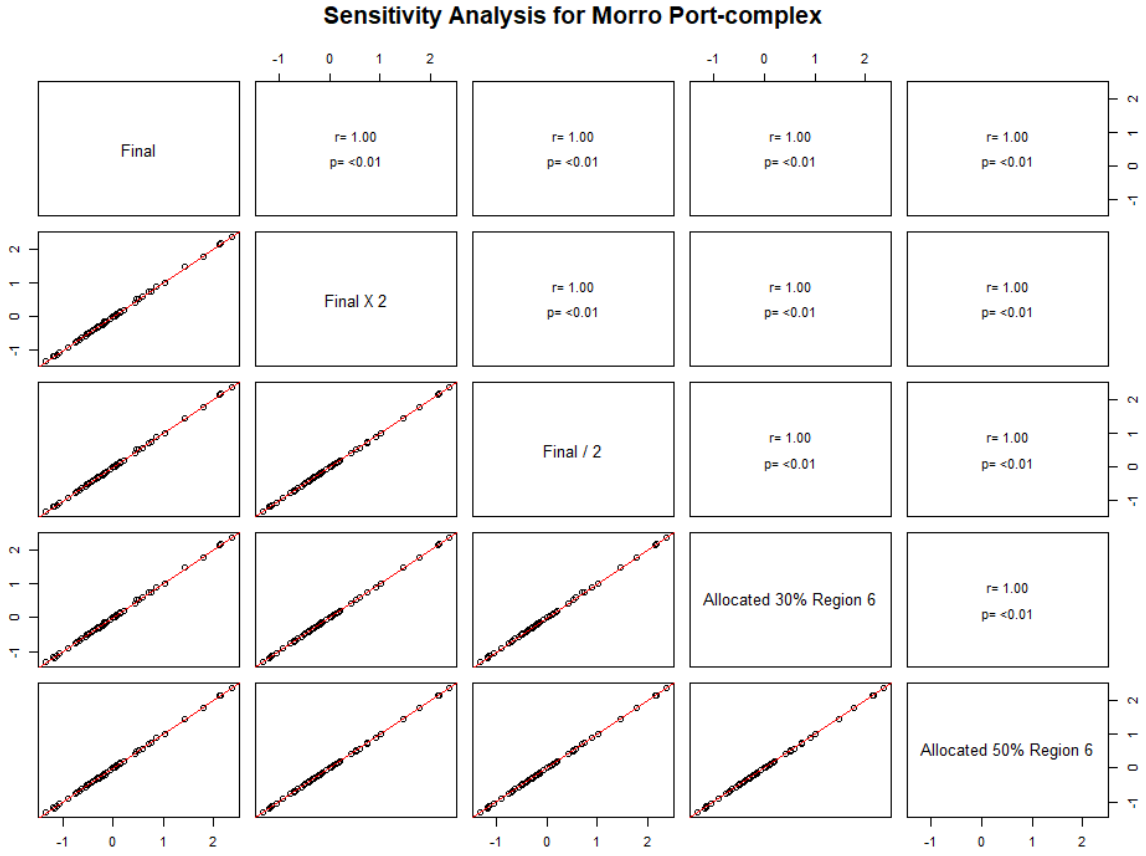
Sensitivity Analysis for Morro Port-complex
Final
r= 1.00
p= <0.01
Final X 2
Final / 2
Allocated 30% Region 6
Allocated 50% Region 6
-1
0
1
2

(F)

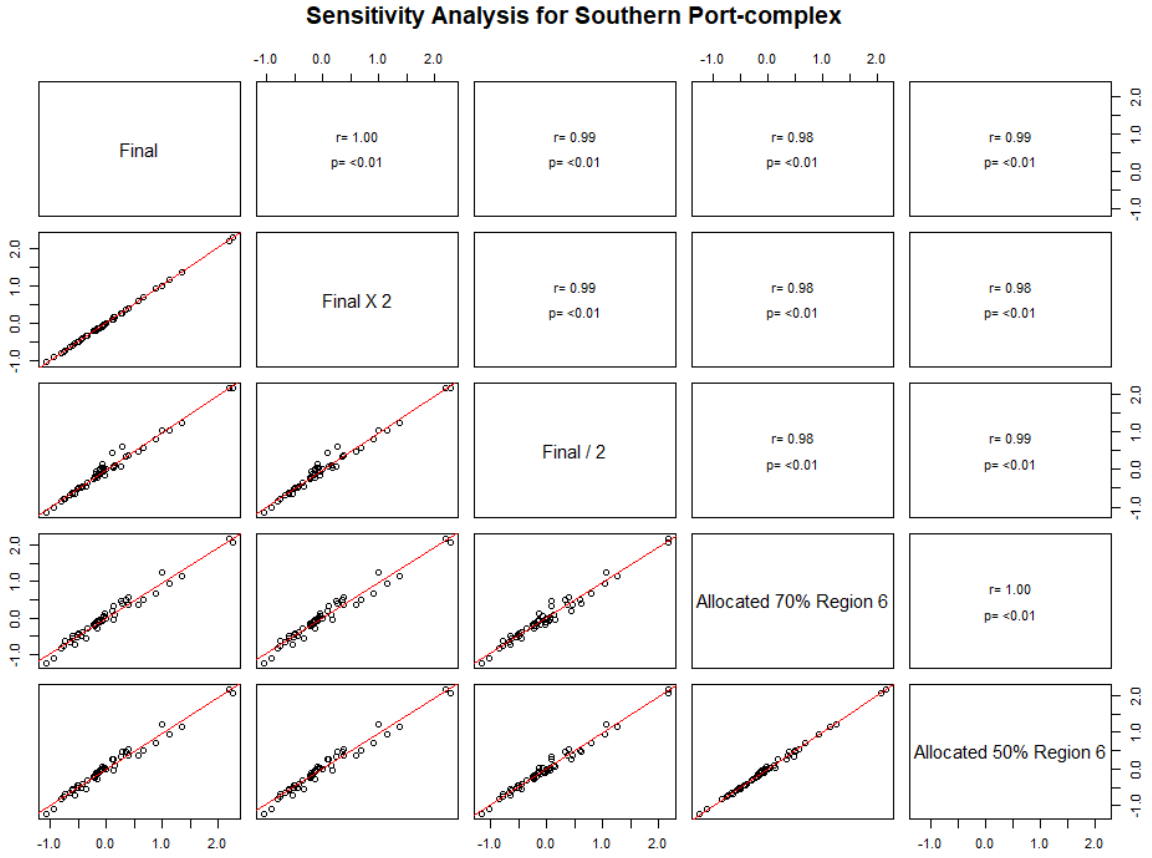
Sensitivity Analysis for Southern Port-complex
Final
r= 1.00
p= <0.01
r= 0.99
p= <0.01
r= 0.98
p= <0.01
r= 0.99
p= <0.01
Final X 2
r= 0.99
p= <0.01
r= 0.98
p= <0.01
r= 0.98
p= <0.01
Final / 2
r= 0.98
p= <0.01
r= 0.99
p= <0.01
Allocated 70% Region 6
r= 1.00
p= <0.01
Allocated 50% Region 6
-1.0
0.0
1.0
2.0

APPENDIX C

Appendix C: Port-complex-specific recruitment deviation estimates from local stock assessment models plotted with 95% confidence intervals. The figures are shown from north to south- (A) Eureka, (B) Ft Bragg, (C) Bodega, (D) San Francisco, (E) Monterey, (F) Morro Bay, (G) Southern, and finally the coastwide model (H) California. Dark blue indicates the estimated recruitment deviations, and light blue lines indicate the 95% confidence intervals. Southern distinctively shows the greatest uncertainty across ports, but deviations are comparable to other port-complexes from 1999 forward. Port-complexes show the greatest uncertainty in moderate recruitment years (1985-1998, 2005-2007).

(A)

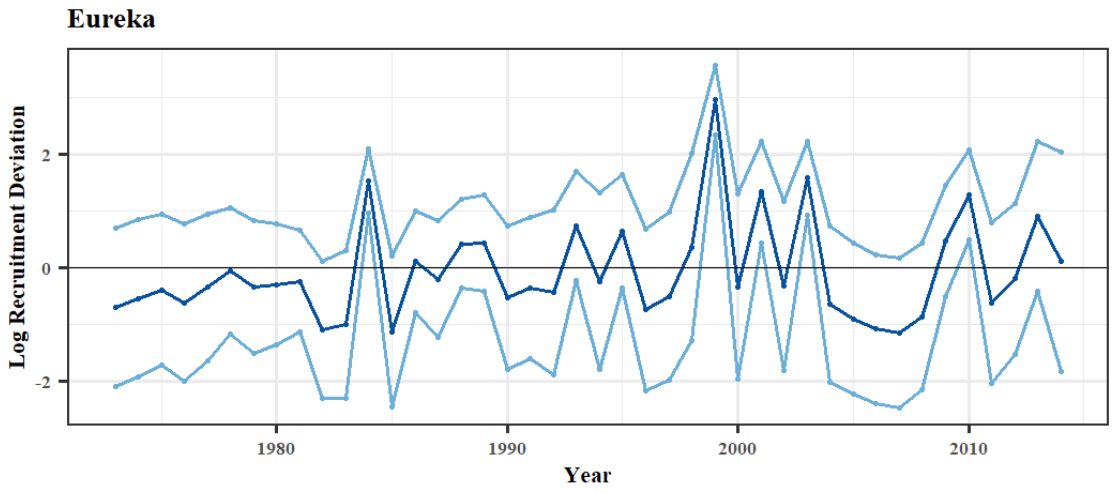

(B)

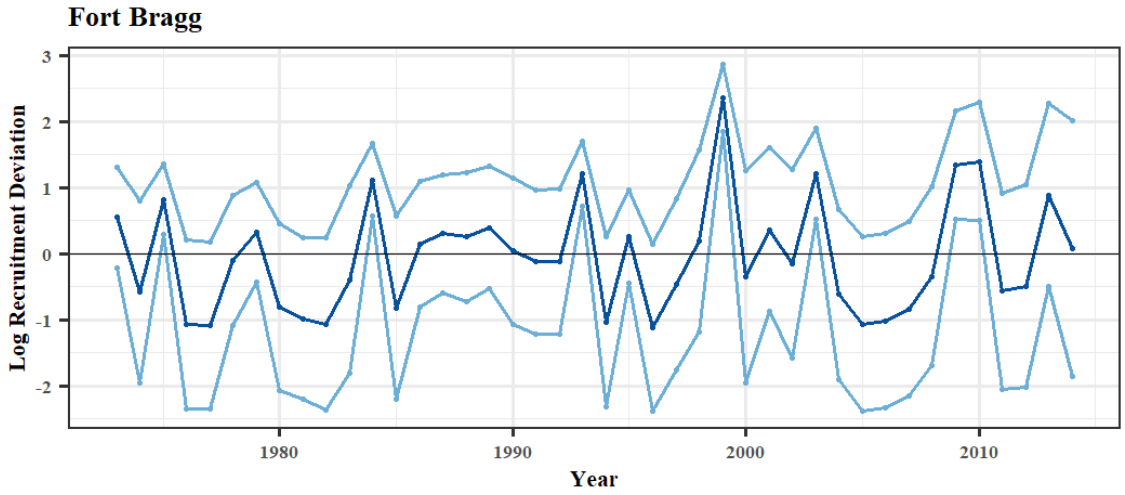
Fort Bragg
Log Recruitment Deviation
3
2
1
0
-1
-2
1980
1990
2000
2010
Year

(C)

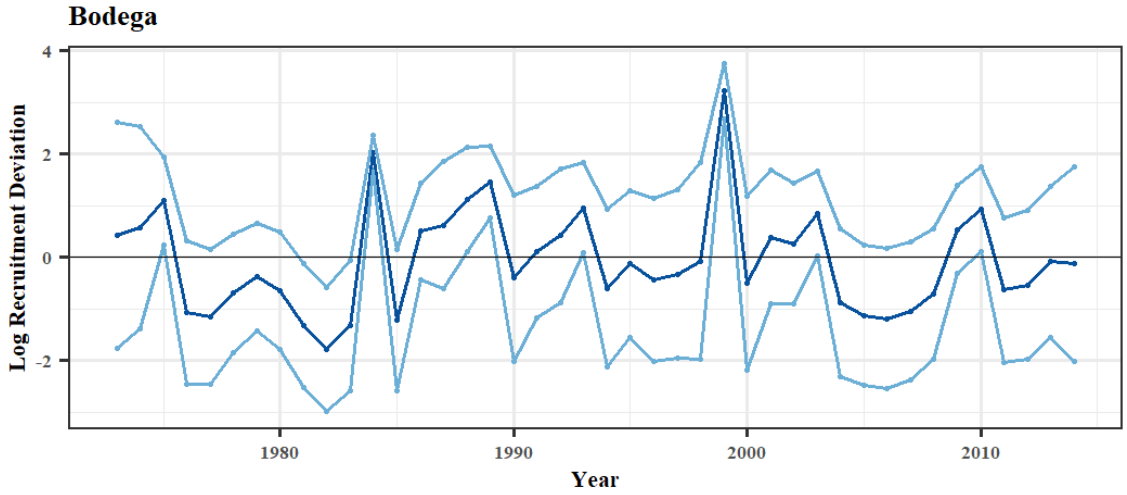
Bodega
Log Recruitment Deviation
4
2
0
-2
1980
1990
2000
2010
Year

(D)

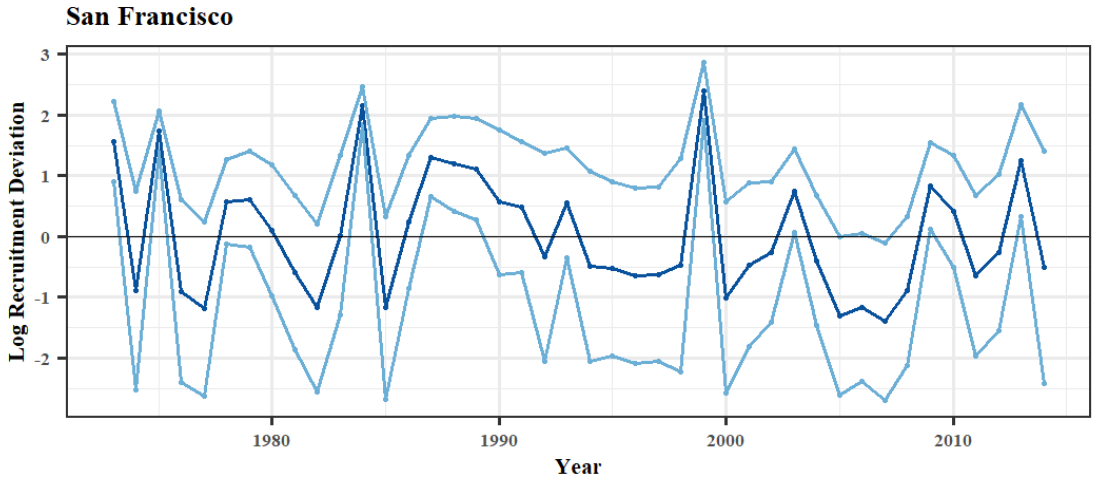
San Francisco
Log Recruitment Deviation
3
2
1
0
-1
-2
1980
1990
2000
2010
Year

(E)

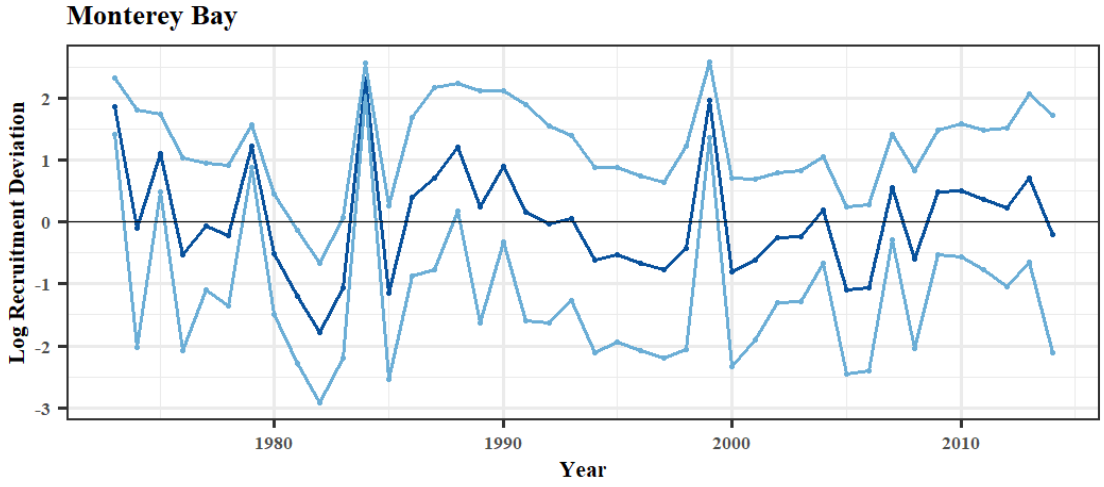
Monterey Bay
Log Recruitment Deviation
2
1
0
-1
-2
-3
1980
1990
2000
2010
Year

(F)

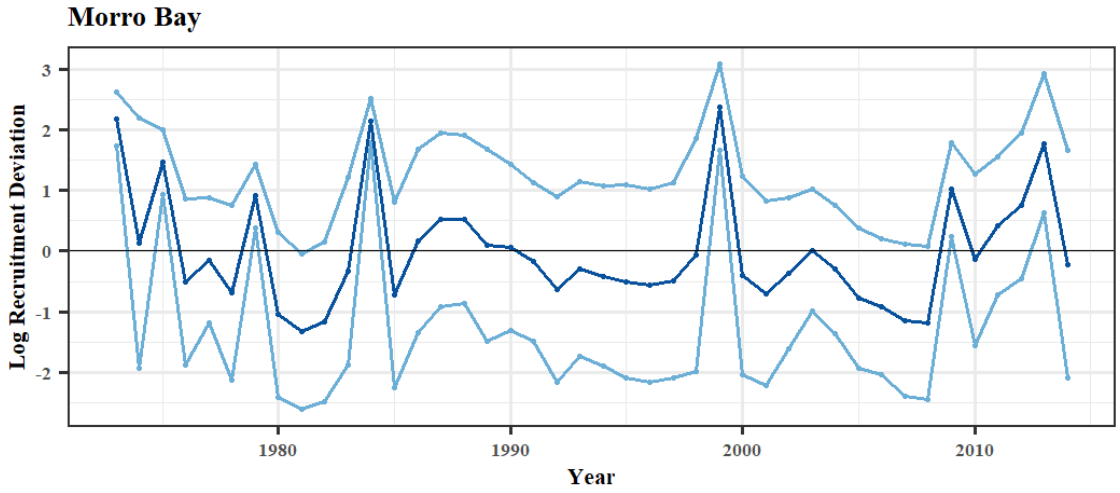
Morro Bay
Log Recruitment Deviation
3
2
1
0
-1
-2
1980
1990
2000
2010
Year

(G)

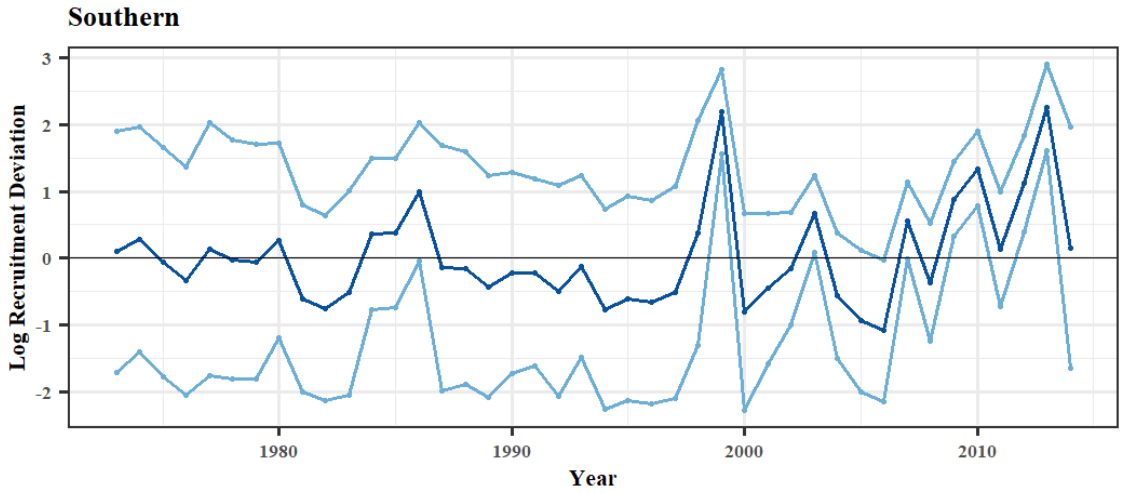
Southern
Log Recruitment Deviation
3
2
1
0
-1
-2
1980
1990
2000
2010
Year

(H)

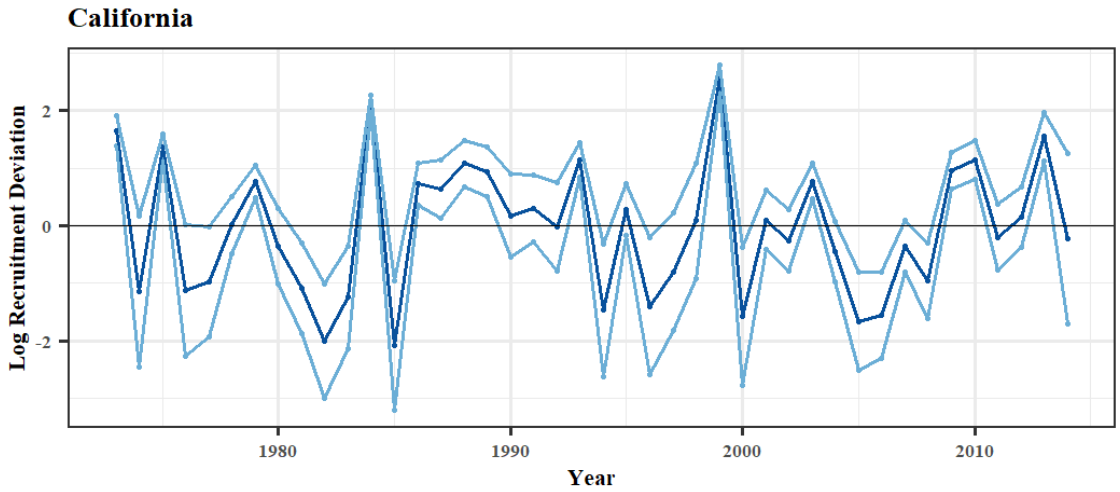
California
Log Recruitment Deviation
2
0
-2
1980
1990
2000
2010
Year

APPENDIX D

Appendix D: The frequency distribution of capture of young Chilipepper Rockfish is shown across latitudes surveyed by the Northwest Fisheries Science Center (NWFSC) groundfish surveys. Age-0 and -1 fish are almost exclusively captured at southern latitudes, which could imply bias in the survey due to variability in timing of survey and age of individuals (early summer vs. late summer and the respective difference in size of individuals), bias of survey habitat coverage throughout the coast, variability in growth rate of individuals throughout the coast, variability in natural mortality rate throughout the coast, or it could be empirical evidence for equatorward alongshore transport of young-of-the-year and subsequent northward propagation of young adults. Plots are shown for (A) age-0, (B) age-1, (C) age-2, (D) age-3, and (E) distribution of all individuals captured by the NWFSC surveys. While the latitudes presented here span from 32°N to 48°N while this study only spans form 32°N to 42°N.

(A)

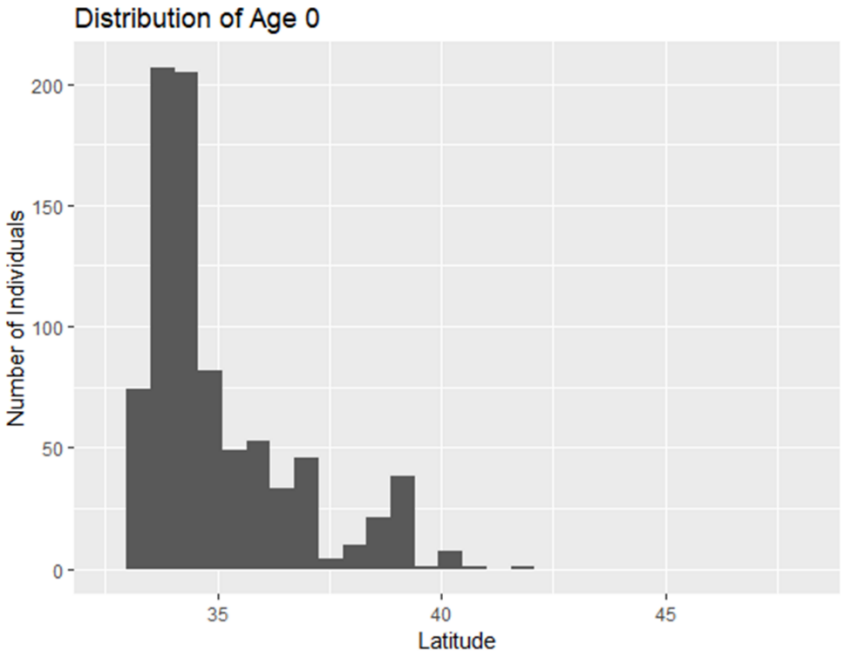

(B)

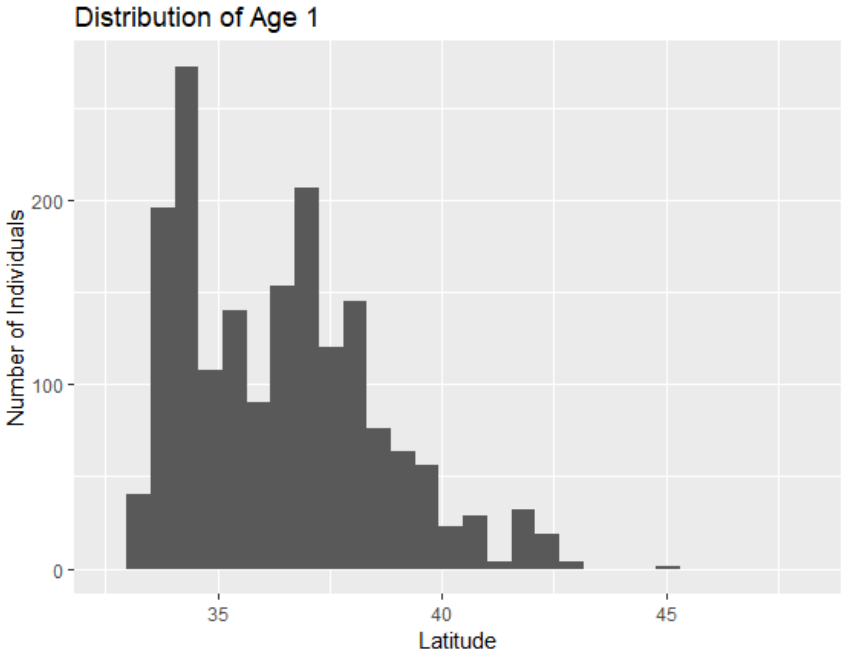
Distribution of Age 1
Number of Individuals
200
100
0
35
40
45
Latitude

(C)

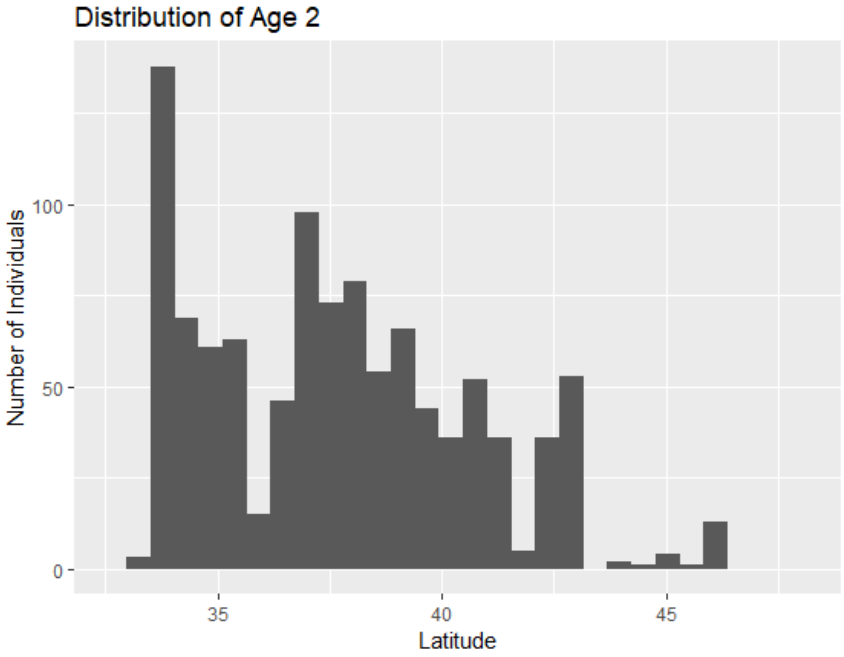
Distribution of Age 2
Number of Individuals
100
50
0
35
40
45
Latitude

(D)

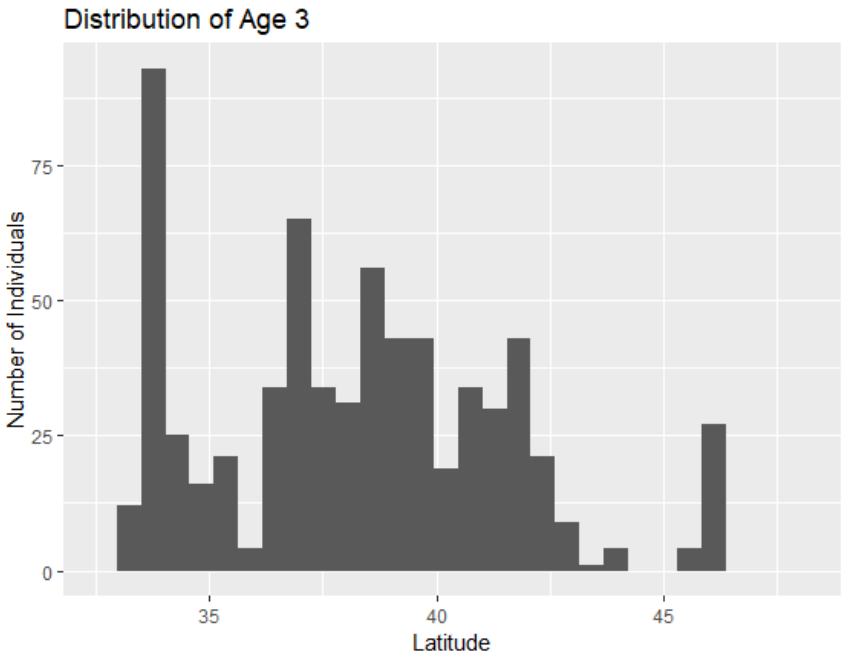
Distribution of Age 3
Number of Individuals
75
50
25
0
35
40
45
Latitude

(E)

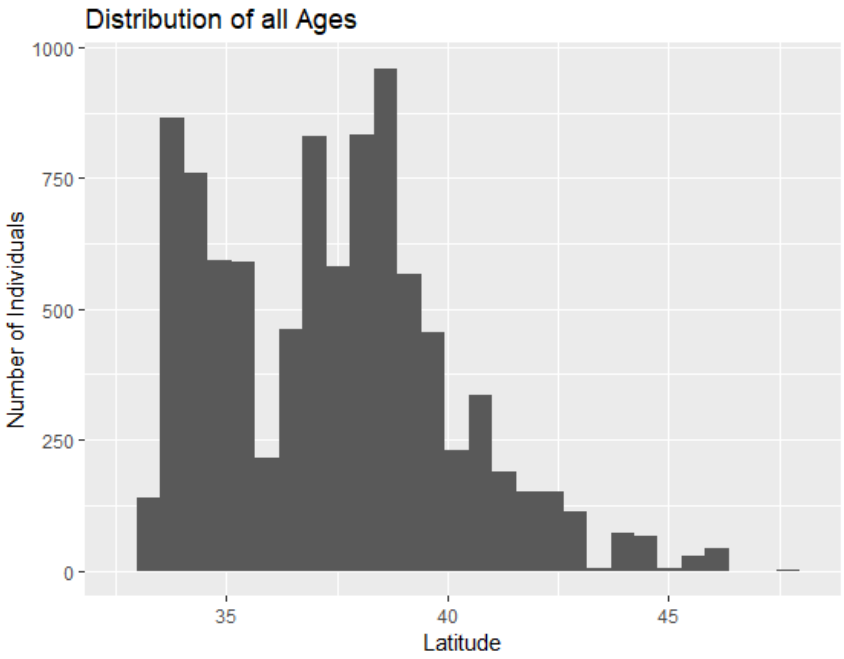
Distribution of all Ages
Number of Individuals
1000
750
500
250
0
35
40
45
Latitude

APPENDIX E

Appendix E: Port-complex-specific recruitment deviation estimates from local stock assessment models plotted against predicted model fits from all generalized additive models with ΔAICc < 2. The figures are shown from north to south- (A) Eureka, (B) Ft Bragg, (C) Bodega, (D) San Francisco, (E) Monterey, (F) Morro Bay, (G) and Southern. Refer to Table 8 for each model covariates and extended details about deviance explained and AICc scores of models.

(A)

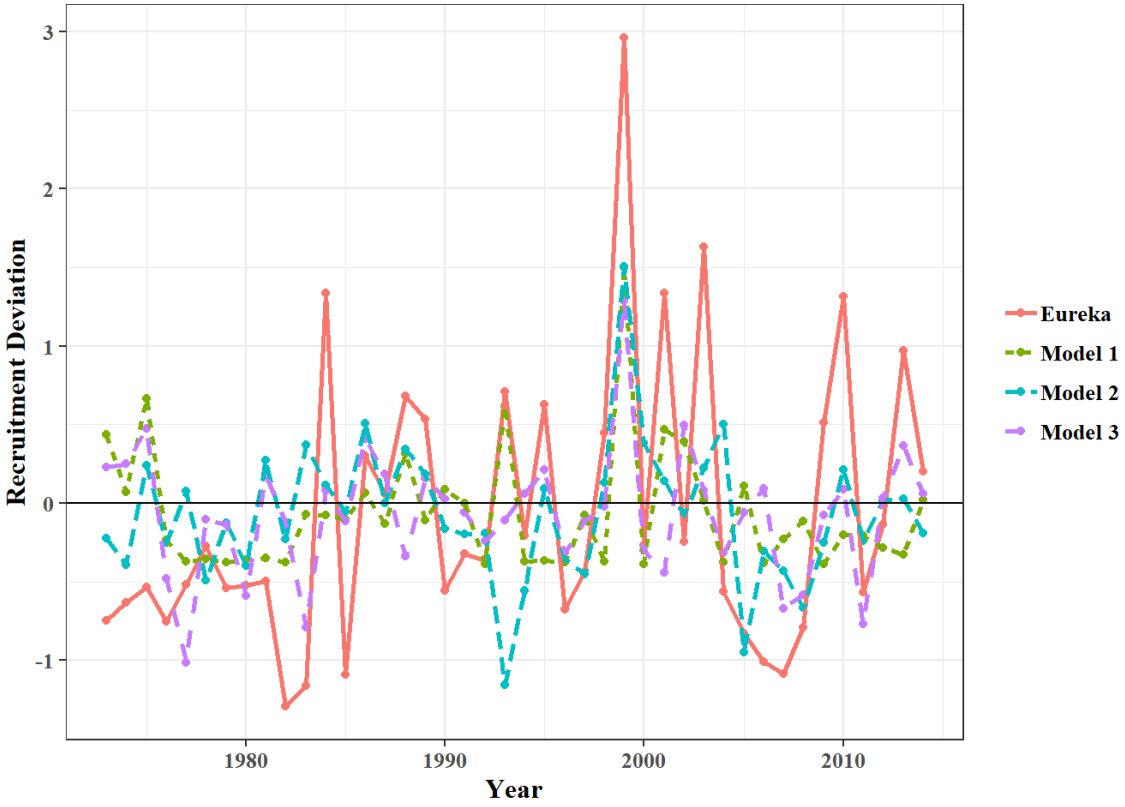

(B)

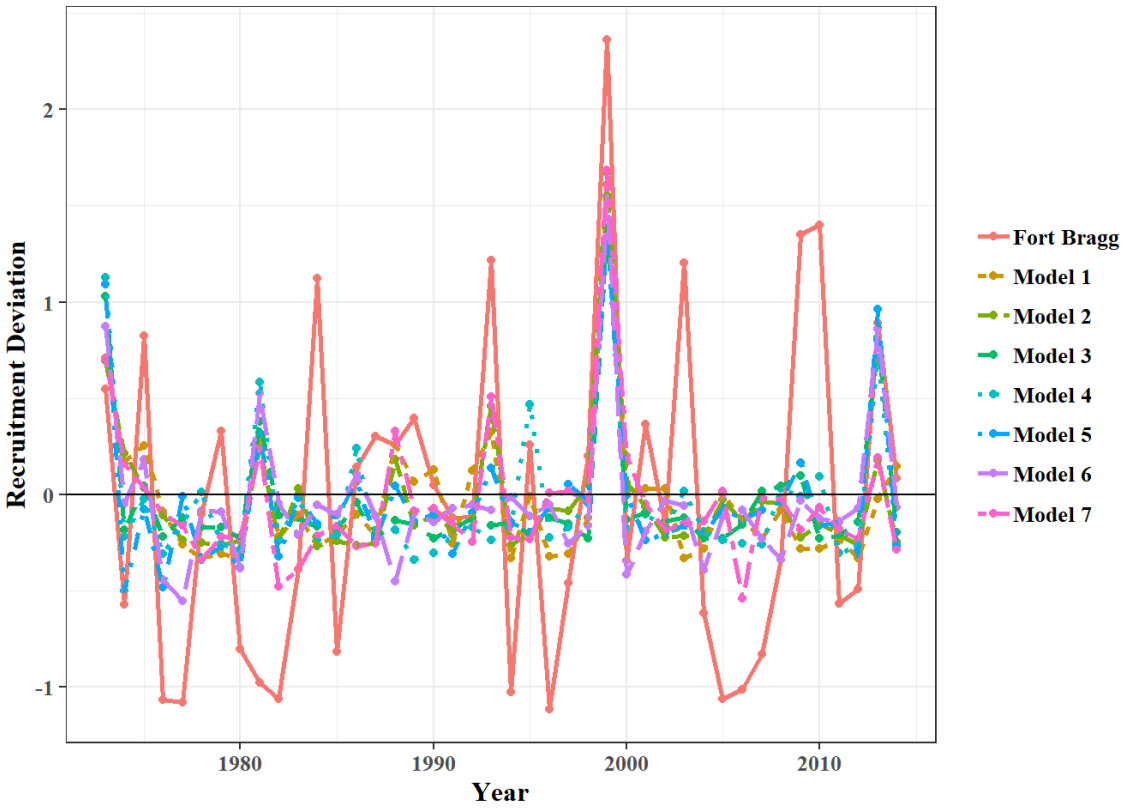
Recruitment Deviation
2
1
0
-1
1980
1990
2000
2010
Year
Fort Bragg
Model 1
Model 2
Model 3
Model 4
Model 5
Model 6
Model 7

(C)

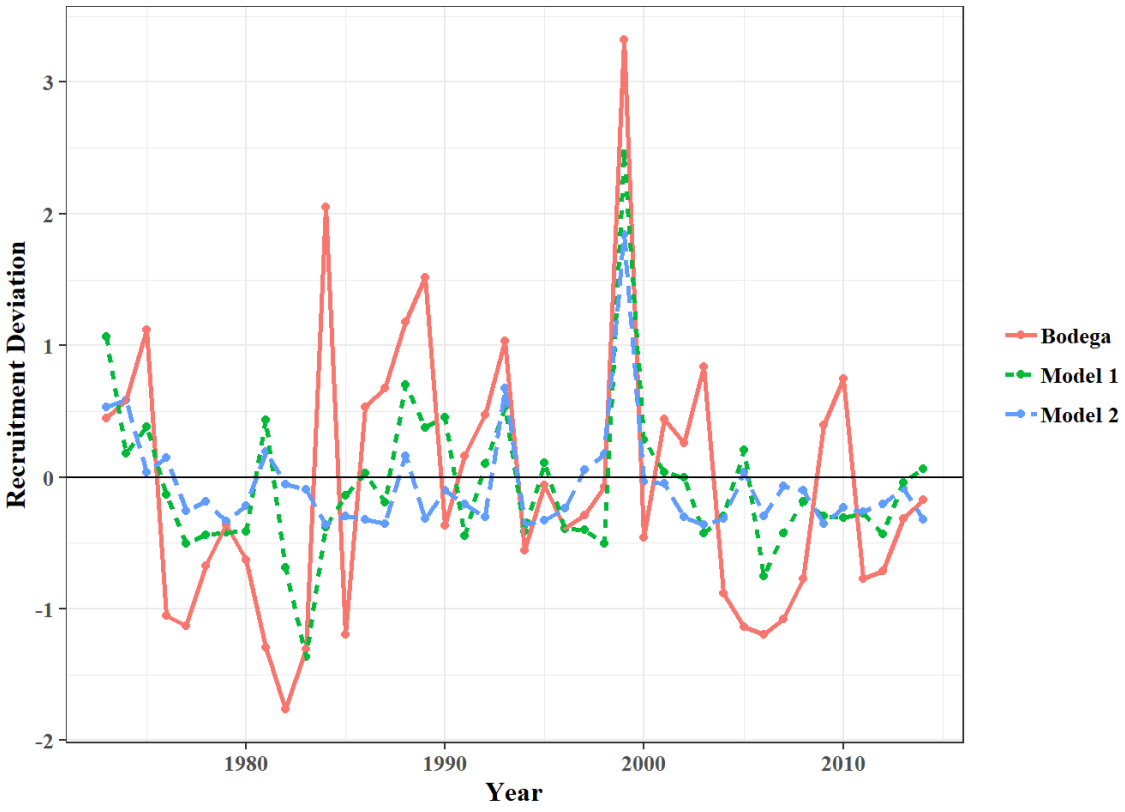
Recruitment Deviation
3
2
1
0
-1
-2
1980
1990
2000
2010
Year
Bodega
Model 1
Model 2

(D)

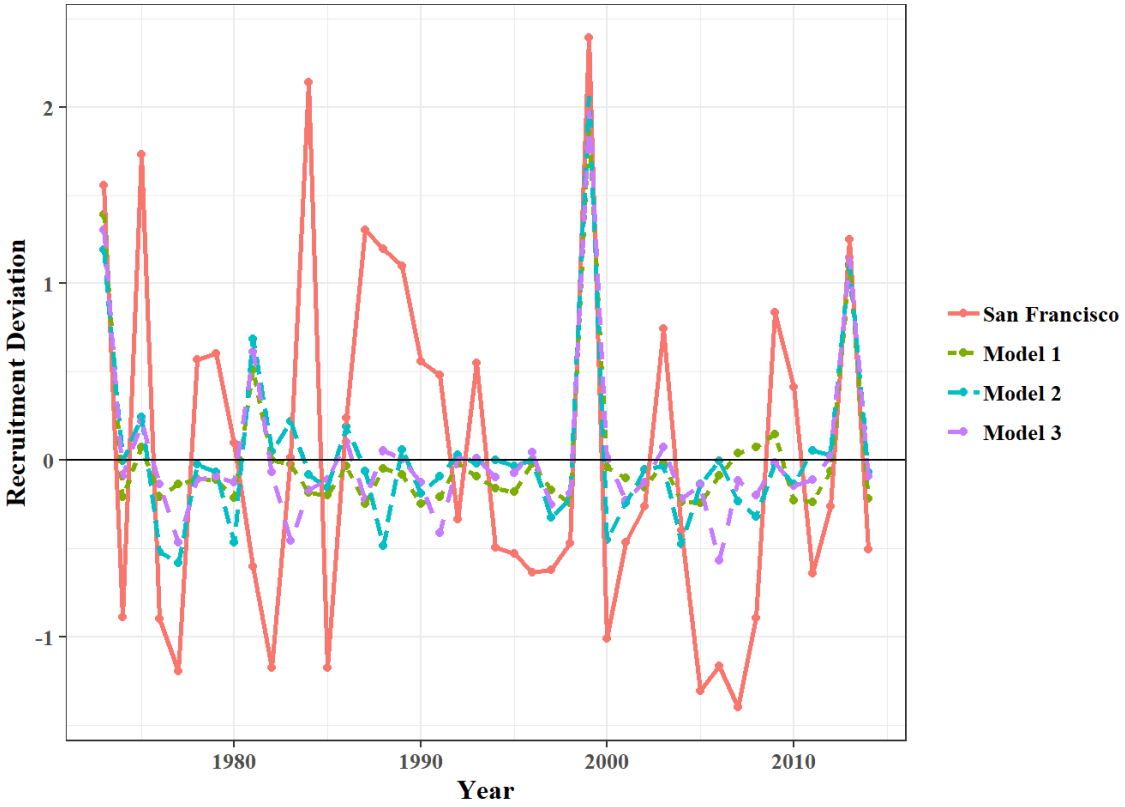
Recruitment Deviation
2
1
0
-1
1980
1990
2000
2010
Year
San Francisco
Model 1
Model 2
Model 3

(E)

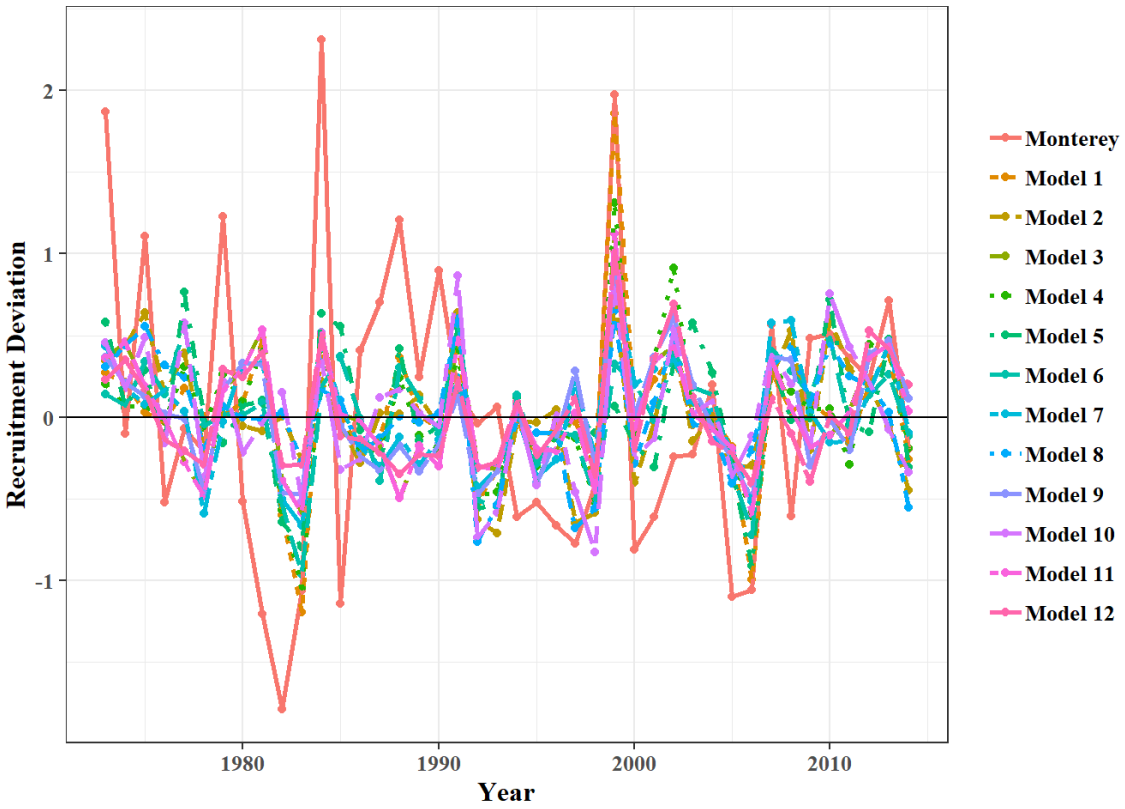
Recruitment Deviation
2
1
0
-1
1980
1990
2000
2010
Year
Monterey
Model 1
Model 2
Model 3
Model 4
Model 5
Model 6
Model 7
Model 8
Model 9
Model 10
Model 11
Model 12

(F)

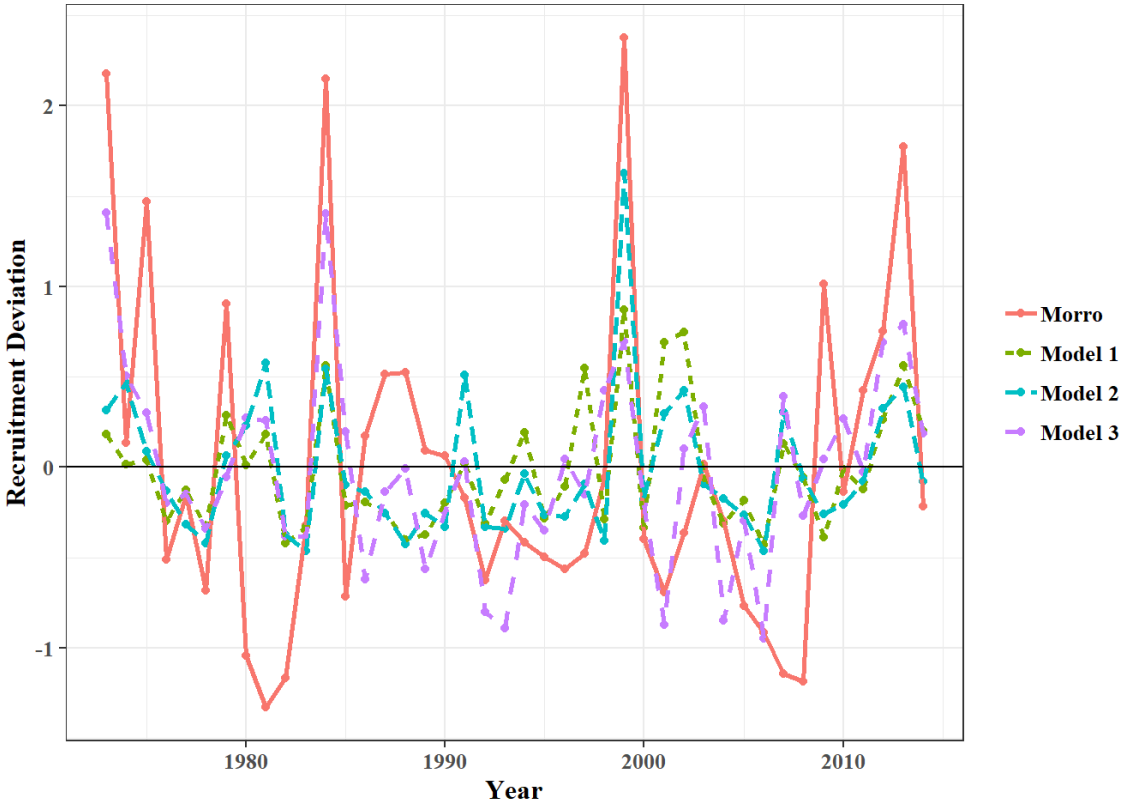
Recruitment Deviation
2
1
0
-1
1980
1990
2000
2010
Year
Morro
Model 1
Model 2
Model 3

(G)

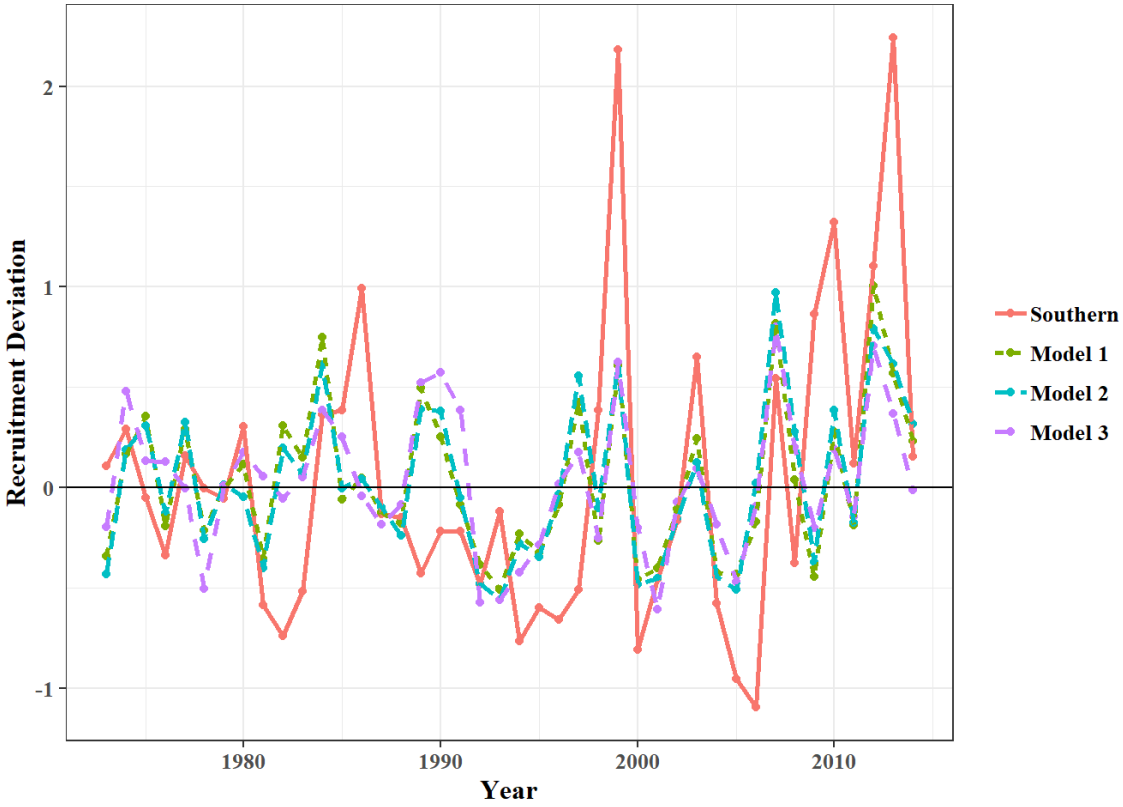
Recruitment Deviation
2
1
0
-1
1980
1990
2000
2010
Year
Southern
Model 1
Model 2
Model 3

APPENDIX F

Appendix F: As length and age data were subset for port-complex-specific stock assessments, I decided to also empirically examine biological characteristics that may vary latitudinally. I make no assertion that my seven port-complex designations are biologically-independent of one another, but as reproductive characteristics are known to vary throughout their range (Beyer et al. 2015; LeFebvre et al. 2018) I decided to take the opportunity to examine if growth characteristics vary as well, as these could contribute to variability in fecundity. First, I examined if growth varied across port-complexes by fitting the Von Bertalanffy growth curve, the curve used to describe length-at-age relationships for Chilipepper Rockfish (Field et al. 2015).

The equation for the Von Bertalanffy growth curve is

$$L(t) = L_{\infty}(1 - e^{-k(t-t_0)})$$

where L is length at time t, L_{∞} is the average maximum asymptotic length, k is the rate at which L_{∞} is reached, and t_0 is the hypothetical length when age is zero. I parameterized the Von Bertalanffy growth curve with non-linear least squares regression using the nls function from the "stats" package in r (Bates & Chambers, 1992). Chilipepper Rockfish are known to exhibit sex-specific growth parameters (males tend to grow faster and reach a smaller maximum length, while females grow slower but reach a larger maximum length), so separate models were fit for male and female growth for each port-complex. The parameters of the growth curve were then compared between port-complexes, and a significant difference was determined based on the bounds of the 95% confidence intervals for each parameter.

		Eureka	Fort Bragg	Bodega	San Francisco	Monterey	Morro Bay	Southern
Female	**L_{inf} (CI 95%)**	50.42, (49.49 to 51.45)	50.49, (49.80 to 51.23)	48.91, (48.46 to 49.37)	49.70, (48.91 to 50.54)	51.73, (50.09 to 53.58)	52.30, (51.06 to 53.65)	51.06, (50.06 to 52.13)
Female	**k (CI 95%)**	0.20, (0.19 to 0.21)	0.197, (0.19 to 0.21)	0.22, (0.21 to 0.23)	0.19, (0.18 to 0.20)	0.18, (0.17 to 0.20)	0.16, (0.15 to 0.17)	0.17, (0.16 to 0.18)
Female	**t_0 (CI 95%)**	-0.86, (-1.03 to -0.71)	-0.96, (-1.05 to -0.87)	-0.87, (-0.95 to -0.78)	-1.10, (-1.20 to -1.01)	-1.10, (-1.22 to -0.98)	-1.30, (-1.39 to -1.20)	-1.46, (-1.53 to -1.41)
Male	**L_{inf} (CI 95%)**	35.41, (34.81 to 36.05)	35.72, (35.23 to 36.24)	36.01, (35.67 to 36.38)	35.34, (34.89 to 35.82)	35.62, (35.08 to 36.20)	37.10, (36.60 to 37.62)	35.97, (35.56 to 36.41)
Male	**k (CI 95%)**	0.33, (0.30 to 0.36)	0.35, (0.32 to 0.38)	0.35, (0.33 to 0.37)	0.35, (0.32 to 0.37)	0.34, (0.32 to 0.36)	0.30, (0.28 to 0.32)	0.28, (0.26 to 0.29)
Male	**t_0 (CI 95%)**	-0.88, (-1.13 to -0.67)	-0.74, (-0.91 to -0.58)	-0.81, (-0.94 to -0.69)	-0.77, (-0.91 to -0.65)	-0.79, (-0.90 to -0.69)	-0.94, (-1.06 to -0.82)	-1.41, (-1.50 to -1.33)

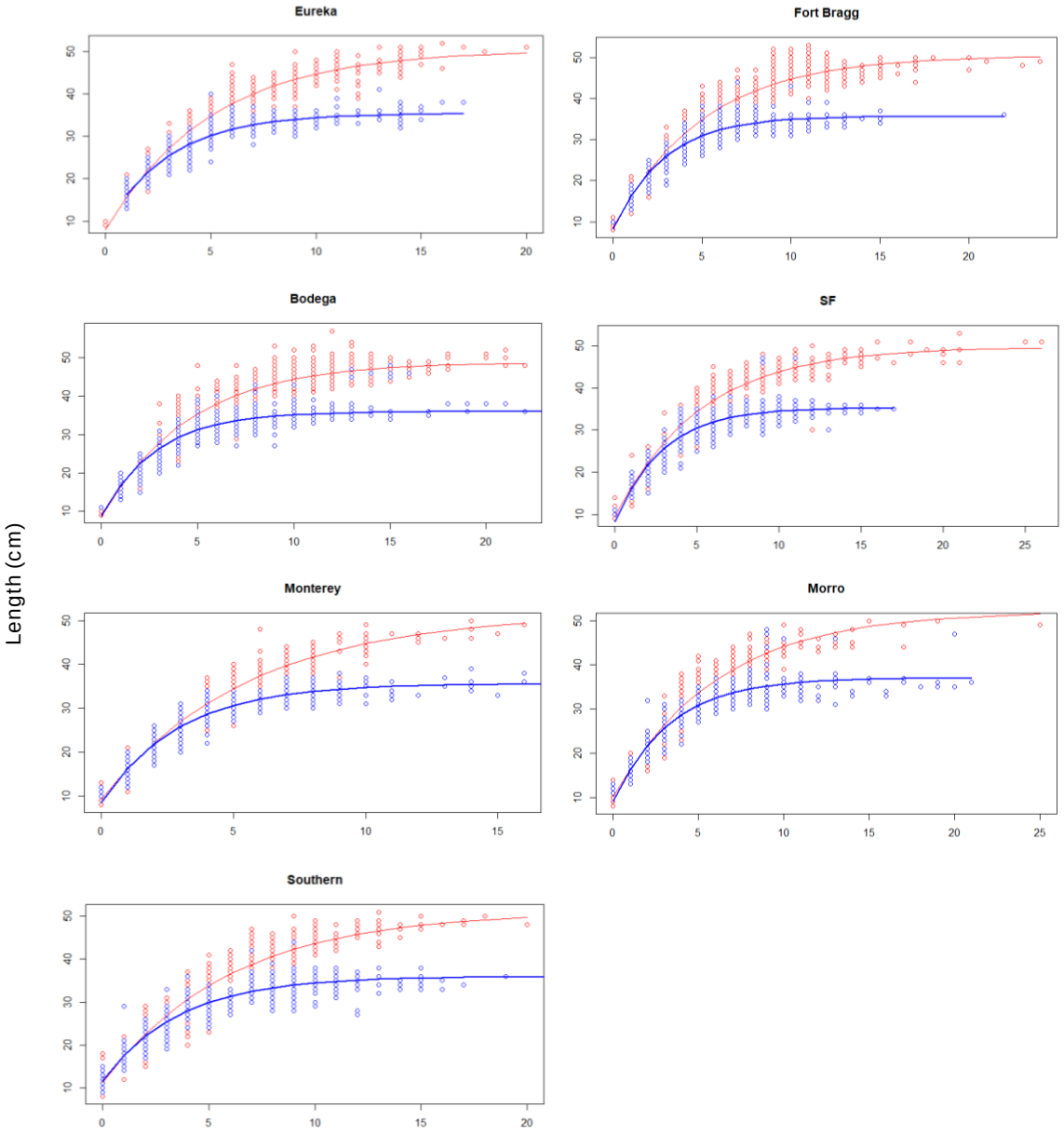
Eureka
Fort Bragg
Bodega
SF
Monterey
Morro
Southern
Length (cm)
Age (years)

APPENDIX G

Appendix G: Biomass estimates for each port-complex are largely determined by landings, and because estimates of landings were assimilated from a variety of data sources (Figure 5) the raw values of biomass aren't as reliable for interpretation. In contrast, CPUE estimates were available to the models from fishery-independent surveys for 1977 - 2015. The trends in biomass from 1977 forward should largely reflect the actual spatiotemporal distribution of biomass of Chilipepper Rockfish throughout this range.

Again, I make no assertion that these are independent stocks, but there is substantial variability in biomass trends across port-complexes. Eureka and Fort Bragg show a very similar trajectory with a steep decline beginning in the early 1970s, remaining low throughout the next thirty years, and increasing since 2001. This was likely catapulted by the strong 1999 year-class.

Bodega shows a decline after 1975, and similarly to northern ports, a steep increase around 2001. This increase was maximized in 2010, followed by another decline to its current biomass. While the rise above the "virgin" biomass at Bodega would lead to concerns in a formal assessment of an closed fish stock, this could be attributed to a variety of causes including lower fishing pressure, better oceanographic conditions, or a northward shift of fish from the San Francisco port-complex, which has been in decline since the 1970s.

San Francisco, Monterey and Morro show very similar trajectories, though San Francisco and Morro are more similar to one another than Monterey. All three ports began to decline in biomass soon after 1950, when the trawl fishery began. San Francisco and Morro approached virgin biomass again around 1980, followed by another decline. In contrast to northern ports, the decline was more incremental, reaching the lowest biomass in the late 1990s. Following course with all previous ports, the biomass began to increase again around 2001.

The Southern port-complex has the most dissimilar biomass trajectory, though it is also the least informed with minimal commercial landings. The biomass began to decline around 1970, plateauing between the late 1970s and 2000. In 2001 the increase began and by 2015 the biomass seems to be at about virgin status. The biomass appears to have rebounded at the edges of the stock, while the central region between San Francisco and Morro have had a harder time recovering. This could be due to the larger collections of biomass in these areas, though.

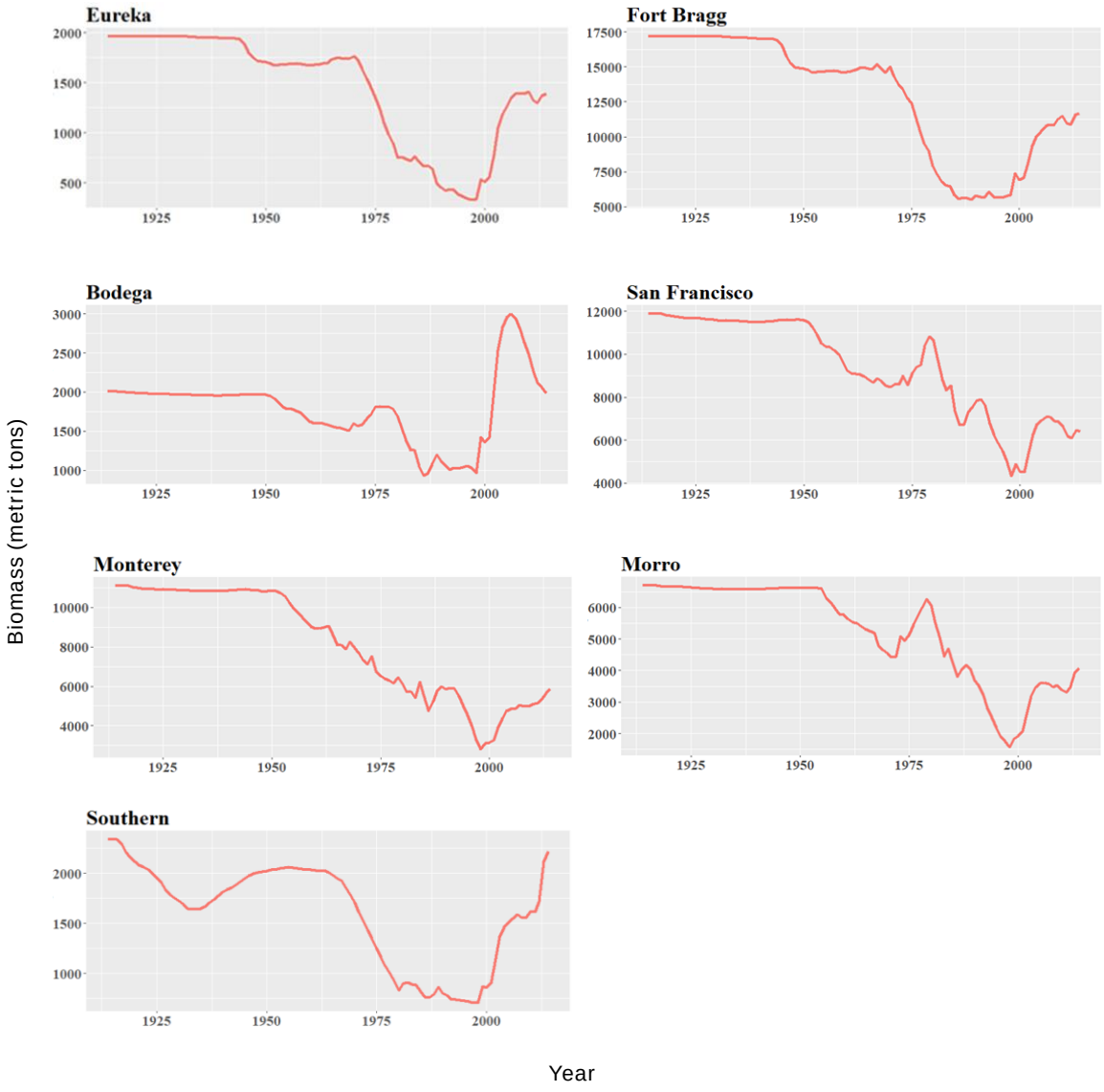
Eureka
Fort Bragg
Bodega
San Francisco
Monterey
Morro
Southern
Biomass (metric tons)
Year
1925
1950
1975
2000